A STUDY OF INTERFERENCE BETWEEN MODULATED LIGHT BEAMS

THESIS

submitted by

CATHERINE WYKES

for the degree of

Ph. D.

University of Edinburgh.

September 1971

I wish to thank Professor N. Feather for making available the facilities of the Department of Natural Philosophy for this research. I also wish to thank my supervisor, Mr. R.M. Sillitto for his guidance, advice and encouragement. My thanks also to all the other members of the Atomic and Electron Physics and Quantum Optics group for much advice, discussion and the loan of equipment, and in particular, to my husband for his constant help and support. I would like also to thank Mr. J. Stevens and the technical staff of the department.

I wish, too, to acknowledge my debt to my parents, to the Department of Education in Dublin, and the staff of University College, Galway to whom I owe my education.

The research was supported by a grant from the Science Research Council to whom I would also like to express my gratitude.

SUMMARY

A paper by Janossy and Nagy is discussed in which it was questioned whether interference would be observed in the probability distribution of a particle scattered by a scattering centre which can occupy two positions, but is at only at one of them at any given time. Some errors in this paper are pointed out. A paper by Mandel which shows that interference is expected in such an experiment from the viewpoint of classical physics, when the scattered particles are photons, is discussed. This discussion requires the use of classical optical coherence theory, some of whose results are derived. Since the method of alternating the scatterer discussed by Mandel is not practically realizeable, it is necessary to consider alternative methods. It is shown that two sinusoidally modulated optical shutters which are operated in anti-phase are not suitable for demonstrating the required effect. A method of doing the experiment which divides a light beam in two, and passes these beams in different directions through an electro-optic crystal which has an applied alternating electric field, is described. To explain the method, a description of the behaviour of light in birefringent and electro-optic materials is given, a computer program is described which calculates the visibility of the fringes produced by two beams travelling through an electro-optic crystal in various directions, and an approximate expression for the same quantity is derived. It is shown that the required experimental conditions can be approximately produced by passing a light beam through two pinholes, and a single electro-optic crystal. The experimental set-up is described, and the method of measurement of the visibility is discussed. The experimental results are given, and it is shown that the required effect has been demonstrated. Finally, two possible applications of the experiment are briefly discussed.

CONTENTS

CHAPTER I

I. INTRODUCTION

Janossy and Nagy[1] in a paper published in 1956, discuss the problem of a particle scattered by a scattering centre which is at one of two positions at any time, but never at both. They question whether interference is observed in the probability distribution of the particle in this case.

II. A SUMMARY OF THE JANOSSY AND NAGY PAPER

They consider first the case of a screen containing two slits, and a photographic plate which can be illuminated through the slits. There is a mechanical shutter in front of each slit. The shutters are initially closed, but one or other is opened at random. The photographic plate is developed after one shutter has been opened. Clearly the intensity distribution of the photographic plate is uniform - no interference is observed - since only one path has been open.

It is impossible to formulate exactly the system described above quantum-mechanically. A simpler problem is then treated - the scattering of an electron by a 'split' proton. (It is not explicitly stated what is meant by a 'split' proton, but if the situation is to be analagous to the optical system first described, it would seem to be a proton which can occupy two positions, but is only at one of these at any given time.)

The co-ordinates of the protons are denoted by $\underline{R}$, and those of the

electron by $\underline{r}$. The Schrödinger equation is then

$$\frac{-\hbar^2}{2m}\nabla^2\Psi - \frac{e^2}{\underline{R}-\underline{r}}\Psi = i\hbar\frac{\partial\Psi}{\partial t} \qquad (1.1)$$

If the wave function of the proton is $\Psi(\underline{R})$, this becomes

$$\frac{-\hbar^2}{2m}\nabla^2\Psi - e^2\int\frac{|\Psi(\underline{R})|^2}{(\underline{R}-\underline{r})}d\underline{R} = i\hbar\frac{\partial\Psi}{\partial t} \qquad (1.2)$$

The proton's wave function is now written as a 'split' wave function

$$\Psi(\underline{R}) = \frac{1}{\sqrt{2}}[\delta(\underline{R}-\underline{R}_1) + \delta(\underline{R}-\underline{R}_2)] \qquad (1.3)$$

where δ is not the Dirac wave function, but a function which differs from zero only over a small though finite range. Substitution of eq.(1.3) into eq.(1.2) gives the Schrödinger equation for the scattering of the electron, and the solution shows interference.

A more detailed treatment of the problem shows that the solution is not quite so simple.

The wave function of the electron and the proton can be denoted by $\Phi(\underline{R},\underline{r},t)$. The Schrödinger equation then becomes

$$\frac{-\hbar^2}{2m}\nabla^2_{\underline{r}}\Phi - \frac{\hbar^2}{2m}\nabla^2_{\underline{R}}\Phi - \frac{e^2}{\underline{r}-\underline{R}} = i\hbar\frac{\partial\Phi}{\partial t} \qquad (1.4)$$

The initial condition

$$\Phi_1(\underline{R},\underline{r},t=0) = \delta_1(\underline{r}-\underline{r}_1).\delta_2(\underline{R}-\underline{R}_1).e^{i\underline{p}\cdot\underline{r}/\hbar}$$

is imposed, where the δs are, as before, narrow functions with sharp maxima. This corresponds to a proton around $\underline{R}$, and an electron round $\underline{r}$, with momentum $\underline{p}$. There will be scattering of the electron when it is in the vicinity of the proton.

Another possible initial condition is

$$\Phi_2(\underline{R}, \underline{r}, t=0) = \delta_1(\underline{r}-\underline{r}_1).\delta_2(\underline{R}-\underline{R}_2).e^{i\underline{p}\cdot\underline{r}/\hbar}$$

A 'split' proton is then described by

$$\Phi_{12}(\underline{R}, \underline{r}, t=0) = \frac{1}{\sqrt{2}}\left[\Phi_1(\underline{R}, \underline{r}, t=0) + \Phi_2(\underline{R}, \underline{r}, t=0)\right] \quad (1.5)$$

From the linearity of the Schrödinger equation, the solution to eq.(1.4) is just the superposition of the solutions with initial states Φ_1 and Φ_2. Hence, the solution for any time t may be represented by

$$\Phi_{12}(\underline{R}, \underline{r}, t) = \frac{1}{\sqrt{2}}\left[\Phi_1(\underline{R}, \underline{r}, t) + \Phi_2(\underline{R}, \underline{r}, t)\right]$$

Φ_{12} is the wave function of the electron and the proton. The probability distribution of the electron at a time t is found by averaging over the co-ordinates of the proton, giving

$$\rho_{12}(\underline{r}, t) = \int |\Phi_{12}(\underline{R}, \underline{r}, t)|^2 d\underline{R} \quad (1.6)$$

This is substituted into eq.(1.5) giving

$$\rho_{12}(\underline{r},t) = \frac{1}{2}\left[\int|\Phi_1(\underline{R},\underline{r},t)|^2 d\underline{R} + \int|\Phi_2(\underline{R},\underline{r},t)|^2 d\underline{R}\right] \qquad (1.7)$$

The cross-terms disappears when the diffusion of the wave-function and the effect of the electron on the proton are neglected.

It is seen from eq.(1.7) that there is no interference in the probability distribution of the electron.

There is some further discussion of this problem in the rest of the paper, but it will be shown in the next section that the previous argument is incorrect, so that the rest of the paper is not of interest.

III. ERRORS IN THE DISCUSSION OF JANOSSY AND NAGY

The most obvious error in the quantum mechanics of the previous section is in the derivation of eq.(1.5) of the probability distribution of the electron when scattered by the proton. This should be found by finding first the probability amplitude $\psi(\underline{r},t)$ given by

$$\psi(\underline{r},t) = \int \Phi(\underline{R},\underline{r},t)\, d\underline{R}$$

for scattering off the first proton which gives the probability distribution $\rho(\underline{r},t)$ as follows

$$\rho_1(\underline{r},t) = \psi_1(\underline{r},t).\psi_1^*(r,t) = \left|\int \Phi_1(\underline{R},\underline{r},t)\, d\underline{R}\right|^2$$

The probability amplitude of the electron scattered by the 'split' proton is then

$$\Psi_{12}(\underline{r},t) = \int(\Phi_1 + \Phi_2)\,d\underline{R} = \int\Phi_1\,d\underline{R} + \int\Phi_2 d\underline{R}$$

and the probability distribution is given by

$$\rho_{12}(\underline{r},t) = \left|\int\Phi_1\,d\underline{R}\right|^2 + \left|\int\Phi_2 d\underline{R}\right|^2 + 2\,\mathrm{Re}\left[\int\Phi_1 d\underline{R}\,.\int\Phi_2\,d\underline{R}\right]$$

There is, in general, an interference term in this distribution. This is contrary to the conclusion reached by Janossy and Nagy.

There is ambiguity about what is meant by a 'split' proton. The wave functions in eq.(1.3) and eq.(1.8) describe a particle in a superimposed state. This does not mean, as seems to be implied, that the particle is switching randomly in time from one position to the other, but simply that if its position is measured it will be found to be at either one position or the other. The wave function of the scattered electron contains, at all times, terms which describe the effect of scattering by the proton at each of the two positions.

The situation which is implied by analogy with the first section of the paper is one where the electron can be scattered from only one scattering centre at a given time. This requires the introduction of time dependence into the description of the scatterer. Such a treatment is given in the next section.

IV. A QUANTUM MECHANICAL DESCRIPTION INCLUDING TIME-DEPENDENCE OF THE POSITION OF THE SCATTERER.

The electron's initial state may be denoted by $|\Psi_i\rangle$ and its final state by $|\Psi_f\rangle$. It gets to the final state by an through an interaction,

described by an operator V, the probability amplitude being given by

$$\langle \Psi_f | V | \Psi_i \rangle$$

The interaction operator consists of two parts, each of which can be separated into time-dependent and space-dependent parts, as follows

$$V_1 = \mathcal{R}(\underline{R} - \underline{R}_1)\, T_1(t) \qquad V_2 = \mathcal{R}(\underline{R} - \underline{R}_2)\, T_2(t)$$

where $\underline{R}_1$ and $\underline{R}_2$ are the positions of the scatterers, and $T_1(t)$ and $T_2(t)$ vary in time, so that one or other is always zero.

If the electron is scattered by the first scatterer, the probability amplitude is given by

$$\phi_1(\underline{r}, t) = \langle \Psi_f | \mathcal{R}(\underline{R} - \underline{R}_1)\, T_1(t - \tau) | \Psi_i \rangle$$

where τ_1 is the time taken for the electron to travel from the scatterer to $\underline{r}$.

The probability amplitude of the electron scattered by the second scatterer is

$$\phi_2(\underline{r}, t) = \langle \Psi_f | \mathcal{R}(\underline{R} - \underline{R}_2) T_2(t - \tau_2) | \Psi_i \rangle$$

The total amplitude is then

$$\phi(\underline{r}, t) = \phi_1(\underline{r}, t) + \phi_2(\underline{r}, t)$$

The transition probability is then

$$\phi\phi^* = |\langle\psi_f|R(\underline{R}-\underline{R}_1)T_1(t-\tau_1)|\psi_i\rangle|^2 + |\langle\psi_f|R(R-R_2)T_2(t-\tau_2)|\psi_i\rangle|^2$$

$$+ 2\,\mathrm{Re}\,[\langle\psi_f|R(\underline{R}-\underline{R}_1)T_1(t-\tau_1)|\psi_i\rangle\langle\psi_i|R^*(\underline{R}-\underline{R}_2)T_2^*(t-\tau_2)|\psi_i\rangle]$$

Though either $T_1(t)$ or $T_2(t)$ is always zero for any t, it is clear that $T_1(t-\tau_1)$ and $T_2(t-\tau_2)$ can be both non-zero. Hence, the cross-term does not necessarily vanish, so that interference is in general observed.

V. A CLASSICAL DESCRIPTION BY MANDEL

In a later paper[2], Mandel has shown that such an experiment performed using photons is expected to show interference from the view-point of classical physics. He derived the important condition that the switching time of the scatterer must be less than, or of the order of the coherence time of the photons. This paper is discussed in detail in the next chapter.

Sudarshan and Mehta have shown[3] that there is strict equivalence between the statistical distribution of the radiation field calculated classically and calculated quantum-mechanically. Hence, both quantum and classical physics predict that the scattered photon distribution should show interference in such an experiment.

This, then, is the experiment which has been performed, the particles used being photons and the double scatterer being produced by electro-optic modulation of the light beam.

CHAPTER 2

I. OPTICAL COHERENCE THEORY

The interference of light beams can be discussed in terms of classical optical coherence theory, so it is useful to summarise some of its definitions and results. The treatment that follows is fairly close to that of Born and Wolf[4].

Any light signal may be represented by a function $V^{(r)}(t)$, where V is a real function which may, for example, represent the electric vector at a fixed point in space. This function may be written as a Fourier integral

$$V^{(r)}(t) = \int_0^\infty a(\nu) \cos[\phi(\nu) - 2\pi\nu t]\, d\nu \qquad (2.1)$$

With this function may be associated a complex function

$$V(t) = \int_0^\infty a(\nu) \exp[i\,\phi(\nu) - 2\pi i\nu t]\, d\nu \qquad (2.2)$$

which is known as the complex analytic signal where

$$V(t) = V^{(r)}(t) + V^{(i)}(t)$$

and $$V^{(i)}(t) = \int a(\nu).\sin[\phi(\nu) - 2\pi\nu t]\, d\nu$$

Further, $V^{(r)}(t)$ may be represented as

$$V^{(r)}(t) \qquad \int_{-\infty}^{+\infty} v(\nu) \exp(-2\pi i\nu t)\, d\nu$$

with $v(-\nu) = v^*(\nu)$ since $V^{(r)}$ is real,

giving $v(\nu) = \frac{1}{2}a(\nu).\exp[i\phi(\nu)]$ from (2.1)

$$\therefore\ V(t) = 2\int_0^\infty v(\nu)\exp(-2\pi i\nu t)\,d\nu$$

This may be written in the form

$$V(t) = A(t)\exp\{i[\phi(t) - 2\pi\bar{\nu}t]\}$$

where $A(t)=\sqrt{VV^*}$ and $\Phi(t) = 2\pi\bar{\nu}t + \tan^{-1}(V^{(i)}/V^{(r)})$

$$\therefore\ A(t)\exp[i\Phi(t)] = 2\int_0^\infty v(\nu)\exp[-2\pi i(\nu-\bar{\nu})t]\,d\nu = 2\int_{-\bar{\nu}}^\infty g(\mu).\exp(-2\pi i\mu t)\,d\mu \qquad (2.3)$$

When the light amplitude has appreciable values only in the frequency range $\Delta\nu$ where $\Delta\nu \ll \bar{\nu}$, then the integral has components only for low values of μ. (2.3)

Hence $A(t).\exp[i\Phi(t)]$ is slowly varying compared with $\bar{\nu}$.

A two pinhole experiment can be discussed in terms of the complex analytic signal. In Fig.(2.1) is shown a screen containing two pinholes, and a second screen. If the pinholes are illuminated, then the signals at P_1 and P_2 may be represented by $V(P_1,t)$ and $V(P_2,t)$.

The average intensities at P_1 and P_2 may be represented by

$$I(P_1) = \langle V(P_1,t)\,V^*(P_1,t)\rangle$$

and

$$I(P_2) = \langle V(P_2,t)\,V^*(P_2,t)\rangle$$

The signal at Q is the sum of the signals from P_1 and P_2 and is given by

$$V(Q,t) = K_1 V(P_1, t-t_1) + K_2 V(P_2, t-t_2)$$

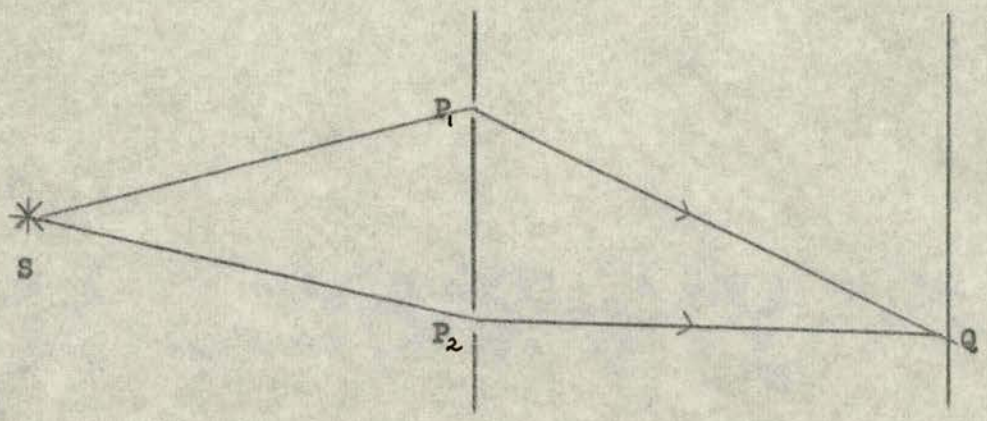

Fig.2.1

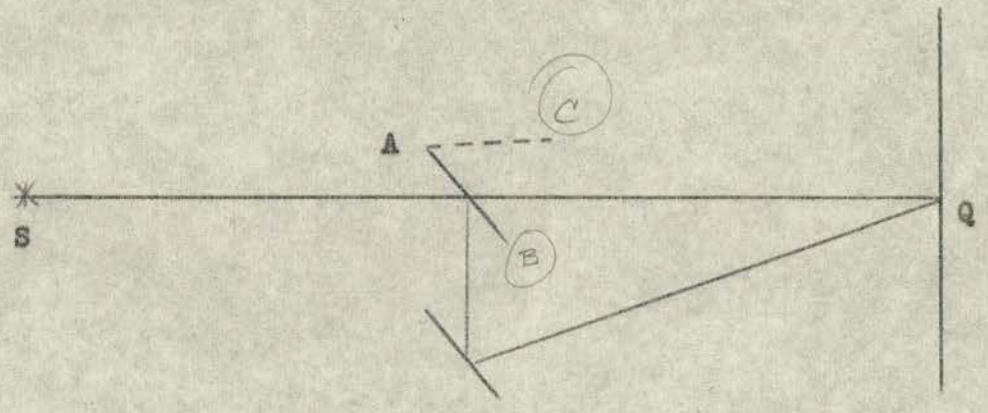

Fig.2.2

where t_1 and t_2, are the times taken for light to travel from P_1 and P_2 respectively, to Q, and K_1 and K_2 are inversely proportional to P_1Q and P_2Q, are also dependent on the geometry, and are time dependent if the transmission of the pinholes is changing in time. They may be separated into time-dependent and time independent parts

$$K_1 = k_1 G_1(t) \qquad K_2 = k_2 G_2(t)$$

The average intensity at Q is then given by

$$I(Q) = k_1 k_1^* \langle G_1(t-t_1)\, G_1^*(t-t_1)\, V_1(t-t_1) V_1^*(r-r_1)\rangle + k_2 k_2^* \langle G_2(t-r_2)\, G_2^*(r-r_2)\, V_2(r-r_2) V_2^*(r-r_2)\rangle$$
$$+ k_1 k_2^* \langle G_1(t-r_1)\, G_2^*(r-r_2)\, V_1(r-r_1) V_2^*(r-r_2)\rangle + k_1^* k_2 \langle G_1^*(r-r_1)\, G_2(r-r_2)\, V_1^*(r-r_1) V_2(r-r_2)\rangle \tag{2.4}$$

Taking first the case where the transmission of the pinholes does not vary with time, when $G_1(t)$ and $G_2(t)$ are constant and may be equated to unity, the intensity at Q is

$$I(Q) = k_1 k_1^* \langle V_1(r-r_1) V_1^*(r-r_1)\rangle + k_2 k_2^* \langle V_2(r-r_2) V_2^*(r-r_2)\rangle$$
$$+ k_1 k_2^* \langle V_1(r-r_1) V_2^*(r-r_2)\rangle + k_1^* k_2 \langle V_1^*(r-r_1) V_2(r-r_2)\rangle$$

If the field is assumed to be stationary, i.e. $\langle V(r)\rangle$ is independent of the time origin, and $\langle V(r-r_1) V_1^*(r-r_1)\rangle$ depends only on the difference $t_1 - t_2$, then

$$\langle V_1(r-r_1) V_1^*(r-r_1)\rangle = I_1$$

$$\langle V_2(r-r_2) V_2^*(r-r_2)\rangle = I_2$$

where I_1 and I_2 are the average intensities at P_1 and P_2, and

$$I(Q) = |k_1^2| I_1 + |k_2^2| I_2 + 2 \mathrm{Re} |k_1 k_2^*| \langle V_1(t-t_1) V_2^*(t-t_2) \rangle$$

The function $\langle V_1(t-t_1) V_2^*(t-t_2) \rangle$ is known as the mutual coherence of the vibrations at P_1 and P_2, the vibrations at P_1 being considered at a time τ later than those at P , τ being equal to $t_1 - t_2$. It is written

$$\Gamma_{12}(\tau) = \langle V_1(t) V_2^*(t+\tau) \rangle$$

The terms $|k_1^2| I_1$ and $|k_2^2| I_2$ clearly give the intensities at Q which would be obtained if only P_1 or P_2 respectively were open. These may be written as $I^{(1)}(Q)$ and $I^{(2)}(Q)$.

$\Gamma_{12}(\tau)$ may be normalized, giving

$$\gamma_{12}(\tau) = \frac{\Gamma_{12}(\tau)}{\sqrt{I^{(1)}} \sqrt{I^{(2)}}}$$

and the intensity at Q then becomes

$$I(Q) = I^{(1)} + I^{(2)} + 2 \sqrt{I^{(1)}} \sqrt{I^{(2)}} \mathrm{Re} [\gamma_{12}(\tau)]$$

The normalization condition ensures that $|\gamma_{12}(\tau)| \leq 1$, for by the Schwarz inequality

$$\left| \int_{-\infty}^{+\infty} V_1(t) V_2^*(t+\tau) d\tau \right|^2 \leq \int_{-\infty}^{\infty} V_1(t) V_1^*(t) dt \int_{-\infty}^{+\infty} V_2(t+\tau) V_2^*(t+\tau) d\tau$$

If the light used is monochromatic, i.e. if the range of its spectral components, $\Delta\nu$, is much less than its mean frequency $\bar{\nu}$, then it is useful to write

$$\gamma_{12}(\tau) = |\gamma_{12}(\tau)| \exp[i(\alpha_{12}(\tau)) - 2\pi\bar{\nu}\tau]$$

where $\alpha_{12}(\tau) = 2\pi\bar{\nu}\tau + \arg[\gamma_{12}(\tau)]$

Then

$$I(Q) = I^{(1)} + I^{(2)} + 2\sqrt{I^{(1)}}\sqrt{I^{(2)}}\,|\gamma_{12}(\tau)|\cos[\alpha_{12}(\tau) - 2\pi\bar{\nu}\tau]$$

In the same way as with eq.(2.3), $\gamma_{12}(\tau)$ and $\alpha_{12}(\tau)$ are very slowly varying compared with $\cos(2\pi\nu t)$ and $\sin(2\pi\nu t)$.

The intensity of the light in the region of Q thus consists of an almost uniform background, $I_1(Q)+I_2(Q)$, upon which is superimposed a sinusoidal intensity variation. The intensity maxima and minima near Q are, to a good approximation, given by

$$I_{max} = I^{(1)} + I^{(2)} + 2\sqrt{I^{(1)}}\sqrt{I^{(2)}}\,|\gamma_{12}(\tau)|$$

$$I_{min} = I^{(1)} + I^{(2)} - 2\sqrt{I^{(1)}}\sqrt{I^{(2)}}\,|\gamma_{12}(\tau)|$$

The visibility of the fringes around Q is given by

$$V(Q) = \frac{I_{max} - I_{min}}{I_{max} + I_{min}} = \frac{2\sqrt{I^{(1)}}\sqrt{I^{(2)}}}{I^{(1)} + I^{(2)}}\,|\gamma_{12}(\tau)|$$

If the ratio of the contributions from P_1 and P_2 is

$$\frac{\sqrt{I^{(1)}}}{\sqrt{I^{(2)}}} = \beta$$

then

$$V(Q) = \frac{2\beta}{1+\beta^2}\,|\gamma_{12}(\tau)|$$

II. VISIBILITY OF FRINGES OBTAINED WITH MODULATED LIGHT

The case where the transmission of the pinholes varies with time can now be considered. In the cases under consideration, $G_1(t)$ and $G_2(t)$ are either random in time as in Mandel's discussion, or fluctuating at frequencies much lower than the fluctuation frequencies of the light signal, so that the averaging processes over G_1 and G_2 can be considered to be independent of averaging over V. Thus eq.(2.3) may be rewritten as

$$I(Q) = k_1 k_1^* \langle G_1(t-t_1) G_1^*(t-t_1)\rangle \langle V_1(t-t_1) V_1^*(t-t_1)\rangle$$

$$+ k_2 k_2^* \langle G_2(t-t_2) G_2^*(t-t_2)\rangle \langle V_2(t-t_2) V_2^*(t-t_2)\rangle$$

$$+ k_1 k_2^* \langle G_1(t-t_1) G_2^*(t-t_2)\rangle \langle V_1(t-t_1) V_2^*(t-t_2)\rangle$$

$$+ k_1^* k_2 \langle G_1^*(t-t_1) G_2(t-t_2)\rangle \langle V_1^*(t-t_1) V_2(t-t_2)\rangle$$

If the average intensities transmitted by the pinholes are the same, then $\langle G_1(t) G_1^*(t)\rangle = \langle G_2(t+\tau) G_2^*(t+\tau)\rangle$ so that the intensity at Q becomes

$$I(Q) = \langle G_1(t) G_1^*(t)\rangle [I^{(1)} + I^{(2)}]$$

$$+ 2\sqrt{I^{(1)}}\sqrt{I^{(2)}}\ \mathrm{Re}[\langle G_1(t) G_2^*(t+\tau)\rangle\ \gamma_{12}(\tau)]$$

A function $M_{12}(\tau)$ may be defined as

$$M_{12}(\tau) = \frac{\langle G_1(t)\, G_2^*(t+\tau)\rangle}{\langle G_1(t) G_1^*(t)\rangle^{1/2} \langle G_2(t+\tau) G_2^*(t+\tau)\rangle} = \frac{\langle G_1(t)\, G_2^*(t+\tau)\rangle}{\langle G_1(t)\, G_1^*(t)\rangle} \qquad (2.7)$$

$$\therefore \; \mathrm{Re}\,[M_{12}(\tau)] = \frac{\mathrm{Re}\langle G_1(t)\, G_1^*(t+\tau)\rangle}{\langle G_1(t)\, G_1^*(t)\rangle} \tag{2.8}$$

$$\therefore \; I(Q) = \langle G_1(t) G_1^*(t)\rangle [I^{(1)} + I^{(2)}] + 2\sqrt{I^{(1)}}\sqrt{I^{(2)}}\, \mathrm{Re}[M_{12}(\tau).\, \gamma_{12}(\tau)] \tag{2.9}$$

The visibility of the fringes around Q is then either

$$V_M(Q) = \mathrm{Re}\,[M_{12}(\tau)].\; |\gamma_{12}(\tau)|.\; \frac{2\beta}{1+\beta^2} \tag{2.10}$$

$$= \mathrm{Re}\,[M_{12}(\tau)]\, V(Q) \qquad \text{if } |M_{12}(\tau)| \text{ is positive}$$

or $$= -\mathrm{Re}\,[M_{12}(\tau)]\, V(Q) \qquad \text{if } |M_{12}(\tau)| \text{ is negative}$$

$$\therefore \; V_M(Q) = |\mathrm{Re}\,[M_{12}(\tau)]|\, V(Q)$$

Again, it follows from the Schwarz inequality, that

$$|M_{12}(\tau)| \leq 1$$

Thus the visibility is, in general, reduced by the modulation of the transmission of the pinholes. It will be seen that it is this change in the visibility which is of interest.

III. INTERFERENCE OF TWO BEAMS MODULATED RANDOMLY IN ANTI-PHASE

The system discussed by Mandel is illustrated in Fig.2.2. A light beam is divided into two beams by the mirror pivoted at A in Fig. 2.2 which can be rapidly rotated through 45° to position AB or AC. If the shutter

is switched at random from one state to the other, it produces a modulation which can be represented by a real function G(t) taking the values 0 or 1 at random. The switching of the shutter effectively produces two slits which can be considered equivalent to the two pinholes in the previous discussion.

The modulation functions are then given by

$$G_1(t) = G(t)$$

$$G_2(t) = 1 - G(t)$$

Then $\mathrm{Re}\,[M_{12}(\tau)] = M_{12}(\tau)$

The successive intervals t' during which G(t) is constant are assumed to be uncorrelated, and to have the probability distribution

$$p(t')\,dt' = \frac{1}{T}\exp\left(-\frac{t'}{T}\right)dt'$$

where T is the mean interval.

Hence,

$$M_{12}(\tau) = \frac{\langle G(t)\,[1 - G(t+\tau)]\rangle}{\langle G^2(t)\rangle^{1/2}\langle [1-G(t+\tau)]^2\rangle^{1/2}}$$

Now $\langle G^2(t)\rangle = \langle G^2(t+\tau)\rangle = \langle G(t)\rangle = \frac{1}{2}$

$$\therefore\quad M_{12}(\tau) = \frac{\frac{1}{2} - \langle G(t)\,G(t+\tau)\rangle}{\frac{1}{2}} = 1 - 2\langle G(t)\,G(t+\tau)\rangle$$

It has been shown by Rice[5] that

$$\langle G(t)\,G(t+\tau)\rangle = \frac{1}{4}\left[1 - \exp\left(-\frac{2(\tau)}{T}\right)\right]$$

The visibility of the fringes in this case is then given by

$$V_M(Q) = \frac{1}{2}\left[1 - \exp\left(-2\frac{|\tau|}{T}\right)\right]|\gamma_{12}(\tau)|$$

For a spectral line of Gaussian shape

$$|\gamma_{12}(\tau)| = \exp\left|-2\pi^2\Delta\nu^2\tau^2\right|$$

$$\therefore V_M(Q) = \frac{1}{2}\exp\left(-2\pi^2\Delta\nu^2\tau^2\right)\left[1 - \exp\left(-2\frac{|\tau|}{T}\right)\right]$$

The shape of this function depends on the relative values of τ, $\Delta\nu$, and T. It can be seen that interference will be observed only if

$$T \gtrsim \tau \gg 1/\Delta\nu$$

i.e. (i) the time delay between the beams must be less than the coherence time, $c/\Delta\nu$, of the light, (this is a general condition for the observation of interference) and

(ii) the switching time must be less than the coherence time.

In Fig.(2.3), Vm(Q) is plotted against τ for different values of the ratio $\frac{\Delta\nu}{T}$. It is seen that as the switching time is decreased, the visibility of the fringes increases. The visibility is zero at zero path difference, as the light at this point has come from one or other slit, but never both.

Mandel concludes by observing that the shutter need not be switched at random, nor must the modulation be rectangular, but that the effect could be observed using sinusoidal modulation.

V. INTERFERENCE OF TWO LIGHT BEAMS MODULATED SINUSOIDALLY IN ANTI-PHASE

Sinusoidally modulated light may be produced by passing a light beam through an electro-optic crystal which is placed between crossed polarisers,

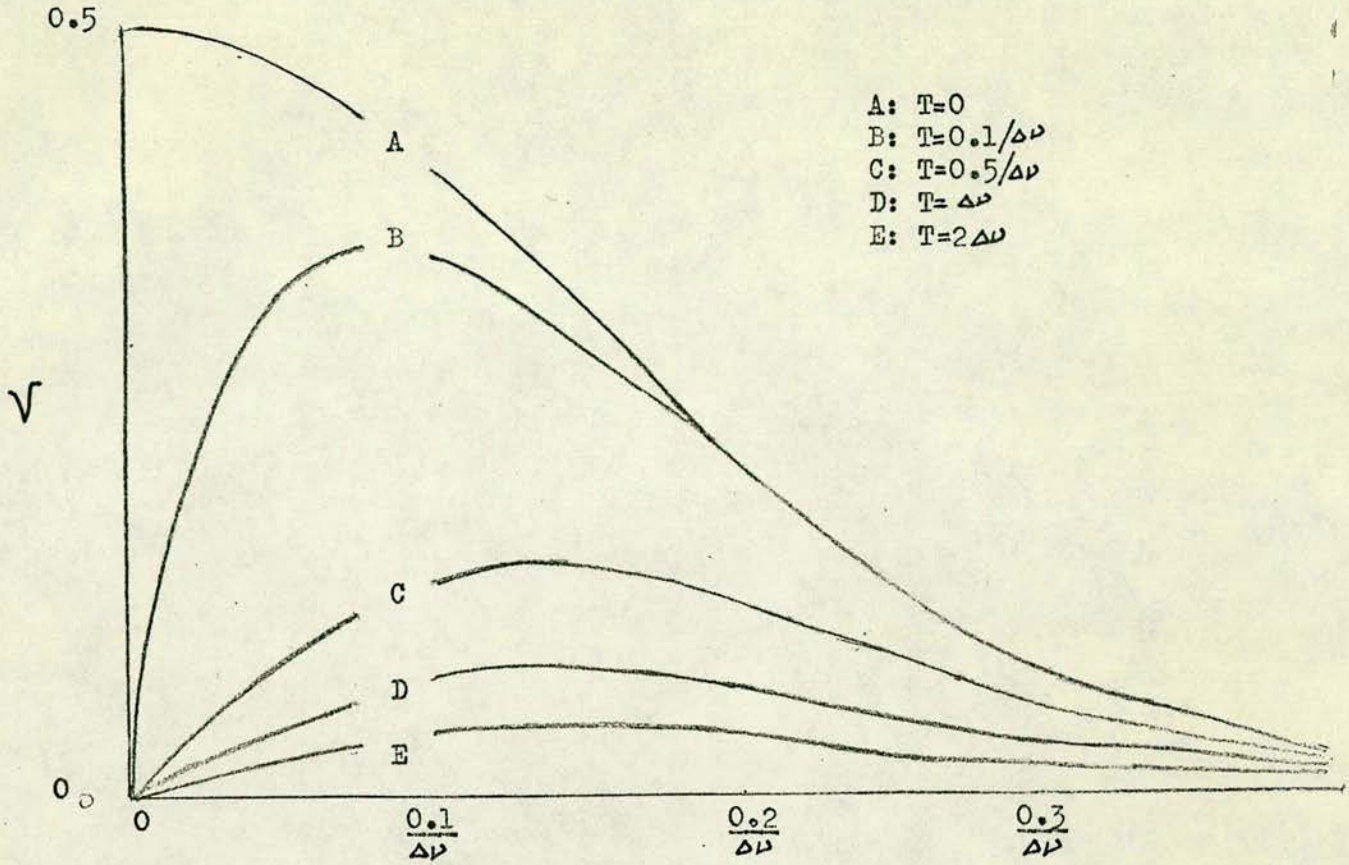
0.5
A
B
C
D
E
V
0
0
0.1/Δν
0.2/Δν
0.3/Δν
A: T=0
B: T=0.1/Δν
C: T=0.5/Δν
D: T= Δν
E: T=2Δν

Fig.2.3

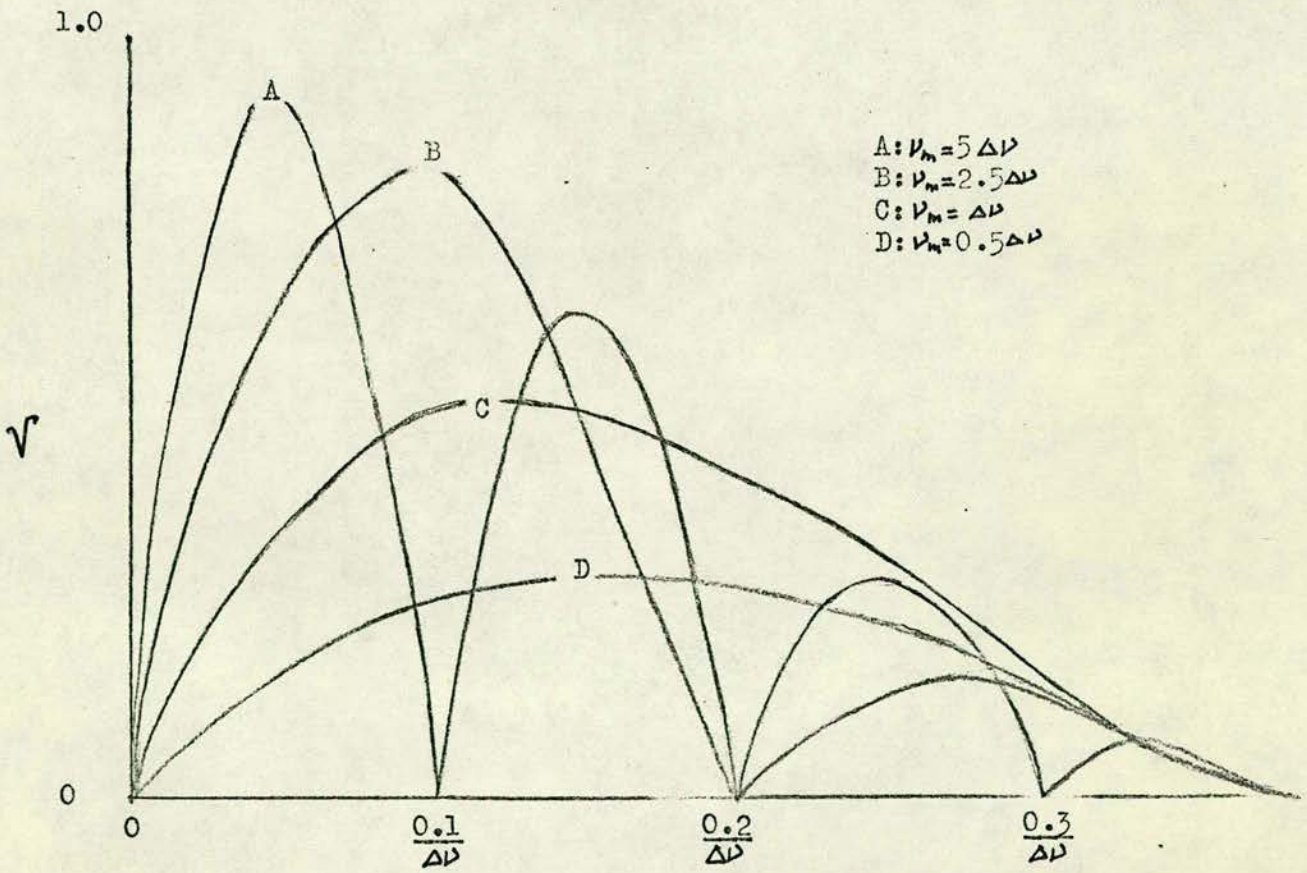
1.0
A
B
C
D
V
0
0
0.1/Δν
0.2/Δν
0.3/Δν
A: νm=5Δν
B: νm=2.5Δν
C: νm= Δν
D: νm=0.5Δν

Fig.2.4

and to which an alternating electric field is applied. If the incident light is described by V(t), then the output signal from such a system is given by p $\mathrm{Sin}(\omega_M t)V(t)$, where p is a constant which is proportional to the amplitude of the electric field, and ω_M is the frequency of the field.

The two pinhole experiment can again be considered, with two such electro-optic shutters, one at each pinhole, operated in anti-phase. The modulation functions are, in this case,

$$G_1(t) = p \sin(\omega_M t)$$

$$G_2(t) = p \cos(\omega_M t)$$

if the amplitudes of the modulating electric fields are the same.

The function $M_{12}(\tau)$ becomes, in this case,

$$M_{12}(\tau) = \mathrm{Re}\,[M_{12}(\tau)] = \frac{\langle p^2 \sin(\omega_M t)\cos(\omega_M (t+\tau))\rangle}{\langle p^2 \sin^2(\omega_M t)\rangle^{1/2} \langle p^2 \cos^2(\omega_M (t+\tau))\rangle^{1/2}}$$

The averaging can now be done by integrating over one period of the modulation, giving

$$\mathrm{Re}\,|M_{12}(\tau)| = \sin(\omega_M \tau)$$

The visibility of the fringes is then given by

$$V_M(Q) = |\sin(\omega_M \tau)|\,|\gamma_{12}(\tau)|\,\frac{2\beta}{1+\beta^2}$$

In Fig.2.4, $V_M(Q)$ is plotted against τ for various values of $\nu_M/\Delta\nu$. It is seen that the visibility goes to zero at zero path difference. With sinusoidal modulation, there is light being transmitted at all times from each pinhole, except at the instant when $\mathrm{Cos}(\omega_M t)$ and $\mathrm{Sin}(\omega_M t)$ are

equal to zero, so that even at zero path difference, there are contributions from both slits, so that interference should be observed. The disappearance of the fringes is then surprising, but can be understood by looking at how the intensity of the light varies in time when the path difference between the beams is around zero. The light intensity may be averaged over the period of the light and not over the modulation, and the intensity $I(t,\tau)$ is then given by

$$I(t,\tau) = I^{(1)} \sin^2(\omega_M t) + I^{(2)} \cos^2(\omega_M(t+\tau))$$

$$+ 2 \sin(\omega_M t).\cos\omega_M(t+\tau).\sqrt{I^{(1)}}\sqrt{I^{(2)}}\,|\gamma_{12}(\tau)|\cos[\alpha_{12}(\tau) - 2\pi\bar{\nu}\tau]$$

Around $\tau = 0$, the function $\cos(\alpha_{12}(\tau) - 2\pi\bar{\nu}\tau)$ will vary between +1 and -1, so that the maximum and minimum intensities in this region are given by

$$I_1 = I^{(1)} \sin^2(\omega_M t) + I^{(2)}\cos^2(\omega_M(t+\tau')) + 2\sqrt{I^{(1)}}\sqrt{I^{(2)}} \sin(\omega_M t)\cos(\omega_M(t+\tau'))|\gamma_{12}(\tau')|$$

$$I_2 = I^{(1)} \sin^2(\omega_M t) + I^{(2)}\cos^2(\omega_M(t+\tau')) - 2\sqrt{I^{(1)}}\sqrt{I^{(2)}} \sin(\omega_M t)\cos(\omega_M(t+\tau'))|\gamma_{12}(\tau')|$$

If $\frac{\omega_M}{2\pi} = \nu_M << \bar{\nu}$, so that $\omega_M\tau' \simeq \omega_M\tau'' \simeq 0$, and if the light is quasi-monochromatic, so that $|\gamma_{12}(\tau')| \simeq |\gamma_{12}(\tau'')| \simeq |\gamma_{12}(0)| \simeq 1$

then
$$I_1 \simeq I^{(1)} \sin^2(\omega_M t) + I^{(2)}\cos^2(\omega_M t) + \sqrt{I^{(1)}}\sqrt{I^{(2)}} \sin(2\omega_M t)$$

$$I_2 \simeq I^{(1)} \sin^2(\omega_M t) + I^{(1)}\cos^2(\omega_M t) - \sqrt{I^{(1)}}\sqrt{I^{(2)}} \sin(2\omega_M t)$$

In Table 2.1 are given the values of I_1 and I_2 at different times in the modulation cycle. During the first quarter cycle, I_1 is larger than I_2, in the second quarter cycle I_2 is larger than I_1, during the third I_1 is greater than I_2, and during the last I_2 is larger than I_1. Clearly,

$\omega_1\tau$	I_1	I_2
0	$I^{(2)}$	$I^{(2)}$
$\frac{\pi}{4}$	$\frac{1}{2}(I^{(1)}+I^{(2)})+\sqrt{I^{(1)}}\sqrt{I^{(2)}}\lvert\gamma_{12}(0)\rvert$	$\frac{1}{2}(I^{(1)}+I^{(2)})-\sqrt{I^{(1)}}\sqrt{I^{(2)}}\lvert\gamma_{12}(0)\rvert$
$\frac{\pi}{2}$	$I^{(1)}$	$I^{(1)}$
$\frac{3\pi}{4}$	$\frac{1}{2}(I^{(1)}+I^{(2)})-\sqrt{I^{(1)}}\sqrt{I^{(2)}}\lvert\gamma_{12}(0)\rvert$	$\frac{1}{2}(I^{(1)}+I^{(2)})+\sqrt{I^{(1)}}\sqrt{I^{(2)}}\lvert\gamma_{12}(0)\rvert$
π	$I^{(2)}$	$I^{(2)}$
$\frac{5\pi}{4}$	$\frac{1}{2}(I^{(1)}+I^{(2)})+\sqrt{I^{(1)}}\sqrt{I^{(2)}}\lvert\gamma_{12}(0)\rvert$	$\frac{1}{2}(I^{(1)}+I^{(2)})-\sqrt{I^{(1)}}\sqrt{I^{(2)}}\lvert\gamma_{12}(0)\rvert$
$\frac{3\pi}{2}$	$I^{(1)}$	$I^{(1)}$
$\frac{7\pi}{4}$	$\frac{1}{2}(I^{(1)}+I^{(2)})-\sqrt{I^{(1)}}\sqrt{I^{(2)}}\lvert\gamma_{12}(0)\rvert$	$\frac{1}{2}(I^{(1)}+I^{(2)})+\sqrt{I^{(1)}}\sqrt{I^{(2)}}\lvert\gamma_{12}(0)\rvert$
2π	$I^{(2)}$	$I^{(2)}$

Table 2.1

the maxima and minima of the interference pattern are reversed during alternate quarter cycles of the modulation cycle, so that the average intensities at the two positions are the same. The disappearance of the fringes at zero path difference is due to this effect. The reason for the inversion of the fringe pattern is found in the form of the amplitude modulation. When the amplitude is given by p $\mathrm{Sin}(\omega_H t)$, then it is seen that the phase of the light is reversed every half cycle of the modulation. This phase reversal occurs in both beams, but is delayed by a quarter of a cycle in one with respect to the other. Thus, some of the time, the two beams are in phase, and some of the time they are in anti-phase. When the two beams are in phase, then the intensity at zero path difference is a maximum, and when they are in anti-phase, the intensity there is a minimum.

The requirement of the experiment is that only one of the two light paths is open at any time, This condition is approximately reproduced when the two light beams are sinusoidally modulated in anti-phase, though obviously there is an overlap in the open times of the two shutters. However the change in the visibility which is produced by the modulation is more significantly affected by phase reversal effects than by amplitude modulation - in fact the visibility could be changed by simply reversing the phase of the light beams periodically, without any amplitude modulation at all.

Hence, the required effect, though present when sinusoidal modulation is used, is combined with phase reversal effects. It had been planned originally to do the experiment this way, and some work was done on the design of a Mach-Zender interferometer for this purpose. However, a

better method was devised. Some discussion of the properties of electro-optic crystals is required to explain the method. This will be given in the next chapter.

CHAPTER 3

I. THE BEHAVIOUR OF LIGHT IN BIREFRINGENT MEDIA

The propagation of light can be discussed in terms of Maxwell's equations, and of the relations which describe the behaviour of materials under the influence of the electro-magnetic field. (see, for example, Born and Wolf[6].)

Many crystals are non-conducting, and magnetically isotropic, but show electric anisotropy. In this case, the electric displacement $\underline{D}$, is not in the same direction as the electric field $\underline{E}$. The simplest case is that in which the relationship between $\underline{D}$ and $\underline{E}$ is given by a tensor equation of the form

$$D_k = \sum_e \epsilon_{ke} E_e$$

where x,y,z refer to some set of co-ordinate axes in the crystal, k and l stand for x,y,z in turn, and the ϵ_{ke} are constants of the crystal.

The electric and magnetic energy densities are given by

$$w_e = \frac{1}{8\pi} \underline{E} \cdot \underline{D} = \frac{1}{8\pi} \sum_{ke} E_k \epsilon_{ke} E_e$$

$$w_m = \frac{1}{8\pi} \underline{B} \cdot \underline{H} = \frac{1}{8\pi} \mu \underline{H}^2$$

where $\underline{B}$ is the magnetic induction, and $\underline{H}$ is the magnetic vector.

It can be shown that the energy flux per unit volume is

$$\frac{1}{4\pi} [\underline{E} \cdot \dot{\underline{D}} + \underline{B} \cdot \dot{\underline{H}}] = \frac{1}{4\pi} \sum_{kl} E_k \epsilon_{kl} \dot{E}_e + \frac{1}{8\pi} \frac{d}{dt} (\mu \underline{H}^2)$$

This is satisfied only if

$$\frac{1}{4\pi} \sum_{kl} E_k \epsilon_{kl} E_e = \frac{dw_e}{dt} = \frac{1}{8\pi} \sum_{kl} \epsilon_{kl} (E_k \dot{E}_e + E_e \dot{E}_k)$$

i.e. if $\sum_{kl} \epsilon_{kl} (E_k \dot{E}_e - E_e \dot{E}_k) = 0$

giving

$$\sum_{kl}(\epsilon_{kl} - \epsilon_{lk})E_k \dot{E}_e = 0$$

This means that $\epsilon_{kl} = \epsilon_{lk}$ for all l,k.

The electrical energy density can then be written

$$\begin{aligned} w_e &= \frac{1}{8\pi}[\underline{E}\cdot\underline{D}] \\ &= \frac{1}{8\pi}[\epsilon_{xx}E_x^2 + \epsilon_{yy}E_y^2 + \epsilon_{zz}E_z^2 + 2\epsilon_{xy}E_xE_y + 2\epsilon_{yz}E_yE_z + 2\epsilon_{zx}E_zE_x] \end{aligned} \tag{3.1}$$

The co-ordinate system (x,y,z) may be rotated to (x',y',z') so that the cross-terms in eq.(3.1) vanish, giving

$$w_e = \frac{1}{8\pi}[\epsilon_{x'}E_{x'}^2 + \epsilon_{y'}E_{y'}^2 + \epsilon_{z'}E_{z'}^2] \tag{3.2}$$

The energy must be positive (or zero), hence the right-hand side of eq.(3.2) is the equation of an ellipsoid, which may be written

$$\epsilon_x E_x^2 + \epsilon_y E_y^2 + \epsilon_z E_z^2 = \text{constant}$$

where x',y',z', are now written x,y,z for convenience. These axes are known as the principal di-electric axes. Clearly

$$D_x = \epsilon_x E_x \qquad D_y = \epsilon_y E_y \qquad D_z = \epsilon_z E_z \tag{3.3}$$

so that

$$w_e = \frac{1}{8\pi}\left[\frac{D_x^2}{\epsilon_x} + \frac{D_y^2}{\epsilon_y} + \frac{D_z^2}{\epsilon_z}\right]$$

The vectors $\underline{E}$, $\underline{D}$, $\underline{H}$, $\underline{B}$ will be proportional to $\exp[i\omega(\frac{n}{c}\underline{r}\cdot\underline{s} - t)]$ for a monochromatic plane wave of angular frequency ω, propagated in the direction $\underline{S}$, with velocity c/n_s.

From Maxwell's equations it can be shown that

$$n_s\underline{S}\times\underline{H} = \underline{D} \qquad n_s\underline{S}\times\underline{E} = \mu\underline{H}$$

and from these

$$\underline{D} = -\frac{n_s^2}{\mu}[\underline{E} - \underline{S}(\underline{S}\cdot\underline{E})] \tag{3.4}$$

Thus $\underline{D}$ is perpendicular to $\underline{S}$. This is true for any medium. In the case of a birefringent crystal (one showing electrical anisotropy) eq.(3.4) can be written

$$E_K = \frac{n_s^2 s_K (\underline{E} \cdot \underline{S})}{n_s^2 - \mu \epsilon_K} \tag{3.5}$$

where $\underline{D}$ is substituted from eq.(3.3).

Putting $s_x = l$, $s_y = m$, and $s_z = n$, then eq.(3.5) can be manipulated to give

$$\frac{l^2}{\frac{1}{n_s^2} - \frac{1}{\mu \epsilon_x}} + \frac{m^2}{\frac{1}{n_s^2} - \frac{1}{\mu \epsilon_y}} + \frac{n^2}{\frac{1}{n_s^2} - \frac{1}{\mu \epsilon_z}} = 0 \tag{3.6}$$

Writing $V_x^2 = \frac{c^2}{\mu \epsilon_x}$, $V_y^2 = \frac{c^2}{\mu \epsilon_y}$, $V_z^2 = \frac{c^2}{\mu \epsilon_z}$, $V_p^2 = \frac{c^2}{n_s^2}$

eq.(3.6) becomes

$$\frac{l^2}{V_p^2 - V_x^2} + \frac{m^2}{V_p^2 - V_y^2} + \frac{n^2}{V_p^2 - V_z^2} = 0 \tag{3.7}$$

and eq.(3.5) becomes

$$E_x = \frac{V_x^2}{V_x^2 - V_p^2} \, l^2 (\underline{E} \cdot \underline{S}) \tag{3.8}$$

Eq.(3.6) is a quadratic equation in V_p, so that for every $\underline{S}$, there are two allowed phase velocities. The ratios $E_x : E_y : E_z$ may be found by substitution into eq.(3.5), and corresponding ratios for $\underline{D}$, may be found from eq.(3.4). Thus, in an anisotropic medium, two monochromatic plane waves of different linear polarization and different phase velocity can travel in any given direction.

There is an interesting relationship between the ellipsoid and the

allowed velocities and polarization directions. This can be demonstrated as follows.

The electric energy density is given by

$$W_e = \frac{1}{8\pi}\left(\frac{D_x^2}{\epsilon_x} + \frac{D_y^2}{\epsilon_y} + \frac{D_z^2}{\epsilon_z}\right)$$

Thus, for constant energy density

$$\frac{D_x^2}{\epsilon_x} + \frac{D_y^2}{\epsilon_y} + \frac{D_z^2}{\epsilon_z} = \text{Constant} \qquad (3.9)$$

For a wave travelling in a direction $\underline{S}$ with direction cosines l,m,n with allowed polarization directions $\underline{D}'$ and $\underline{D}''$, it can be seen that these latter must satisfy eq.(3.9), and also that

$$\underline{D}' \cdot \underline{S} = 0 \qquad \underline{D}'' \cdot \underline{S} = 0$$

Both vectors lie on a plane normal to $\underline{S}$. Because they must satisfy eq.(3.9), they must be radii of the ellipse which is the intersection of that plane and the ellipsoid. They must also satisfy eq.(3.4)

$$D_x = -\frac{n_s^2}{\mu}\left[E_x - \ell(\underline{s}\cdot\underline{E})\right]$$

This can be written

$$D_x = -\frac{n_s^2}{\mu}\left[\frac{D_x}{\epsilon_x} - \ell\left(\ell\frac{D_x}{\epsilon_x} + m\frac{D_y}{\epsilon_y} + n\frac{D_z}{\epsilon_z}\right)\right]$$

This condition is satisfied by the two vectors which are the semi-axes of the ellipse which is the intersection of the ellipsoid and the plane normal to $\underline{S}$. This is shown as follows. Let $\underline{D}$ be one of the semi-axes. Then

$$\underline{D}^2 = D_x^2 + D_y^2 + D_z^2$$

If it is a semi-axis, it must be either a maximum or a minimum. Its direction can be found using Lagrange's method of undetermined multipliers. Introducing two constants, λ_1, and $2\lambda_2$, a function F may be constructed such that

$$F = D_x^2 + D_y^2 + D_z^2 + 2\lambda_1(D_x\ell + D_y m + D_z n)$$

$$+ \lambda_2\left[\frac{D_x^2}{\epsilon_x} + \frac{D_y^2}{\epsilon_y} + \frac{D_z^2}{\epsilon_z} - C\right]$$

The condition for an extreme value of F is that $\frac{\partial F}{\partial D_x}$, $\frac{\partial F}{\partial D_y}$, $\frac{\partial F}{\partial D_z}$ should vanish, i.e.

$$D_x + \lambda_1\ell + \lambda_2\frac{D_x}{\epsilon_x} = 0 \quad D_y + \lambda_1 m + \lambda_2\frac{D_y}{\epsilon_y} = 0 \quad D_z + \lambda_1 m + \lambda_2\frac{D_z}{\epsilon_z} = 0 \qquad (3.10)$$

Multiplying by D_x, D_y, and D_z respectively and adding,

$$D^2 + \lambda_2 C = 0$$

Again, multiplying by l,m,n and adding,

$$\lambda_1 + \lambda_2\left[\ell\frac{D_x}{\epsilon_x} + m\frac{D_y}{\epsilon_y} + n\frac{D_z}{\epsilon_z}\right]$$

Substituting for λ_1, and λ_2 into eq.(3.10)

$$D_x^2 = -\frac{D^2}{C}\left[\frac{D_x}{\epsilon_x} - \ell\left(\ell\frac{D_x}{\epsilon_x} + m\frac{D_y}{\epsilon_y} + n\frac{D_z}{\epsilon_z}\right)\right]$$

This is the same as eq.(3.4), if

$$\frac{n_s^2}{\mu} = \frac{D^2}{C}$$

Thus, the two directions $\underline{D}'$ and $\underline{D}''$ are the semi-axis of the ellipse, and the velocities $V_p = \frac{c}{n_s}$, are proportional to the lengths of the semi-axes.

Now an ellipsoid is constructed :

$$\frac{x^2}{\epsilon_x} + \frac{y^2}{\epsilon_y} + \frac{z^2}{\epsilon_z} = 1 \qquad (3.11)$$

which is similar to the ellipsoid (3.9), but with all its dimensions multiplied by a factor $\sqrt{\frac{c}{D^2}}$. The ellipse formed by the intersection of this ellipsoid with the plane normal to $\underline{S}$ and passing through the origin, has also semi-axes in the directions $\underline{D}'$ and $\underline{D}''$, but their magnitudes are now given by

$$r' = n'\sqrt{\mu} \qquad r'' = n''\sqrt{\mu}$$

For most materials, $\mu \sim 1$, hence the lengths of these axes are now equal to $\frac{c}{v_p'}$, $\frac{c}{v_p''}$.

Eq.(3.11) is known as the index ellipsoid, or the ellipsoid of wave-normals. If it is known, then the allowed vibration directions, and the associated phase velocities, can be found for any direction of travel in the medium.

The index ellipsoid is often written

$$\frac{x^2}{n_1^2} + \frac{y^2}{n_2^2} + \frac{z^2}{n_3^2} = 1 \qquad (3.12)$$

where n_1, n_2, n_3 are known as the principal refractive indices.

If light travels in the direction of one of the axes, it can be seen that the allowed vibration directions are in the directions of the other axes, and that the phase velocities are given by n_k , where the n_k are the appropriate principal refractive indices.

Any wave travelling through a birefringent medium will be effectively resolved into two polarization components, which will travel with different

velocities. A linearly polarised wave will, in general, become elliptically polarised, and an elliptically polarised wave will have its ellipticity changed.

There are two directions for which the intersection of the ellipsoid and the plane normal to the direction of travel of the wave, becomes a circle. This is a property of an ellipsoid. This will be shown in the next section, and an expression for these directions will be found.

These directions are known as the optic axes of the medium. A wave travelling along an optic axis will suffer no change in polarisation. In some materials, there is only one optic axis. Such media are called uni-axial. Materials with two optic axes are called bi-axial.

II. THE BEHAVIOUR OF LIGHT IN ELECTRO-OPTIC MEDIA

An electro-optic material is one whose index ellopsoid is changed by the application of an electric field. Of interest here is the first-order effect, where the ellipsoid may be represented by

$$\frac{x^2}{n_1^2} + \frac{y^2}{n_2^2} + \frac{z^2}{n_3^2} + f(x, y, z, E_x, E_y, E_z) = 1$$

where f is of the form

$$f = (E_x \; E_y \; E_z).(x^2 \; y^2 \; z^2 \; 2yz \; 2zx \; 2xy).\begin{pmatrix} r_{11} & r_{12} & r_{13} \\ r_{21} & r_{22} & r_{23} \\ r_{31} & r_{32} & r_{33} \\ r_{41} & r_{42} & r_{43} \\ r_{51} & r_{52} & r_{53} \\ r_{61} & r_{62} & r_{63} \end{pmatrix}$$

and E_x, E_y, and E_z are the components of the electric field, while the r_{ij} are constants of the medium. Many of the r_{ij} vanish, and others are equal to one another, depending on the symmetry of the crystal.

The material which is of immediate concern is Ammonium Di-hydrogen Phosphate (ADP), for which all the constants vanish except $r_{41} = r_{52}$, and r_{63}.

Hence the index ellipsoid of ADP with an electric field $\underline{E}$ applied, is

$$\frac{x^2}{n_1^2} + \frac{y^2}{n_2^2} + \frac{z^2}{n_3^2} + 2r_{41} E_x\, yz + 2r_{41} E_y\, zx + 2r_{63} E_z\, xy = 1$$

and since for ADP $n_1 = n_2$, the ellipsoid further simplifies to

$$\frac{x^2}{n_1^2} + \frac{y^2}{n_1^2} + \frac{z^2}{n_3^2} + 2r_{41} E_x\, yz + 2r_{41} E_y\, zx + 2r_{63} E_z\, xy = 1 \qquad (3.13)$$

III. THE ALLOWED VIBRATION DIRECTIONS AND ASSOCIATED VELOCITIES FOR ANY DIRECTION OF TRAVEL OF LIGHT IN ANY BIREFRINGENT MEDIUM

A complete description of the behaviour of a light wave travelling through an electro-optic medium is obtained by finding the two allowed vibration directions and the associated phase velocities for that wave direction. If the initial polarization of the wave is known, then its state after travelling a given distance through the medium can be found.

If the wave is travelling in a direction $\underline{S}$, with direction cosines l, m, n, then the allowed vibration directions and associated phase velocities are given by the directions and magnitudes of the semi-axes of the ellipse specified by the equations

$$\left.\begin{aligned} E &= 1 \\ S &= 0 \end{aligned}\right\} \qquad \begin{aligned} &(3.14)(a) \\ &(3.14)(b) \end{aligned}$$

where the first equation is the equation of the index ellipsoid, and $S = 0$ is the plane normal to $\underline{S}$ and is given by

$$S = \ell x + my + nz = 0$$

The index ellipsoid equation may be written in the form

$$Ax^2 + By^2 + Cz^2 + 2Fxy + 2Gyz + 2Hzx = 1 \tag{3.15}$$

The semi-axes of the ellipse (3.14) may be found by rotating the co-ordinate system, x, y, z to x', y', z', such that eq.(3.14(b)) becomes

$$z' = S = 0 \tag{3.16}$$

so that the equation of the ellipse is now

$$A'x'^2 + B'y'^2 = 1$$

The magnitudes of the axes are then $1/\sqrt{A'}$ and $1/\sqrt{B'}$, and their directions are the directions of the x'- and y'- axes.

This rotation may be represented by a rotation matrix, and the matrix is found in two steps as follows:

(i) The co-ordinate system (x, y, z) is first rotated to a system (x", y", z") such that z" is in the direction $\underline{S}$. The directions of x" and y" can be chosen arbitrarily, and are taken here so that the rotation is in the xz plane.

The transformation can be expressed as a matrix equation

$$\begin{pmatrix} x'' \\ y'' \\ z'' \end{pmatrix} \quad \begin{pmatrix} \frac{-m}{\sqrt{\ell^2+m^2}} & \frac{\ell}{\sqrt{\ell^2+m^2}} & 0 \\ \frac{-\ell n}{\sqrt{\ell^2+m^2}} & \frac{-mn}{\sqrt{\ell^2+m^2}} & \sqrt{\ell^2+m^2} \\ \ell & m & n \end{pmatrix} \begin{pmatrix} x \\ y \\ z \end{pmatrix}$$

Eq.(3.14(b)) becomes

$$z'' = 0 \tag{3.17}$$

and if eq.(3.14(a)) is transformed, and eq.(3.17) is substituted into it, it becomes

$$A''x''^2 + B''y''^2 + 2C''x''y'' = 1$$

where

$$\begin{aligned} A'' &= (Am^2 + B\ell^2 - 2F\ell m)/(\ell^2 + m^2) \\ B'' &= [(A\ell^2n^2 + Bm^2n^2 + 2F\ell mn^2)/(\ell^2 + m^2)] \\ &\quad - 2Gmn - 2H\ell n + C(\ell^2 + m^2) \\ C'' &= [(\ell mnA - \ell mnB - 2F(m^2n - \ell^2n))/(\ell^2 + m^2)] \\ &\quad + 2G\ell - 2Hn \end{aligned} \tag{3.18}$$

(ii) The co-ordinate system (x", y", z") can now be rotated to (x', y', z') where z' = z", and eq.(3.14) becomes

$$A'x'^2 + B'y'^2 = 1 \tag{3.19}$$

As this rotation is about the z-axis, which remains unaltered, only the rotation of x" and y" need be considered. If these are rotated through an angle θ, then the rotation matrix is of the form

$$\begin{pmatrix} x' \\ y' \end{pmatrix} = \begin{pmatrix} \sin\theta & \cos\theta \\ -\cos\theta & \sin\theta \end{pmatrix} \begin{pmatrix} x'' \\ y'' \end{pmatrix}$$

Thus, the relationship between the two co-ordinate systems may be written

$$\begin{pmatrix} x'' \\ y'' \end{pmatrix} = \begin{pmatrix} q_{11} & q_{12} \\ -q_{12} & q_{11} \end{pmatrix} \begin{pmatrix} x' \\ y' \end{pmatrix}$$

where $q_{11}^2 + q_{12}^2 = 1$ (3.20)

The values of q_{11} and q_{12} must be such that when eq.(3.19) is transformed to the system (x', y', z'), the co-efficient of the term x'y' is zero. This co-efficient is

$$C' = 2A'' q_{11} q_{12} - 2B'' q_{11} q_{12} + 2C'' (q_{11}^2 - q_{12}^2) = 0$$

This is a quadratic equation in q_{11}, (or q_{12}) so that q_{11} may be found in terms of q_{12}, giving

$$q_{11} = \frac{1}{2C''} \left[(B'' - A'') \pm \sqrt{(A'' - B'')^2 + 4C''^2} \right] q_{12}$$

The two values occur because x" and y" may be interchanged. The positive value is chosen here, so that

$$q_{11} = \frac{1}{2C''} \left[(B'' - A'') + \sqrt{(A'' - B'')^2 + 4C''^2} \right] q_{12} \qquad (3.21)$$

Substitution into eq.(3.20) gives

$$\frac{1}{4C''^2} \left[(B'' - A'') + \sqrt{(A'' - B'')^2 + 4C''^2} \right] q_{12}^2 + q_{12}^2 = 1$$

whence

$$q_{12} = \pm \frac{2C''}{\left[2(A'' - B'')^2 + 8C''^2 + 2(B'' - A'') \sqrt{(A'' - B'')^2 + 4C''^2} \right]^{1/2}}$$

The two values occur here because the positive axes can have either of two directions. Again the positive direction is chosen. By substitution into eq.(3.20), q_{11} is then obtained, and is

$$q_{11} = \frac{(B'' - A'') + \sqrt{(A'' - B'')^2 + 4C''^2}}{2(A'' - B'')^2 + 8C''^2 + 2(B'' - A'') \sqrt{(A'' - B'')^2 + 4C''^2}}$$

Finally therefore, the transformation from x,y,z to x', y', z' can be represented by the equation

$$\begin{pmatrix} x' \\ y' \\ z' \end{pmatrix} = \begin{pmatrix} q_{11} & -q_{12} & 0 \\ q_{12} & q_{11} & 0 \\ 0 & 0 & 1 \end{pmatrix} \begin{pmatrix} \frac{-m}{\sqrt{\ell^2+m^2}} & \frac{\ell}{\sqrt{\ell^2+m^2}} & 0 \\ \frac{-\ell n}{\sqrt{\ell^2+m^2}} & \frac{-mn}{\sqrt{\ell^2+m^2}} & \sqrt{\ell^2+m^2} \\ \ell & m & n \end{pmatrix} \begin{pmatrix} X \\ Y \\ Z \end{pmatrix}$$

$$= \begin{pmatrix} \frac{(-mq_{11}+\ell n q_{12})}{\sqrt{\ell^2+m^2}} & \frac{(\ell q_{11}+mnq_{12})}{\sqrt{\ell^2+m^2}} & -\sqrt{\ell^2+m^2}\, q_{12} \\ \frac{(-mq_{12}-\ell n q_{11})}{\sqrt{\ell^2+m^2}} & \frac{(\ell q_{12}-mnq_{11})}{\sqrt{\ell^2+m^2}} & \sqrt{\ell^2+m^2}\, q_{11} \\ \ell & m & n \end{pmatrix} \begin{pmatrix} X \\ Y \\ Z \end{pmatrix} \quad (3.22)$$

This equation may be written

$$\begin{pmatrix} x' \\ y' \\ z' \end{pmatrix} = \begin{pmatrix} \ell_x & m_x & n_x \\ \ell_y & m_y & n_y \\ \ell_z & m_z & n_z \end{pmatrix} \begin{pmatrix} X \\ Y \\ Z \end{pmatrix}$$

where (l_x, m_x, n_x), (l_y, m_y, n_y) and (l_z, m_z, n_z) are the direction cosines of the x'-, y'-, and z'-axes respectively.

The equation of the ellipse (3.14) becomes

$$x'^2[A\ell_x^2 + Bm_x^2 + Cn_x^2 + 2F\ell_x m_x + 2Gm_x n_x + 2Hn_x\ell_x]$$

$$+ y'^2[A\ell_y^2 + Bm_y^2 + Cn_y^2 + 2F\ell_y m_y + 2Gm_y n_y + 2Hn_y\ell_y] = 1$$

Thus, the allowed vibration directions which we may denote by $\underline{X}$

and $\underline{Y}$, are in the directions of the x- and y-axes, and the phase velocities V_x and V_y (say) of waves polarised in these directions are given by

$$V_x^2 = c^2[A\ell_x^2 + Bm_x^2 + Cn_x^2 + 2F\ell_x m_x + 2G m_x n_x + 2H n_x \ell_x]$$

$$V_y^2 = c^2[A\ell_y^2 + Bm_y^2 + Cn_y^2 + 2F\ell_y m_y + 2G m_y n_y + 2H n_y \ell_y]$$

where c is the velocity of light in vacuum.

IV. THE DIRECTIONS OF THE OPTIC AXES IN A BIREFRINGENT MEDIUM

It was previously stated that there are two directions of travel in the crystal for which the ellipse of eq.(3.14) is a circle. This happens when

$$A'' = B''$$

and

$$C'' = 0$$

These two equations in l, m, n and the equation

$$\ell^2 + m^2 + n^2 = 1$$

are three second-order equations, having two solutions. The solutions will, in general, be complicated, but it is interesting to consider the case where F=G=H=0, i.e. where the co-ordinate system has axes in the directions of the principal axes. Eq.(3.16) gives

$$\frac{Am^2 + B\ell^2}{\ell^2 + m^2} \qquad \frac{A\ell^2 n^2 + Bm^2 n^2}{\ell^2 + m^2} + C(\ell^2 + m^2) \tag{3.23}$$

$$\ell m n (A - B) = 0 \tag{3.24}$$

From eq.(3.24) it is seen that either l, m, or n must be zero. Taking the case where n = 0, it is found that

$$\ell = \pm \sqrt{\frac{C-A}{B-A}} \qquad m = \pm \sqrt{\frac{B-A}{C-A}}$$

These will be real only if either

$$B > C > A \qquad \text{or} \qquad A > C > B$$

Similar solutions are obtained by putting l = 0 and m = 0. Only one of these sets of solutions will give real values for the direction cosines of the optic axes. The real solution depends on the values of A, B and C.

The optic axes, then, lie in the plane of the principal axes of greatest and least principal indices, and the angles, ϕ_{max} and ϕ_{min}, made with these axes are given by

$$\cos \phi_{MAX} = \left[\frac{\frac{1}{n^2_{MAX}} - \frac{1}{n^2_{INT}}}{\frac{1}{n^2_{MAX}} - \frac{1}{n^2_{MIN}}} \right]^{1/2} \qquad (3.25)$$

$$\cos \phi_{MIN} = \left[\frac{\frac{1}{n^2_{INT}} - \frac{1}{n^2_{MIN}}}{\frac{1}{n^2_{MAX}} - \frac{1}{n^2_{MIN}}} \right]^{1/2}$$

and

$$\sin \phi_{MAX} = \cos \phi_{MIN}$$

where n_{max}, n_{int}, n_{min} are the principal refractive indices, n_{max} being the greatest, n_{min} being the least, and n_{int} being the intermediate.

It can be shown that if two of the principal refractive indices are equal there is only one optic axis, and it is in the direction of the

remaining principal axis. If, for example, A=B, then eq.(3.23) becomes

$$(1-n^2)A + (1-n^2)C = 0$$

which is satisfied only if $n^2 = 1$, unless A=C. Thus, the optic axis is in the z-direction.

When A=B=C, the medium is isotropic. The ellipsoid becomes a sphere and the intersection of any plane with it is a circle. All waves have the same phase velocity.

V. THE RATIO OF THE TRANSMITTED TO INCIDENT AMPLITUDE OF A WAVE WHICH HAS TRAVELLED THROUGH A POLARISER, BIREFRINGENT MEDIUM, AND ANALYSER

If a crystal is used which has parallel faces separated by h, the normal $\underline{N}$ to the faces having direction $\underline{S}$, with direction cosines α, β, γ is then the distance travelled by a wave in the direction $\underline{S}$, with direction cosines l, m, and n, is

$$d = l / \cos\psi$$

where ψ is the angle between $\underline{S}$ and $\underline{N}$, and is given by

$$\cos\psi = l\alpha + m\beta + n\gamma$$

If the light is polarised by a polariser whose direction is given by a unit vector $\underline{P}_o$, then the polarization $\underline{P}_s$ of a wave travelling in the direction $\underline{S}$ is given by the projection of $\underline{P}_o$ onto a plane normal to $\underline{S}$, and is

$$\underline{P}_s = \frac{1}{N}[\underline{P}_o - (\underline{P}_o \cdot \underline{S})\underline{S}] \qquad (3.26)$$

where N is a normalisation co-efficient, introduced so that $\underline{P}_s$ is a unit vector.

The light travelling through the crystal in the direction $\underline{S}$, and

polarised in the direction $\underline{P}_s$, is resolved into components in the $\underline{X}$ and $\underline{Y}$ directions, which are

$$(\underline{P}_s)_x = (\underline{P}_s \cdot \underline{X}) \frac{1}{N_x} \qquad (\underline{P}_s)_y = (\underline{P}_s \cdot \underline{Y}) \frac{1}{N_y}$$

where N_x and N_y are normalization co-efficients.

The two components travel with velocities V_x and V_y, and their phases after travelling through the crystal are given by

$$\delta_x = \frac{\omega d}{V_x} \qquad \delta_y = \frac{\omega d}{V_y}$$

where ω is the angular frequency of the light.

It should be noted that when the two components emerge from the crystal they will travel in different directions, because they have different refractive indices. However, in all the cases to be considered here, the difference between the two refractive indices is much less than the values of the refractive indices, i.e.

$$\left| \frac{c}{V_x} - \frac{c}{V_y} \right| \ll \frac{c}{V_x}, \frac{c}{V_y} \qquad (3.27)$$

so that the difference in the directions in which the emergent beams travel will be neglected.

If a second polarizer is placed after the crystal, with polarization direction $\underline{Q}_0$, then the two components are resolved along a direction $\underline{Q}_s$, given by

$$\underline{Q}_s = \frac{1}{N_Q} (\underline{Q}_0 - \underline{Q}_0 \cdot \underline{S}) \qquad (3.28)$$

where N_Q is a normalization co-efficient. The resolution of the components in the $\underline{X}$ and $\underline{Y}$ directions gives

$$(\underline{X})_Q = (\underline{P}_s \cdot \underline{X})(\underline{X} \cdot \underline{Q}_s)$$

$$(\underline{Y})_Q = (\underline{P}_s \cdot \underline{Y})(\underline{Y} \cdot \underline{Q}_s)$$

If the incident amplitude is given by

$$A_I = A_o \sin \omega t$$

then the transmitted amplitude is given by

$$A_T = A_o (\underline{P}_s \cdot \underline{X})(\underline{X} \cdot \underline{Q}_s) \sin(\omega t + \delta_x) + A_o (\underline{P}_s \cdot \underline{Y})(\underline{Y} \cdot \underline{Q}_s) \sin(\omega t + \delta_y) \quad (3.29)$$

Evaluation of eq.(3.26) gives the amplitude and phase of the light transmitted by any electro-optic crystal where only first-order effects are important, for any direction of travel in the crystal, any applied electric field, and any polariser and analyser directions, subject to the approximation in eq.(3.25)

VI. THE INTERFERENCE PRODUCED BY TWO LIGHT BEAMS TRAVELLING THROUGH A Z-CUT CRYSTAL AT PARTICULAR ORIENTATIONS, AND WITH AN ALTERNATING ELECTRIC FIELD APPLIED TO THE CRYSTAL IN THE Z-DIRECTION.

The case to be considered here is that of an ADP crystal with faces cut perpendicular to the z-axis, and with an electric field applied in the z-direction. From eq.(3.13) it is seen that the index ellipsoid in this case is given by

$$\frac{x^2}{n_1^2} + \frac{y^2}{n_1^2} + \frac{z^2}{n_3^2} + 2 r_{63} E_z xy = 1 \quad (3.30)$$

If such a crystal is placed between crossed polarisers, a light wave travelling along the z-axis will not be transmitted by the second polariser, as in this case, the optic axis is in the z-direction. When E_z is not zero, however, the crystal becomes bi-axial. The principal axes of the ellipsoid are now in the directions x', y' and z' where z' = z, and x' and y' are at 45° to x and y. This can be seen by substituting

$$x = \frac{1}{\sqrt{2}}(x' + y') \qquad (3.31)$$

$$y = \frac{1}{\sqrt{2}}(-x' + y')$$

$$z = z'$$

into eq.(3.26), giving

$$x'^2\left(\frac{1}{n_1^2} + r_{63}E_z\right) + y'^2\left(\frac{1}{n_1^2} - r_{63}E_z\right) + \frac{z'^2}{n_3^2} = 1$$

In ADP, $n_1 = 1.53$, and $n_3 = 1.48$ ( ). Hence when $r_{63}E_z$ is positive

$$\frac{1}{n_3^2} > \frac{1}{n_1^2}(1 - r_{63}E_z) > \frac{1}{n_1^2}(1 + r_{63}E_z)$$

so the optic axes lie in the y'z' plane, and make angles ϕ with the z-axis given by (from eq.(3.24)),

$$\sin\phi = \sqrt{\frac{2n_3^2 r_{63}E_z}{n_1^2 - n_3^2}}$$

When $r_{63}E_z$ is negative

$$\frac{1}{n_3^2} > \frac{1}{n_1^2}(1 + r_{63}E_z) > \frac{1}{n_1^2}(1 - r_{63}E_z)$$

so the optic axes are in the x'z' plane, and make the same angle ϕ, with the z-axis.

If an alternating electric field, $E_z \sin\omega_4 t$, is applied to the

crystal in the z-direction, and two waves are passed through the crystal, one in the yz plane, and the other in the xz plane, and each making an angle ϕ with the z-axis where

$$\sin\phi = \sqrt{\frac{2n_3^2 r_{63} E_z}{n_1^2 - n_3^2}}$$

then when $\sin\omega_m t = 1$ the first wave will not be transmitted, while some of the second will, and when $\sin\omega_m t = -1$ some of the first wave will be transmitted while some of the second will not. This suggests a method of amplitude-modulating two beams in anti-phase. It is, therefore useful to find the time variation of the amplitudes of the two waves.

The ellipsoid equation may be written

$$A(1+\Delta)x^2 + A(1-\Delta)y^2 + Cz^2 = 1$$

where $\Delta = r_{63}E_z$, $A = 1/n_1^2$, and $C = 1/n_3^2$.

The direction cosines of the two beams are

$$\ell_1 = \beta \qquad m_1 = 0 \qquad n_1 = \sqrt{1-\beta^2} = \alpha$$

$$\ell_2 = 0 \qquad m_2 = \beta \qquad n_2 = \sqrt{1-\beta^2} = \alpha$$

The ellipsoid can be transformed, using the transformation matrix (3.22). It is seen that C" is zero for both beams, because either l or m is zero. The matrices become

$$\begin{pmatrix} 0 & 1 & 0 \\ -\alpha & 0 & \beta \\ \beta & 0 & \alpha \end{pmatrix} \quad \text{and} \quad \begin{pmatrix} -1 & 0 & 0 \\ 0 & -\alpha & \beta \\ 0 & \beta & \alpha \end{pmatrix}$$

Let the directions of the two polarisers be $\underline{P}$ and $\underline{Q}$, given by

$$\underline{P} = \frac{1}{\sqrt{2}}(\underline{i} + \underline{j}) \qquad \underline{Q} = \frac{1}{\sqrt{2}}(\underline{i} - \underline{j})$$

where $\underline{i} = \underline{j}$ are unit vectors in the x and y directions.

It will be seen later that for practical values of the electric field, $\beta \ll 1$, hence

$$(\underline{P}_{s_1} \cdot \underline{X}_1)(\underline{X}_1 \cdot \underline{Q}_{s_1}) = -\frac{1}{2(\alpha^2+1)} \simeq \frac{1}{4}$$

$$(\underline{P}_{s_1} \cdot \underline{Y}_1)(\underline{Y}_1 \cdot \underline{Q}_{s_1}) = \frac{\alpha^2}{2(\alpha^2+1)} \simeq \frac{1}{4}$$

$$(\underline{P}_{s_2} \cdot \underline{X}_2)(\underline{X}_2 \cdot \underline{Q}_{s_2}) = \frac{1}{2(\alpha^2+1)} \simeq \frac{1}{4}$$

$$(\underline{P}_{s_2} \cdot \underline{Y}_2)(\underline{Y}_2 \cdot \underline{Q}_{s_2}) = -\frac{1}{2(\alpha^2+1)} \simeq \frac{1}{4}$$

where $\underline{X}_1\underline{Y}_1$ and $\underline{X}_2\underline{Y}_2$ are the allowed vibration directions for the two waves, and $\underline{P}_{s_1}\underline{Q}_{s_1}$ and $\underline{P}_{s_2}\underline{Q}_{s_2}$ are their initial and final polarization directions.

The phase velocities associated with these polarization directions are given by

$$V_{x_1}^2 = A(1-\Delta) \qquad V_{y_1}^2 = An^2(1+\Delta) + C\ell^2$$

$$V_{x_2}^2 = A(1+\Delta) \qquad V_{y_2}^2 = An^2(1-\Delta) + C\ell^2$$

The transmitted amplitudes are then found from eq.(3.26), and are

$$A_{T_1} = \frac{A_0}{2} \sin\left(\frac{\delta x_1 - \delta y_1}{2}\right) \cdot \cos\left(\omega t + \frac{\delta x_1 + \delta y_1}{2}\right)$$

$$A_{T_2} = \frac{A_0}{2} \sin\left(\frac{\delta x_2 - \delta y_2}{2}\right) \cdot \cos\left(\omega t + \frac{\delta x_2 + \delta y_2}{2}\right)$$

where δ_{x1}, δ_{y1}, δ_{x2}, δ_{y2} are given by

$$\delta_{x_1} = \frac{\omega d}{v_{x_1}} \qquad \delta_{y_1} = \frac{\omega d}{v_{y_1}}$$

$$\delta_{x_2} = \frac{\omega d}{v_{x_2}} \qquad \delta_{y_2} = \frac{\omega d}{v_{y_2}}$$

and the amplitude of the incident wave is $A_o \sin\omega t$

Because $\Delta \ll 1$, the quantities $\frac{1}{v_{x_1}}$, $\frac{1}{v_{y_1}}$, $\frac{1}{v_{x_2}}$, $\frac{1}{v_{y_2}}$ may be expressed as

$$\frac{1}{v_{x_1}} = \frac{1}{\sqrt{A}}\left(1 + \tfrac{1}{2}\Delta\right) \qquad \frac{1}{v_{y_1}} = \frac{1}{\sqrt{A}}\left[1 - \tfrac{1}{2}\left(\tfrac{C}{A}\beta^2 \beta^2 + \Delta - \beta^2\Delta\right)\right]$$

$$\frac{1}{v_{x_2}} = \frac{1}{\sqrt{A}}\left(1 - \tfrac{1}{2}\Delta\right) \qquad \frac{1}{v_{y_2}} = \frac{1}{\sqrt{A}}\left[1 - \tfrac{1}{2}\left(\tfrac{C}{A}\beta^2 - \beta^2 - \Delta + \beta^2\Delta\right)\right]$$

Thus the phase differences $(\delta_{x1} - \delta_{y1})$ and $(\delta_{x_2} - \delta_{y_2})$ are

$$\delta_{x_1} - \delta_{y_1} = \frac{\omega d}{\sqrt{A}}\left[\Delta + \tfrac{1}{2}\beta^2\frac{(C-A)}{A}\right] \qquad \delta_{x_2} - \delta_{y_2} = -\frac{\omega d}{\sqrt{A}}\left[\Delta - \tfrac{1}{2}\beta^2\frac{(C-A)}{A}\right]$$

if $\beta^2\Delta$ is neglected.

From eq.(3.24), it is seen that

$$\beta^2 = \frac{2 n_3^2 r_{63} E_z}{n_1^2 - n_3^2}$$

so that

$$\tfrac{1}{2}\beta^2\frac{(C-A)}{A} = r_{63} E_z = \Delta_o$$

The quantities $\frac{\delta_{x_1} + \delta_{y1}}{2}$ and $\frac{\delta_{x_2} + \delta_{y_2}}{2}$ become

$$\frac{\delta_{x_1} + \delta_{y_1}}{2} \simeq \frac{\omega d}{\alpha\sqrt{A}} = \delta$$

$$\frac{\delta_{x_2} + \delta_{y_2}}{2} \simeq \frac{\omega d}{\alpha\sqrt{A}} = \delta$$

Thus the transmitted amplitudes are, if $\frac{\omega d}{\alpha\sqrt{A}}\Delta_o \ll 1$

$$A_{T_1} = A_o \sin\left[\frac{\omega d}{\alpha\sqrt{A}}\Delta_o(\sin(\omega_m t) + 1)\right]\cos(\omega t + \delta)$$

$$\simeq A_o \frac{\omega d}{\alpha\sqrt{A}}\Delta_o\left[\sin(\omega_m t) + 1\right]\cos(\omega t + \delta)$$

$$A_{T_2} = A_0 \sin\left[\frac{\omega d}{2\sqrt{A}} \Delta_0 \left(\sin(\omega_M t) - 1\right)\right] \cos(\omega t + \delta)$$

$$\simeq A_0 \frac{\omega d}{2\sqrt{A}} \Delta_0 \left[\sin(\omega_M t) - 1\right] \cos(\omega t + \delta)$$

The amplitudes may be expressed as

$$A_{T_1} = A(1 + \sin\omega_M t)\cos(\omega t + \delta) = G_1(t).\ A\cos(\omega t + \delta)$$

$$A_{T_2} = -A(1 - \sin\omega_M t)\cos(\omega t + \delta) = G_2(t).\ A\cos(\omega t + \delta)$$

The transmitted intensities are

$$I_1(t) = A^2(1 + \sin\omega_M t)^2 \cos^2(\omega t + \delta)$$

$$I_2(t) = A^2(1 - \sin\omega_M t)^2 \cos^2(\omega t + \delta)$$

If $\omega \gg \omega_M$, then these intensities may be averaged over ω, and they become

$$I_1(t) = \frac{A^2}{2}(1 + \sin\omega_M t)^2$$

$$I_2(t) = \frac{A^2}{2}(1 - \sin\omega_M t)^2$$

These quantities can be thought of as being the transmission functions of shutters which are placed in the two beams. They are shown in Fig.3.1, where it is seen that the situation is fairly close to the ideal case, as the overlap between the two shutters is quite small.

Finally, the quantity $M_{12}(\tau)$, can be evaluated for this case, and is

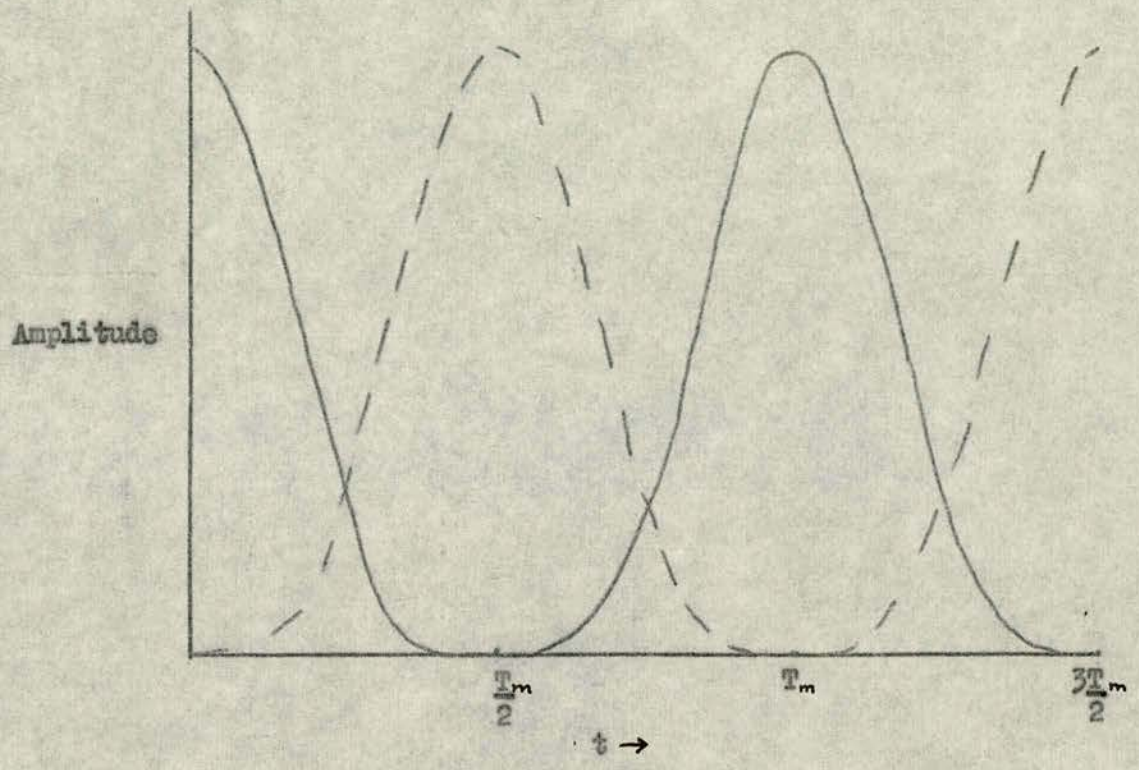
Amplitude
$\frac{T_m}{2}$
T_m
$\frac{3T_m}{2}$
t →

FIG.3.1

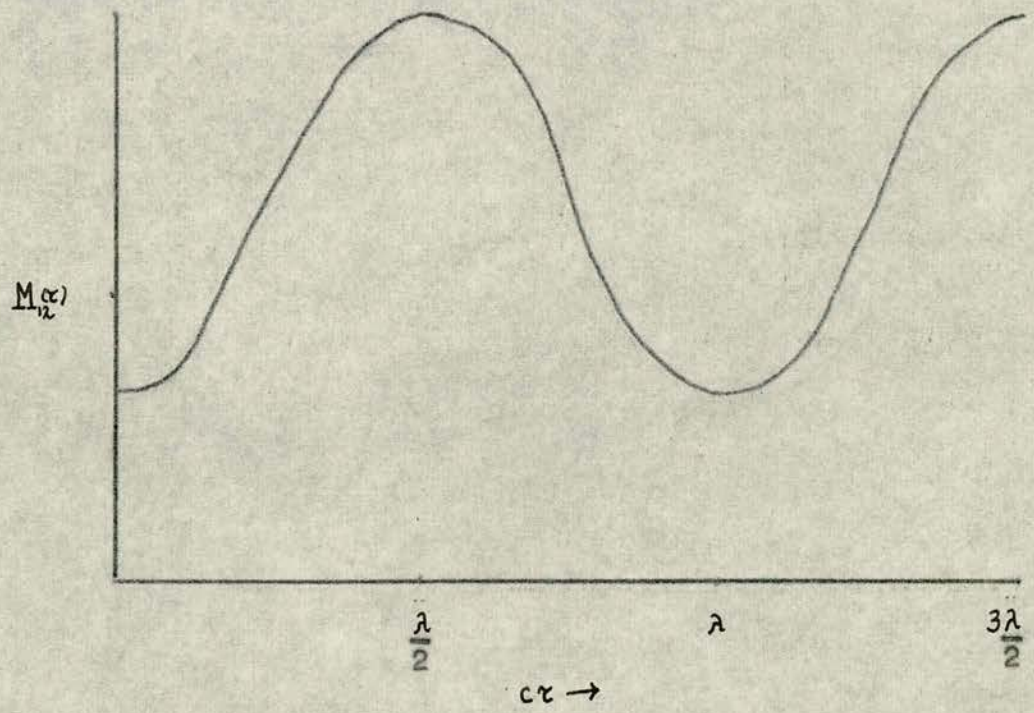
$M_{\lambda}^{(\alpha)}$
$\frac{\lambda}{2}$
λ
$\frac{3\lambda}{2}$
cτ →

FIG.3.2

$$M_{12}(\tau) = \frac{\langle G_1(t)\, G_2^*(t+\tau)\rangle}{\langle G_1^2(t)\rangle}$$

$$= \frac{2}{3}\left[1 - \frac{1}{2}\cos(\omega_M \tau)\right]$$

This is shown in Fig.(3.2).

If the two beams are superimposed, the interference fringes produced will vary in visibility as the path difference between the beams is varied, the variation being the same as the variation of $M_{12}(\tau)$. The value at $c\tau = 0$ is .33.

Thus, if two beams are passed through an ADP crystal as specified in this section, it should be possible to observe the required effect.

VI. THE INTERFERENCE PRODUCED BY TWO LIGHT BEAMS TRAVELLING THROUGH THE ADP CRYSTAL WITH APPLIED ELECTRIC FIELD

In the last section, the behaviour of two light beams travelling through the crystal in two particular directions was examined, and an expression obtained for the visibility of the interference fringes produced by the superposition of two such beams.

It is of interest to examine what happens when the beams are not travelling exactly in these directions. For reasons which will be clear when the experimental set-up is described, it is particularly interesting to examine what happens when the angles between the two beams and the x- (or y-) axis are equal, but the angles made by them with the y- (or x-) axis are varied.

A computer program has been written which evaluates $M_{12}(o)$ for two beams travelling in various directions. (Appendix I).

The quantities

$$(\underline{P}_s \cdot \underline{X})(\underline{X} \cdot \underline{Q}_s), \quad (\underline{P}_s \cdot \underline{Y})(\underline{Y} \cdot \underline{Q}_s), \quad \delta_x, \quad \delta_Y$$

are evaluated for given values of l, m, n, r, E_z, P_o, Q_o.

These quantities vary in time if the electric field E_z is time-varying. The transmitted amplitude for a given electric field strength can be written

$$A_{T_1} = A_o\, G_1'(t).\, Sin\,(\omega t + \delta x_1(t)) + A_o G_1''(t).\, Sin\,(\omega t + \delta y_1(t))$$

The transmitted amplitude of a second beam can be written

$$A_{T_2} = A_o G_2'(t).\, Sin\,(\omega t + \delta x_2(t)) + A_o G_2''(t)\, Sin\,(\omega t + \delta y_2(t))$$

If these two beams are superimposed with a path difference $c\tau$ between them, the total amplitude is

$$A_T = A_{T_1} + A_{T_2}$$

and the intensity is $I = A_T^2$

The intensity can be averaged over the optical period $\frac{2\pi}{\omega}$, for during this time $G_1(t)$ and $G_2(t)$ can be considered to be constant because the modulation frequency is much less than the light frequency. This gives

$$I_{AV} = \frac{A_o^2}{2}\Big[G_1'^2(t) + G_2'^2(t+\tau) + G_1''^2(r) + G_2''^2(t+\tau)$$

$$+ 2\, G_1'(t) G_1''(t) \cos(\delta y_1 - \delta x_1) + 2\, G_2'(t+\tau) G_2''(r+\tau) \cos(\delta y_2 - \delta x_2)$$

$$+ 2\, G_1'(t) G_2'(r+\tau) \cos(\omega\tau + \delta x_1 - \delta x_2) + 2\, G_1'(r)\, G_2''(r+\tau) \cos(\omega\tau + \delta x_1 - \delta y_2)$$

$$+ 2\, G_1''(r) G_2'(r+\tau) \cos(\omega\tau + \delta y_1 - \delta x_2) + 2\, G_1''(r)\, G_2''(r+\tau) \cos(\omega\tau + \delta y_1 - \delta x_2) \quad (3.32)$$

This can be then averaged over the modulation period, to give the intensity which is to be observed at a given path difference. Interference fringes are observed, with the seperation between maxima being given by

$$\Delta d = c(\tau_2 - \tau_1) = \frac{2\pi c}{\omega}$$

The visibility of the fringes around $\tau = 0$ is

$$V_{\tau=0} = \frac{2\langle G_1(t)\, G_2(t)\rangle}{\langle G_1^2(t) + G_2^2(t)\rangle}$$

where $\langle G_1(t)\, G_2(t)\rangle \equiv \langle G_1'(t)\, G_2'(t)\cos(\delta x_1 - \delta x_2) + G_1'(t)\, G_2''(t)\cos(\delta x_1 - \delta y_2)$

$$+ G_1''(r)\, G_2'(t)\cos(\delta y_1 - \delta x_2) + G_1''(r)\, G_2''(r)\cos(\delta y_1 - \delta y_2)\rangle$$

and $\langle G_1^2(t) + G_2^2(r)\rangle \equiv \langle G_1'^2(r) + G_1''^2(r) + G_2'^2(r) + G_2''^2(r)$

$$+ 2G_1'(r)\, G_1''(r)\cos(\delta y_1 - \delta x_1) + 2G_2'(r)\, G_2''(r)\cos(\delta x_2 - \delta y_2)\rangle$$

Each of these quantities is evaluated in the program by evaluating the unaveraged quantities for nineteen different values of $E_z \sin\omega t$ between $+E_z$ and $-E_z$, and then adding those values.

In this way, a value for $M_{12}(o)$ can be found for different wave directions.

VII. AN APPROXIMATE EXPRESSION FOR THE TRANSMITTED TO INCIDENT AMPLITUDE OF A LIGHT WAVE TRAVELLING THROUGH A BIREFRINGENT MEDIUM

An approximate expression for the ratio of transmitted to incident amplitude of a wave travelling through a birefringent medium can be found in terms of the angle made by the optic axes and by the wave, with

the crystal.

From eq.(3.29) it is seen that the transmitted amplitude depends on the angle between the polariser and also the analyser, and the allowed vibration directions, and on the phase velocities of the two components. It is necessary to find approximate expressions for each of these quantities.

(i) An expression for the allowed vibration directions is found as follows.

The allowed vibrations are denoted by $\underline{N}_1$ and $\underline{N}_2$, the wave direction by $\underline{S}$, and the optic axes by $\underline{O}_1$ and $\underline{O}_2$. The ellipse E, formed by the intersection of the plane normal to $\underline{S}$ with the index ellipsoid intersects the circles which are the intersections of $\underline{O}_1$ and $\underline{O}_2$ with the index ellipsoid, in directions which are denoted $\underline{R}_1$ and $\underline{R}_2$. The lengths of the radii $\underline{R}_1$ and $\underline{R}_2$ are equal, as can be seen from eq.(3.18), since the direction cosines of the optic axes are always of the form (1,0,n) (-1,0,n) or (0,m,n) (0,-m,n) etc. It can be shown that the semi-axes of an ellipse are the internal and external bisectors of the angle between any two radii of equal length. Hence $\underline{N}_1$ and $\underline{N}_2$ are the bisectors of the angle between $\underline{R}_1$ and $\underline{R}_2$. $\underline{R}_1$ is perpendicular to $\underline{S}$ and $\underline{O}_1$ so that it is normal to the plane containing $\underline{S}$, and $\underline{O}_1$. Similarly $\underline{R}_2$ is normal to the plane containing $\underline{S}$ and $\underline{O}_2$. The planes (S,O_1) and (S,O_2) intersect the ellipse E, in radii $\underline{R}_1'$ and $\underline{R}_2'$ which are perpendicular to $\underline{R}_1$ and $\underline{R}_2$, as shown in Fig.(3.3). $\underline{N}_1$ and $\underline{N}_2$ are normal to $\underline{S}$, so that the planes $(\underline{N}_1, S)$ and $(\underline{N}_2, S)$ bisect internally and externally the angles between the planes (S,O_1) and (S,O_2).

The principal axes of the crystal are labelled x', y', z'*, with

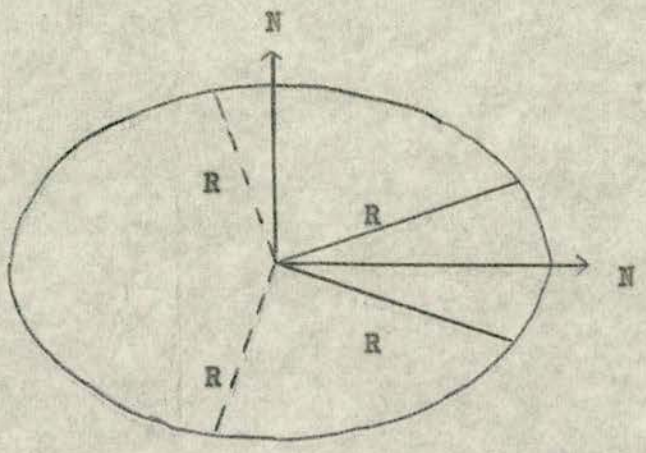

Fig.3.3

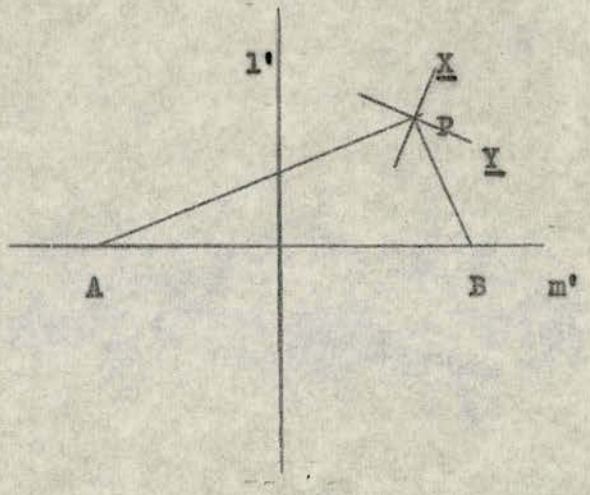

Fig.3.4

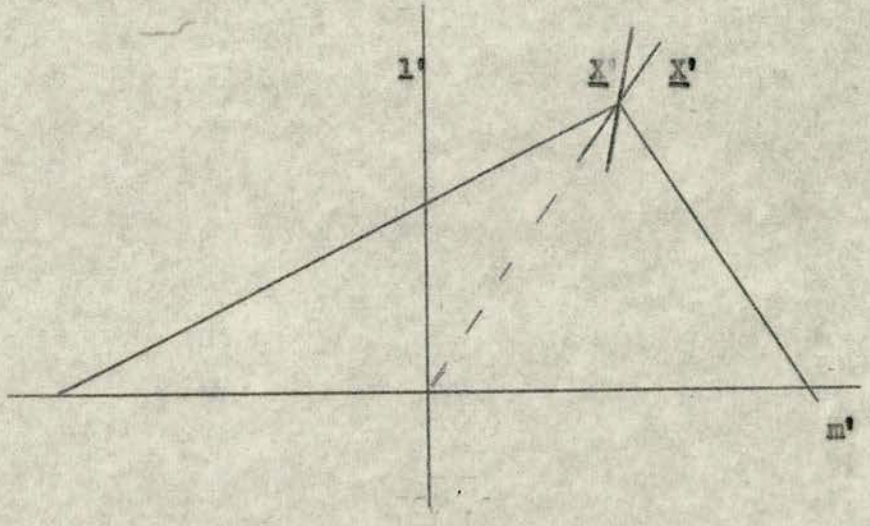

Fig.3.5

the optic axes being coplanar with the z-axis, and the wave direction S having direction cosines l', m', n', and the angle between the optic axes, and the z-axis being β. The wave directions and the optic axes can be represented in two dimensions as in Fig.(3.4), where a direction is represented by its direction cosines l' and m'. The projections of the allowed vibration directions on the xy plane can also be represented as follows.

The intersections of the planes $(\underline{S},\underline{O}_1)$ and $(\underline{S},\underline{O}_2)$ with the x'y' plane are given by the lines AP and BP. The planes $(\underline{N}_1,\underline{S})$ and $(\underline{N}_2,\underline{S})$ then intersect the xy plane in the lines $\underline{X}$ and $\underline{Y}$, which are the projections of $\underline{N}_1$ and $\underline{N}_2$ on the x'y' plane. When l',m', and $\beta \ll 1$, the allowed vibration directions $\underline{N}_1$ and $\underline{N}_2$, which are perpendicular to $\underline{S}$, are almost normal to the z-axis, and hence their projections on the x'y' plane may be used instead of their true directions.

It is required then to find the direction cosines of the lines $\underline{D}_1$ and $\underline{D}_2$.

The slopes of the lines AP and BP with respect to the l'-axis are

$$m_1 = \frac{l'}{m' - \beta} \qquad m_2 = \frac{l'}{m' + \beta} \tag{3.33}$$

In Appendix II, it is shown that the slopes of the bisectors of

* Note: The axes are denoted by x', y', z' rather than x, y, z, because when the case of ADP is discussed, the axes are the principal axes of the ellipsoid, and not the crystal axes as specified in eq.(3.13), and as used in section VI.

these two angles are

$$M_+ = \frac{-1 + m_1 m_2 - \sqrt{(1+m_1^2)(1+m_2^2)}}{m_1 + m_2}$$

$$M_- = \frac{-1 + m_1 m_2 + \sqrt{(1+m_1^2)(1+m_2^2)}}{m_1 + m_2}$$

where $\underline{X}$ has slope M_+, and $\underline{Y}$ has slope M_-.

Substitution from eq.(3.33) gives

$$M_+ = \frac{(m'^2 + \ell'^2 + \beta^2) - \sqrt{(\ell'^2 + m'^2 + \beta^2)^2 - 4m'^2\beta^2}}{2\ell' m'}$$

$$= \frac{(\beta^2 - m'^2 + \ell'^2) - \sqrt{(\beta^2 - m'^2 + \ell'^2)^2 + 4\ell'^2 m'^2}}{2\ell' m'}$$

$$M_- = \frac{(m'^2 + \ell'^2 + \beta^2) + \sqrt{(\ell'^2 + m'^2 + \beta^2)^2 - 4m'^2\beta^2}}{2\ell' m'}$$

$$= \frac{(\beta^2 - m'^2 + \ell'^2) + \sqrt{(\beta^2 - m'^2 + \ell'^2)^2 + 4\ell'^2 m'^2}}{2\ell' m'}$$

The direction cosines (l_x, m_x) and (l_y, m_y) of the vibration directions are found from the slopes as follows.

If $M_+ = \tan\theta$

then

$$\frac{M_+}{\sqrt{1+M_+^2}} = \sin\theta = \ell_x \qquad \frac{1}{\sqrt{1+M_+^2}} = \cos\theta = m_x \tag{3.34}$$

It is necessary to evaluate the quantities $(\underline{P}_s \cdot \underline{X})$ etc. in eq.(3.29) In the case of interest, the polariser and analyser directions $\underline{P}_o$ and $\underline{Q}_o$, are given by

$$P_o = \frac{1}{\sqrt{2}}(\underline{i}' + \underline{j}') \qquad Q_o = \frac{1}{\sqrt{2}}(\underline{i}' - \underline{j}')$$

where $\underline{i}'$ and $\underline{j}'$ are unit vectors in the x' and y' directions.

When l' and m' are small, it can be shown from eq.(3.26) and (3.28)

$$\underline{P}_s \simeq \underline{P}_o \quad , \quad \underline{Q}_s \simeq \underline{Q}_o$$

In this case

$$\underline{P}_s \cdot \underline{X} = \frac{1}{\sqrt{2}}(\ell_x + m_x) \qquad \underline{P}_s \cdot \underline{Y} = \frac{1}{\sqrt{2}}(\ell_y + m_y)$$

$$\underline{Q}_s \cdot \underline{X} = \frac{1}{\sqrt{2}}(\ell_x - m_x) \qquad \underline{P}_s \cdot \underline{Y} = \frac{1}{\sqrt{2}}(\ell_y - m_y)$$

Hence

$$(\underline{P}_s \cdot \underline{X})(\underline{X} \cdot \underline{Q}_s) = \frac{1}{2}(\ell_x^2 - m_x^2)$$

$$(\underline{P}_s \cdot \underline{Y})(\underline{Y} \cdot \underline{Q}_s) = \frac{1}{2}(\ell_y^2 - m_y^2)$$

Because the bisectors are orthogonal, it is seen that

$$\ell_x = m_y, \qquad m_x = \ell_y$$

Eq.(3.22) then becomes

$$\frac{A_T}{A_o} = (\ell_x^2 - m_x^2).\sin\left(\frac{\delta y - \delta x}{2}\right).\cos\left(\omega t + \frac{\delta y + \delta x}{2}\right) \qquad (3.35)$$

$(l_x^2 - m_x^2)$ can be found from eq.(3.34), Putting

$$P = (\beta^2 - m'^2 + \ell'^2) \qquad Q = 2\ell' m'$$

then

$$\ell_x = \frac{P - \sqrt{P^2+Q^2}}{[2(P^2+Q^2 - P\sqrt{P^2+Q^2})]^{1/2}}$$

$$m_x = \frac{Q}{[2(P^2+Q^2 - P\sqrt{P^2+Q^2})]^{1/2}}$$

$$\therefore \ \ell_x^2 - m_x^2 = \frac{2P^2 + Q^2 - 2P\sqrt{P^2+Q^2} - Q^2}{2[P^2+Q^2 - P\sqrt{P^2+Q^2}]}$$

$$= \frac{P^2 - P\sqrt{P^2+Q^2}}{(P^2+Q^2)^2 - P\sqrt{P^2+Q^2}}$$

Multiplying this on top and the bottom by $(P^2+Q^2+P\sqrt{P^2+Q^2})$ it becomes

$$\ell_x^2 - m_x^2 = \frac{[P^3 - P(P^2+Q^2)]\sqrt{P^2+Q^2}}{(P^2+Q^2) - P^2(P^2+Q^2)}$$

which reduces to

$$\ell_x^2 - m_x^2 = \frac{-P}{\sqrt{P^2+Q^2}} = \frac{\ell'^2 - m'^2 - \beta^2}{[(\beta^2 - m'^2 + \ell'^2)^2 + 4m'^2\ell'^2]^{1/2}} \qquad (3.36)$$

(ii) Approximate expressions for the associated phase velocities are found as follows.

Eq.(3.7) may be written

$$\ell'^2(v_p^2 - B)(v_p^2 - C) + m'^2(v_p^2 - A)(v_p^2 - C) + n'^2(v_p^2 - A)(v_p^2 - B) = 0$$

where A, B, C are the inverse squares of the principal indices, and l', m', n' are the direction cosines of the wave direction, and v_p is one of the phase velocities. This is a quadratic equation in v_p^2 and has solutions

$$v_p^2 = \frac{1}{2}[\ell'^2(B+C) + m'^2(A+C) + n'^2(A+B)]$$
$$\pm \frac{1}{2}[\{\ell'^2(B+C) + m'^2(A+C) + n'^2(A+B)\} - 4(\ell'^2BC + m'^2AC + n'^2AB)]^{1/2}$$

This can be re-arranged, with some tedious algebra, into the form

$$v_p^2 = \frac{1}{2}[(A+C) + (A-C)\cos(\theta_1 \pm \theta_2)] \qquad (3.37)$$

where θ_1 and θ_2 are the angles between the wave direction S and the optic axes of the crystal, and are given by

$$\cos\theta_1 = m' \sin\psi + n' \cos\psi$$

$$\cos\theta_2 = -m' \sin\psi + n' \cos\psi$$

where ψ is the angle between the optic axes and the z-axis, and where the optic axes lie in the xz plane, ψ is given by

$$\sin\psi = \sqrt{\frac{B-A}{C-A}}$$

$$\cos\psi = \sqrt{\frac{C-B}{C-A}}$$

from eq.(3.25).

To evaluate the quantity $\delta_y - \delta_x$ in eq.(3.35), it is necessary to find which of these velocities is associated with the allowed vibration direction $\underline{X}$, and which with $\underline{Y}$.

This can be done in the case of ADP, by considering what happens to the optic axes as the electric field is reduced to zero. The optic axes become closer to the z-axis. One of the bisectors is then the radius of the circle normal to the optic-axis, and the other is perpendicular to that radius. The values of v_p^2 in this case are given by

$$v_{p-}^2 = A$$

$$v_{p+}^2 = \frac{1}{2}\left[(A+C) + (A-C)\cos(2\theta)\right]$$

Clearly, v_{p_+} corresponds to the bisector which is the radius of the circle, since the length of this radius is just n_1, where $A = \frac{1}{n_1^2}$.

The radius which is the intersection of the ellipse E and the circle normal to the z-axis, is perpendicular to the plane $(\underline{z},\underline{S})$. Thus, this radius corresponds to the line $\underline{X}$ in Fig.(3.5).

Clearly, when the electric field is applied, the allowed vibration

direction $\underline{X}$ rotates to $\underline{X}^{i}$ as shown in Fig.(3.5), so that v_{p_-} still corresponds to $\underline{X}$ and v_{p_+} to $\underline{Y}$.

$v_{p_+}^2$ and $v_{p_-}^2$ may be written

$$v_{p_+}^2 = \frac{1}{2}[(A+C) + (A-C)(\cos\theta_1\cos\theta_2 - \sin\theta_1\sin\theta_2)]$$

$$v_{p_-}^2 = \frac{1}{2}[(A+C) + (A-C)(\cos\theta_1\cos\theta_2 + \sin\theta_1\sin\theta_2)]$$

If $\theta_1, \theta_2 \ll 1$, then $V_{p_+} \simeq V_{p_-} \simeq A$

$$\therefore \quad \delta_y - \delta_x = \frac{\omega d}{n'c}\left[\frac{1}{V_{p_-}} - \frac{1}{V_{p_+}}\right]$$

$$\propto \frac{\omega d}{n'c}$$

When l', m', and $\beta \ll 1$, then

$$\cos^2\theta_1 = (m'\sin\beta + n'\cos\beta)^2$$

$$\simeq [m'\beta + \{1 - \tfrac{1}{2}(l'^2 + m'^2)\}\{1 - \tfrac{1}{2}\beta^2\}]$$

$$\simeq [1 - (l'^2 + m'^2 + \beta^2 - 2m'\beta)]$$

and $$\sin^2\theta_1 \simeq l'^2 + m'^2 + \beta^2 - 2m'\beta$$

Similarly

$$\cos^2\theta_2 \simeq [1 - (l'^2 + m'^2 + \beta^2 + 2m'\beta)]$$

$$\sin^2\theta_2 \simeq l'^2 + m'^2 + \beta^2 + 2m'\beta$$

$$\therefore \quad \sin\theta_1\sin\theta_2 \simeq [(l'^2 + m'^2 + \beta^2)^2 - 4m'^2\beta^2]^{1/2}$$

$$\simeq [(\beta^2 - m'^2 + l'^2)^2 + 4l'^2m'^2]^{1/2}$$

$$\therefore \quad \delta_x - \delta_y = \frac{\omega d}{n'c}\frac{(n_1^2 - n_3^2)n_1}{n_3^2}[(\beta^2 - m'^2 + l'^2)^2 + 4l'^2m'^2]^{1/2} \qquad (3.38)$$

$\delta_x + \delta_y$ also can be evaluated by putting

$$V_{p+}^2 = \frac{1}{2}\left[(A+C) + (A-C)(\cos\theta_1 \cos\theta_2 - \sin\theta_1 \sin\theta_2)\right]$$

$$\simeq A - \frac{1}{2}(A-C)\sin\theta_1 \sin\theta_2 \simeq A$$

$$V_{p-}^2 = \frac{1}{2}\left[(A+C) + (A-C)(\cos\theta_1 \cos\theta_2 + \sin\theta_1 \sin\theta_2)\right]$$

$$\simeq A + \frac{1}{2}(A-C)\sin\theta_1 \sin\theta_2 \simeq A$$

$$\therefore \frac{1}{V_x} + \frac{1}{V_y} \simeq \frac{1}{\sqrt{A}} + \frac{1}{\sqrt{A}} = 2n_1$$

$$\therefore \delta_x + \delta_y = \frac{\omega d}{n' c} \cdot 2n_1$$

(3.39)

Using the relationships (3.36), (3.37) and (3.38), the ratio of transmitted to incident amplitude may be evaluated, and is

$$\frac{A_T}{A_0} = \frac{\ell'^2 - m'^2 + \beta^2}{\left[(\beta^2 + m'^2 - \ell'^2)^2 + 4m'^2\ell'^2\right]^{1/2}} \cdot \sin\left[\frac{\omega d}{nc}(n_1^2 - n_3^2)\frac{n_1}{n_3^2}\left[\left|\beta^2 + m'^2 - \ell'^2\right|^2 + 4\ell'^2 m'^2\right\}^{\frac{1}{2}}\right] \cdot \cos\left(\omega t + \frac{\omega d}{nc} n_1\right)$$

If the argument of the sin term is much less than unity, as it is in the case of interest, then

$$\frac{A_T}{A_0} = (\ell'^2 - m'^2 + \beta^2) \cdot \frac{\omega d}{n' c}(n_1^2 - n_3^2) \cdot \frac{n_1}{n_3^2} \cdot \cos\left(\omega t + \frac{\omega d}{n' c} n_1\right)$$

In the case of ADP, with an electric field applied in the z-direction, the angle β is given by

$$\beta \simeq \sin\beta = \sqrt{\frac{2n_1^3 r_{63} E_z}{n_1^2 - n_3^2}}$$

$$\therefore \beta^2 = k E_z$$

If an alternating field $E_z \sin\omega t$ is applied to the crystal, then the angle β may be written

$$\beta^2 = \beta_o^2 \sin \omega t$$

The transmitted-to-incident-amplitude ratio is then

$$\frac{A_T}{A_o} = \frac{\omega d}{n_1 c} \left[\ell'^2 - m'^2 + \beta_o^2 \sin\omega_M t\right] \cos\left(\omega t + \frac{\omega d n_1}{c}\right)$$

This equation may be transformed to the system (x,y,z), the crystal axes. From eq.(3.31) it is seen that

$$\ell' = \frac{1}{\sqrt{2}}(\ell + m) \qquad m' = \frac{1}{\sqrt{2}}(\ell - m)$$

Thus

$$\frac{A_T}{A_o} = \frac{\omega d}{nc} \left[2\ell m + \beta_o^2 \sin\omega_M t\right] \cos\left(\omega t + \frac{\omega d n_1}{nc}\right) \qquad (3.40)$$

The value of the function $M_{12}(\tau)$ can be found for two waves travelling in given directions. If the wave directions are (l_1, m_1, n_1) and (l_2, m_2, n_2), then

$$M_{12}(\tau) = \frac{\frac{2}{n_1 n_2}\frac{1}{T_M}\int_0^{T_M}(2\ell_1 m_1 + \beta_o^2 \sin\omega_M t)(2\ell_2 m_2 + \beta_o^2 \sin\omega_M(t+\tau))\,dt}{\frac{1}{n_1^2}\frac{1}{T_M}\int_0^{T_M}(2\ell_1 m_1 - \beta_o^2 \sin\omega_M t)^2 dt + \frac{1}{n_2^2}\frac{1}{T_M}\int_0^{T_M}(2\ell_2 m_2 - \beta_o^2 \sin\omega_M t)^2 dt}$$

$$= \frac{\frac{2}{n_1 n_2}\left(4\ell_1 m_1 \ell_2 m_2 - \frac{\beta_o^4}{2}\cos\omega_M \tau\right)}{\frac{1}{n_1^2}\left(4\ell_1^2 m_1^2 + \frac{\beta_o^4}{2}\right) + \frac{1}{n_2^2}\left(4\ell_2^2 m_2^2 + \frac{\beta_o^4}{2}\right)}$$

Of particular interest is the case where $l_2 = -l$, $m_2 = m_1$, $n_1 = n_2$. Then

$$M_{12}(\tau) = \frac{2\left[\frac{\beta_0^4}{2} - 4\ell_1^2 m_1^2 \cos\omega_H \tau\right]}{2\left[\frac{\beta_0^4}{2} + 4\ell_1^2 m_1^2\right]}$$

$$= \frac{\beta_0^2 \cos\omega_H \tau - 8\ell_1^2 m_1^2}{\beta_0^2 + 8\ell_1^2 m_1^2}$$

(3.41)

It is seen that $M_{12}(\tau)$, and hence the visibility of the fringes produced when the two beams are superimposed, is constant when $l_1 m_1$ is constant. This may be represented by a "contour map", on which the ordinates are the direction cosines (l,m) of waves which super-imposed on waves of direction cosines (-l,m), and the contours are contours of equal visibility. This is shown in Fig.(3.6). The contours are seen to be hyperbolae, with the l and m axes as asymptotes.

If two waves are sent through the crystal so that they are symmetrically located about the y-axis (i.e. m constant), but whose directions about the x-axis are varied, then the variation of $M_{12}(o)$ is given by

$$M_{12}(0) = \frac{\beta_o^4 - 8\ell^2 m_o^2}{\beta_o^4 + 8\ell^2 m_o^2}$$

where m_o is the value of m. This is sketched in Fig.(3.7). It is a Lorentzian curve with limiting values +1 and -1. The half width (i.e. the width at which $M_{12}(o) = 0$ is given by

$$\Delta\ell = \frac{1}{2\sqrt{2}} \cdot \frac{\beta_o^2}{m}$$

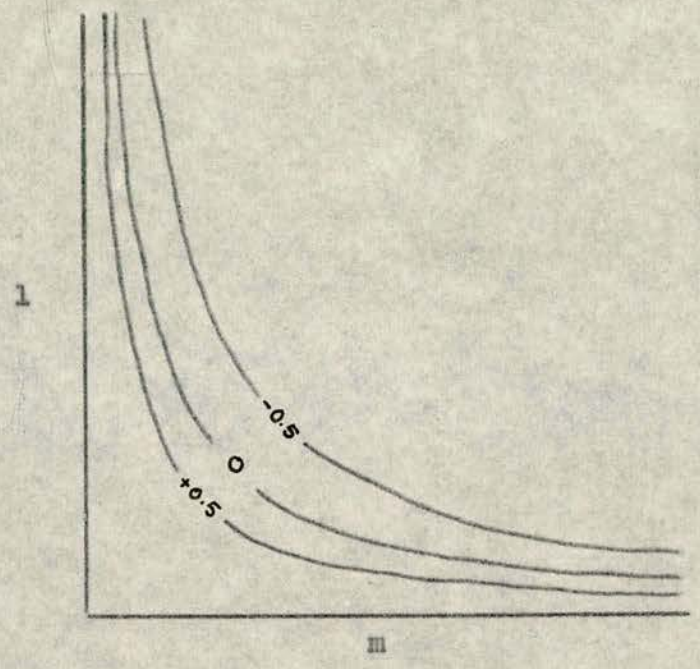

FIG.3.6

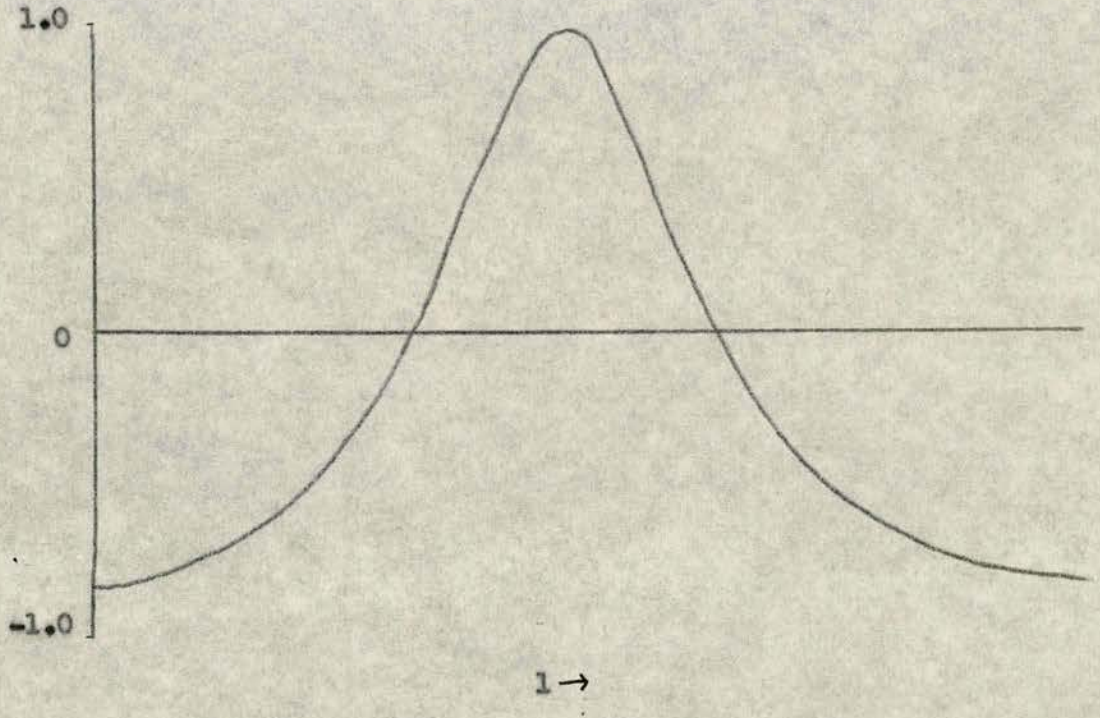

FIG.3.7

The half width depends on the values of m_o and β_o. Since β_o is proportional to the square root of the amplitude of the applied electric field, an experimental determination of this curve allows the electric field amplitude to be measured.

It should be noted that phase reversal of the amplitude of the light occurs when

$$\beta_o^2 > 2lm$$

Since phase reversal effects should be avoided in demonstrating the required effect, it must be ensured that the beams used, which will have finite divergence, do not suffer significant phase reversal.

Finally, values of A/A_o and $M_{12}(0)$ have been calculated with the program, and using the approximate formula (3.39), for various values of l, m, β_o. These are compared in Table 3.1 and it is seen that they are in good agreement up to values of l, m, β_o, of $\sim 10^{-2}$ rad, so that the approximation can be considered valid up to these values.

IX. THE EFFECT OF THE DIVERGENCE OF THE BEAMS, AND OF THE FINITE TRANSIT TIME OF THE LIGHT THROUGH THE CRYSTAL

Any real light beam is divergent, so it is necessary to examine the effect of this on the envelope of modulation, and on $M_{12}(\tau)$.

The case of a beam which consists of a cone of directions centred about a direction (l_o, m_o, n_o) as indicated in Fig.(3.8), is considered here.

Assuming that the initial amplitudes in each direction are the same, then the ratio of transmitted to incident amplitudes is given by

			A_T/A_0 for $E = +E_z$		$M_{12}^{(0)}$	
$\beta_0 \cdot 10^3$	$1 \cdot 10^3$	$m \cdot 10^3$	EXACT	APPROX.	EXACT	APPROX.
1	1.5	1	0.00719	0.00719	-0.213	-0.213
1	1.5	0	0.00987	0.00987	-0.666	-0.666
1	10	5	0.190	0.205	-1.000	-1.000
1	10	0	0.259	0.272	-1.000	-1.000
1	50	25	0.269	5.052	-1.000	-1.000
4	1.5	1	0.0148	0.0148	0.707	0.707
4	1.5	0	0.0175	0.0175	0.286	0.286
4	10	5	0.197	0.213	-0.997	-0.997
4	10	0	0.266	0.280	-0.998	-0.998
4	50	25	0.271	5.059	-1.000	-1.000
4	50	0	0.395	6.740	-1.000	-1.000
10	1.5	1	0.349	0.386	1.000	1.000
10	1.5	0	0.350	0.390	1.000	1.000
10	10	5	0.436	0.584	0.300	0.231
10	10	0	0.482	0.651	-0.025	0.006
10	50	25	0.313	5.431	-0.929	-0.994
10	50	0	0.498	7.111	-0.635	-0.996
40	1.5	1	0.490	3.830	1.000	1.000
40	1.5	0	0.490	3.832	1.000	1.000
40	10	5	0.487	4.027	0.734	0.989
40	10	0	0.472	4.095	0.532	0.980
40	50	25	0.109	8.880	-0.677	-0.553
40	50	0	0.387	10.559	-0.131	-0.721

Table 3.1

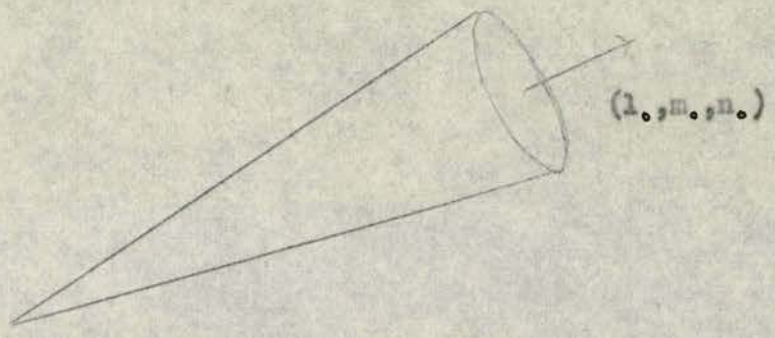

Fig.3.8

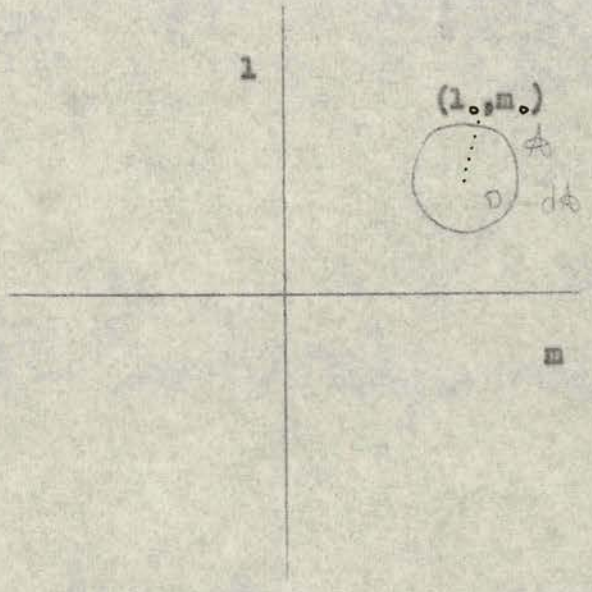

Fig.3.9

$$\int_{\Phi} \frac{A_r}{A_o} d\Phi = \int_{\Phi} \frac{\omega d}{c}(n_1^2 - n_3^2)\frac{n_1}{2n_3^2} \cdot \frac{1}{n}(2\ell m - \beta_o^2)\, d\Phi$$

where $d\Phi$ is an element of area of Φ, as in Fig.(3.9).

The co-ordinate system (l,m) may be transformed to (l'm') where

$$\ell = \ell_o + \ell' \qquad m = m_o + m'$$

Then

$$\int_{\Phi} \frac{A_r}{A_o} d\Phi = \iint_{\Phi} \frac{\omega d}{c}(n_1^2 - n_3^2)\frac{n_1}{2n_3^2} \cdot \frac{1}{n}\left\{2\ell_o m_o + 2(m_o\ell + \ell_o m + \ell' m') - \beta_o^2\right\} d\Phi$$

n is approximately constant for all directions in the beam since l and m are small. The expression then becomes

$$\frac{A_r}{A_o}\Phi = \frac{\omega d}{c}(n_1^2 - n_3^2)\frac{n_1}{2n_3^2} \cdot \frac{1}{n_o}\left[\int_{\Phi}(2\ell_o m_o - \beta_o^2)\, d\Phi + 2m_o\int_{\Phi}\ell' d\Phi + 2\ell_o\int_{\Phi} m' d\Phi + 2\int_{\Phi}\ell' m' d\Phi\right]$$

But since the integration is over a circle, all three remaining integrals are zero. Hence the ratio of transmitted to incident amplitude is

$$\frac{A_r}{A_o}\Phi = \frac{\omega d}{c}(n_1^2 - n_3^2)\frac{n_1}{2n_3^2} \cdot \frac{1}{n_o}(2\ell_o m_o - \beta_o^2)\Phi$$

If the crystal in question is ADP with an applied alternating electric field, this becomes

$$\frac{A_r}{A_o} = \frac{\omega d}{c}(n_1^2 - n_3^2)\cdot\frac{n_1}{2n_3^2} \cdot \frac{1}{n_o}(2\ell_o m_o - \beta_o^2)$$

The remarkable result is obtained that the modulation envelope for a beam of any divergence centred about a direction (l,m,n) is the same as the modulation envelope for a plane wave travelling in the direction (l,m,n).

This result has also been obtained using a computer program (Appendix III). In Table 3.1 are shown the results calculated with the program and by the approximation. The approximation is seen to be good up to values of 10^{-2} rad.

			$M_{12}(0)$		
β_0	l	m	Uncorrected	Divergence correction	Transit time correction
5.10^{-4}	10^{-3}	0	-0.826	-0.826	-0.839
7.10^{-4}	10^{-3}	0	-0.710	-0.710	-0.727
5.10^{-3}	10^{-2}	0	-0.826	-0.822	-0.840
7.10^{-3}	10^{-2}	0	-0.711	-0.701	-0.728
5.10^{-2}	10^{-1}	0	-0.076	-0.141	-0.032
7.10^{-2}	10^{-1}	0	-0.092	-0.050	-0.091

Table 3.2

(ii) An exact correction for the effect of the finite transit time of the light through the crystal would be rather difficult, but it is shown below that the effect is quite small even when the transit time is 1/12th of the modulation cycle as was the case in the experiment.

The only part of the expression for the transmitted to incident amplitude which varies with the variation of the electric field is $\beta_0^2 \sin\omega_M t$. The average value of this quantity during the modulation cycle is

$$\langle \beta_0^2 \sin\omega t \rangle = \beta_0^2 \int_t^{t+t_0} \sin\omega t' dt' = \beta_0^2 . \sin\omega t . \frac{\sin(\omega t_0/2)}{\omega t_0/2}$$

Where t_0 is the transit time of the light in the crystal. When $\omega t_0 = 1/12$, then

$$\frac{\sin(\omega t_0/2)}{(\omega t_0/2)} = .0005$$

so that the effect could be expected to be small.

An approximate calculation of the effect on $M_{12}(\tau)$ was made by a modification of the program (Appendix IV) as follows.

The crystal can be considered to be made up of a series of shorter crystals, across which the electric field can be considered to be constant during the time taken for the light to traverse it, but the fields across successive crystals are out of phase with one another by appropriate amounts. The light is initially polarised in a direction $\underline{P}$, with amplitude A Sin t, and in the first crystal this is resolved along $\underline{X}_1$ and $\underline{Y}_1$, where these are the allowed vibration directions, with an angle O, between $\underline{X}_1$ and $\underline{P}$. The wave travels through the first crystal phases of the components are changed by δ_{x_1} and δ_{y_1}. The components

along $\underline{P}$ and $\underline{Q}$, where $\underline{Q}$ is perpendicular to $\underline{P}$, are

$$A_0\left[1 - \sin(2\theta_1)\cdot \sin^2\left(\frac{\delta_{y_1} - \delta_{x_1}}{2}\right)\right]^{1/2} \sin(\omega t + \phi)$$

$$A_0 \cdot \sin 2\theta_1 \cdot \sin\left(\frac{\delta_{y_1} - \delta_{x_1}}{2}\right) \cdot \cos\left(\omega t + \frac{\delta_{y_1} + \delta_{x_1}}{2}\right)$$

where $$\tan\phi = \frac{\cos^2\theta_1 \sin\delta_{x_1} + \sin^2\theta_1 \sin\delta_{y_1}}{\cos^2\theta_1 \cos\delta_{x_1} + \sin^2\theta_1 \cos\delta_{y_1}}$$

$$= \frac{\sin\left(\frac{\delta_{x_1} + \delta_{y_1}}{2}\right) + \tan\left(\frac{\delta_{y_1} - \delta_{x_1}}{2}\right)\cdot \cos 2\theta_1 \cdot \cos\left(\frac{\delta_{y_1} + \delta_{x_1}}{2}\right)}{\cos\left(\frac{\delta_{x_1} + \delta_{y_1}}{2}\right) + \tan\left(\frac{\delta_{y_1} - \delta_{x_1}}{2}\right)\cdot \cos 2\theta_1 \cdot \sin\left(\frac{\delta_{y_1} + \delta_{x_1}}{2}\right)}$$

If $\delta_{y_1} - \delta_{x_1} << 1$, then $\tan\phi \simeq \tan\left(\frac{\delta_{x_1} + \delta_{y_1}}{2}\right)$

It is seen that when $\delta_{y_1} - \delta_{x_1}$ is small, as it is when the wave direction is close to the z-axis of the crystal, and when the crystal is short, then the amplitude along $\underline{P}$ is almost unchanged and the phase is changed by $\frac{\delta_{x_1} + \delta_{y_1}}{2}$, while there is a small component along $\underline{Q}$ whose phase is approximately 90^0 out of phase with the component in the direction $\underline{P}$.

When the two components pass through the second crystal, they are each resolved along the directions $\underline{X}_2$ and $\underline{Y}_2$ where these are the allowed vibration directions in the second crystal. These components suffer phase changes δ_{x_2} and δ_{y_2}. On emerging from the second crystal the components in the $\underline{X}_2$ and $\underline{Y}_2$ directions can be resolved along $\underline{P}$ and $\underline{Q}$. These components are

$$\underline{P}: \quad A_0\left[1 - \sin^2 2\theta_1 \sin^2\left(\frac{\delta_{y_1} - \delta_{x_1}}{2}\right)\right]^{1/2} \cdot \left[1 - \sin^2 2\theta_1 \sin^2\left(\frac{\delta_{y_2} - \delta_{x_2}}{2}\right)\right]^{1/2} \cdot$$

$$\sin\left(\omega t + \frac{\delta_{x_1} + \delta_{y_1}}{2} + \frac{\delta_{x_1} + \delta_{y_2}}{2}\right) \quad +$$

$$A_o \sin 2\theta_1 \cdot \sin\left(\frac{\delta y_1 - \delta x_1}{2}\right) \cdot \sin 2\theta_2 \cdot \sin\left(\frac{\delta y_2 - \delta x_2}{2}\right) \cdot$$

$$\sin\left(\omega t + \frac{\delta y_1 + \delta x_1}{2} + \frac{\delta y_2 + \delta x_2}{2}\right)$$

$$\underline{Q}: \quad A_o \sin 2\theta_2 \cdot \sin\left(\frac{\delta y_2 - \delta x_2}{2}\right) \cdot \left[1 - \sin^2 2\theta_1 \cdot \sin^2\left(\frac{\delta y_1 - \delta x_1}{2}\right)\right]^{1/2} \cdot$$

$$\cos\left(\omega t + \frac{\delta y_1 + \delta x_1}{2} + \frac{\delta y_2 + \delta x_2}{2}\right) +$$

$$A_o \sin 2\theta_1 \cdot \sin\left(\frac{\delta y_1 - \delta x_1}{2}\right)\left[1 - \sin^2 2\theta_2 \cdot \sin^2\left(\frac{\delta y_2 - \delta x_2}{2}\right)\right]^{1/2} \cdot$$

$$\cos\left(\omega t + \frac{\delta x_1 + \delta y_1}{2} + \frac{\delta x_2 + \delta y_2}{2}\right)$$

where θ_2 is the angle between $\underline{P}$ and $\underline{X}_2$.

If $\delta x_1 - \delta y_2 \ll 1$, and $\delta x_2 - \delta y_2 \ll 1$, then these may be written

$$\underline{P}: \quad A_o \sin\left[\omega t + \frac{\delta x_1 + \delta y_1}{2} + \frac{\delta x_2 + \delta y_2}{2}\right]$$

$$\underline{Q}: \quad A_o\left[\sin 2\theta_1 \cdot \sin\left(\frac{\delta x_1 - \delta y_1}{2}\right) + \sin 2\theta_2 \cdot \sin\left(\frac{\delta x_2 - \delta y_2}{2}\right)\right] \cdot$$

$$\cos\left[\omega t + \frac{\delta x_1 + \delta y_1}{2} + \frac{\delta x_2 + \delta y_2}{2}\right] \qquad (3.42)$$

It is seen that the amplitude in the $\underline{P}$ direction is almost unchanged, and the phase change is $\frac{\delta x_1 + \delta y_1 + \delta x_2 + \delta y_1}{2}$. The amplitude transmitted in the $\underline{Q}$ direction is increased after the light has traversed each crystal, and the phase is changed. The light signal in the $\underline{Q}$ direction after traversing n crystals may be expressed as

$$A_T = A_o\left[\sum_{i=1}^{n} \sin 2\theta_i \cdot \sin\left(\frac{\delta x_i - \delta y_i}{2}\right)\right] \cdot \cos\left[\omega t + \frac{1}{2}\sum_{i=1}^{n}(\delta x_i + \delta y_i)\right] \qquad (3.43)$$

where δ_{xi} and δ_{yi} are the phase changes of the components along $\underline{X}_i$ and $\underline{Y}_i$, the allowed vibration directions in the i-th crystal and θ_i is the angle between $\underline{P}$ and $\underline{X}_i$.

In the modified program, the crystal was divided into ten sections, and the amplitude and phase in eq.(3.40) were calculated for different values of $E_z \sin\omega t$. This enabled $M_{12}(o)$ to be evaluated. The results of this computation are shown in Table , where they are compared with the results of the uncorrected program. It is seen that the values are almost unchanged.

CHAPTER 4

I. EXPERIMENTAL REQUIREMENTS

An alternating electric field must be produced along the z-axis of an ADP crystal which is cut with optically polished faces perpendicular to that axis. Two coherent or quasi-coherent beams of parallel light should be passed through this crystal in directions which are determined by the magnitude of the electric field, and by the considerations of Sections VI and VII, Chapter 4. The crystal must be placed between crossed polarisers, whose polarisation directions are parallel to the x- and y-axes of the crystal. The two light beams should then be superimposed to produce interference fringes, whose visibility can be measured. The path difference between the two beams must be variable over a range of distances which allows a few cycles of the modulated visibility pattern to be observed. So that this path difference is not unmanageably large, micro-wave modulation should be used. The crystal should therefore be placed in a micro-wave resonant cavity. The fringe spacing in the interference pattern should be large enough to allow half a fringe or less to be resolved or less, and its intensity measured.

II. OPTICAL ARRANGEMENT

The arrangement is as shown in Fig.(4.1).

The light source used is a laser. This has obvious advantages over a thermal source. The long coherence length of the laser means that large path differences can be introduced between the two beams without a

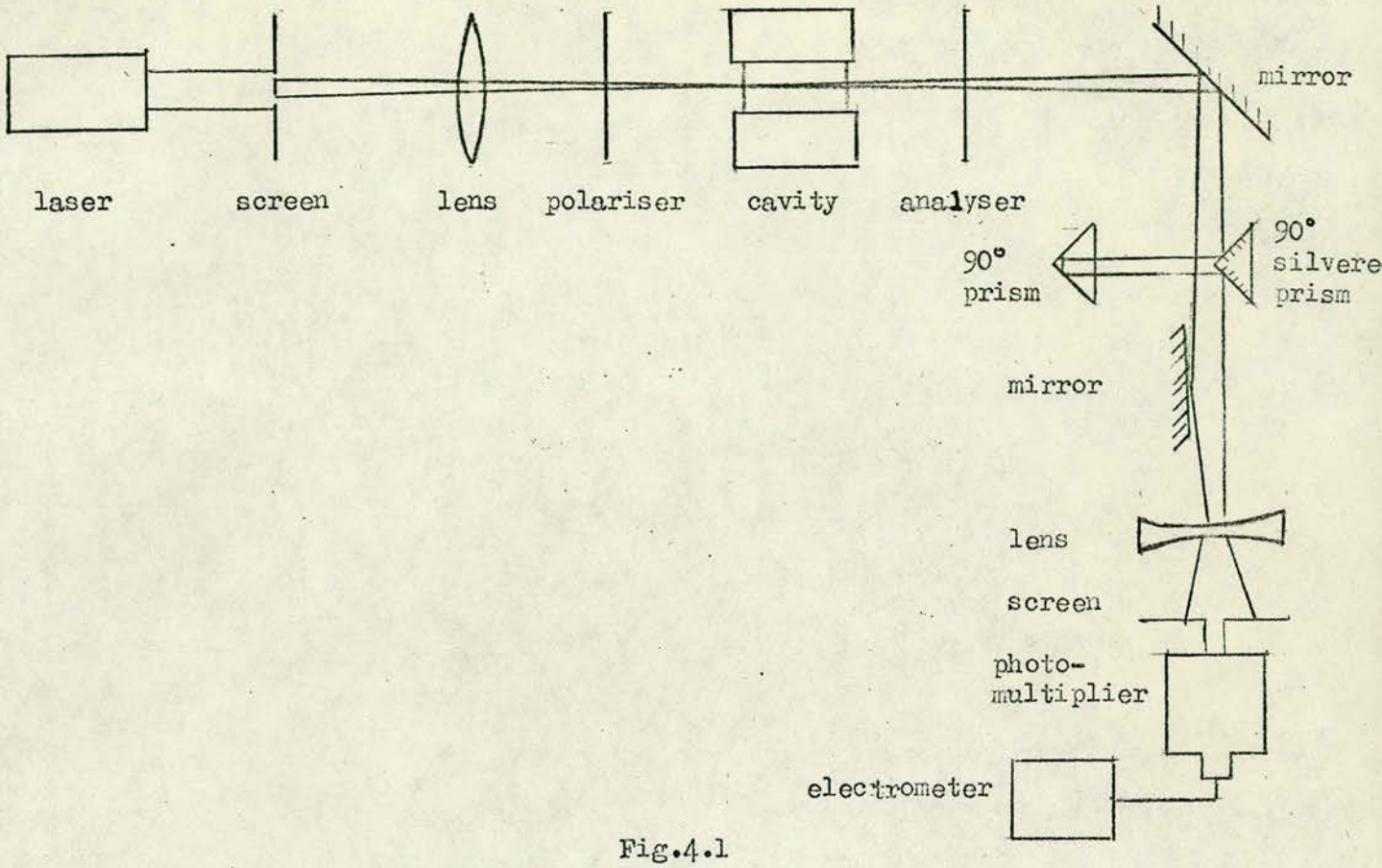
laser
screen
lens
polariser
cavity
analyser
mirror
90°
prism
90°
silvered
prism
mirror
lens
screen
photo-
multiplier
electrometer

Fig.4.1

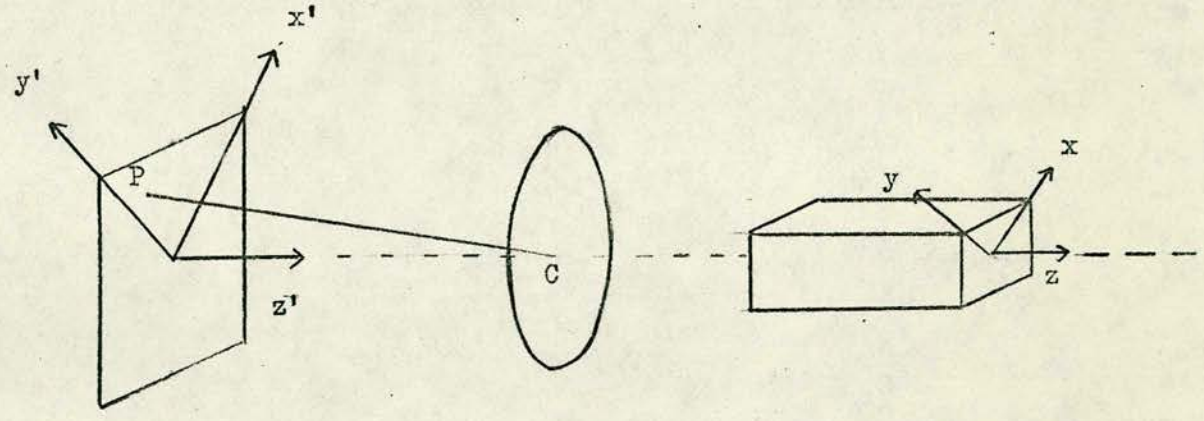
x'
y'
P
z'
C
y
x
z

Fig.4.2

significant reduction in the visibility of the fringes. The intensity of the laser makes the measurement of the visibility of the fringes much easier, and combined with the small divergence of the beam, makes the adjustment of the interferometer much simpler.

A screen with two pinholes is situated in the focal plane of a convex lens. The screen can be traversed vertically and horizontally, and two vernier scales allow its position to be noted. When the pinholes are illuminated, two beams of almost parallel light emerge from the lens, making angles with the optic axis of the lens, which are determined by their position in the screen with respect to that axis. The optic axis of the lens is parallel to the z-axis of the crystal. After passing through the cavity, the two beams are reflected through 90^{o}. This reflection is necessary because of the geometry of the laboratory. One beam is then reflected through 90^{o} by a silvered 90^{o} prism, and is then successively reflected internally by the two faces of a second 90^{o} prism, and is then reflected off the second face of the first prism. The separation of these two prisms is variable, enabling the path difference between the two beams to be varied. The slotted disc, which can be rotated by means of a stepping motor, allows one or both of the beams to be cut off. The second beam is then reflected at almost grazing incidence at a mirror, so that the two beams converge towards a concave lens which then spreads them out so that they overlap. In the region where the beams overlap, interference fringes are obtained. A slit of approximately half a fringe width is placed in the interference region, so that this much of the light falls onto a photomultiplier. The slit can be traversed across the fringe pattern. In this way, the intensity of the maxima and minima can be measured. The first polariser is situated infront of the resonant

cavity, and the second is after the slit.

The angles made by the two beams with the optic axis of the system can be found as follows. In Fig.(4.2) are shown the crystal axes (x,y,z). Another set of axes (x',y',z') are shown whose origin is the point of intersection of the optic axes and the screen, the x'- and y'-axes being parallel to the x- and y-axes, and in the plane of the screen, and the z'-axis being parallel to the z-axis. If light is sent through a point at $(x_1', y_1', 0')$, the light will emerge from the lens as a beam of parallel light, the direction of the beam being parallel to PC, the line joining the point $(x_1', y_1' 0)$ to the centre of the lens. The direction cosines of PC with respect to the x-, y-, z-axes are

$$\frac{x_1'}{PC}, \quad \frac{y_1'}{PC}, \quad \frac{\sqrt{1 - x_1'^2 - y_1'^2}}{PC}$$

respectively. If x', and y', are much smaller than PC, then $PC \simeq f_1$, where f_1 is the focal length of the lens. The direction cosines then b become

$$\frac{x_1'}{f_1}, \quad \frac{y_1'}{f_1}, \quad \frac{\sqrt{1 - x_1'^2 - y_1'^2}}{f_1}$$

As the x-, y-, z-axes are parallel to the x-, y-, z-axes, these are also the direction cosines with respect to the latter axes.

The position of the beam with respect to the optic axis of the lens is determined by the direction of the light incident on the hole in the screen (see Fig.4.3). The size of the beam is determined either by the divergence of the light incident on the hole (Fig.4.4) or the diffraction produced at the hole, (Fig.4.5) whichever is the greater.

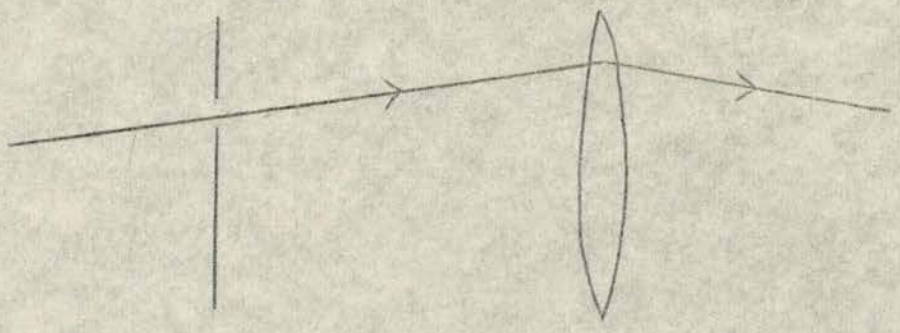

Fig.4.3

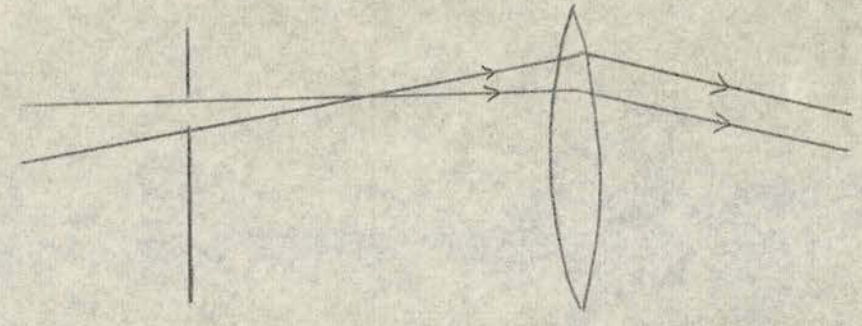

Fig.4.4

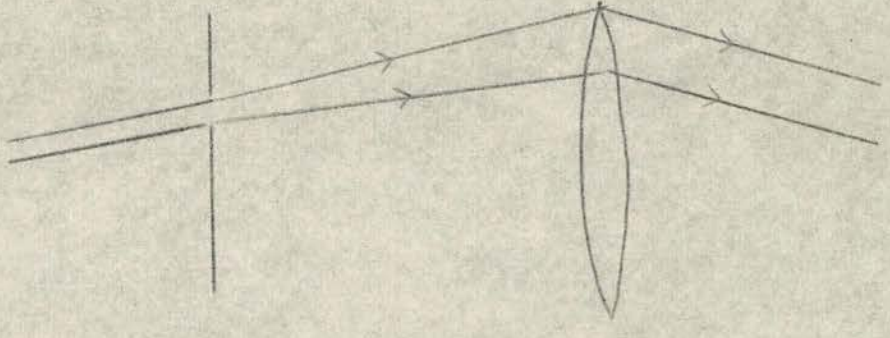

Fig.4.5

The light emerging from the lens will not be truly parallel, because of the finite size of the pinhole. The light coming from a point in the screen with co-ordinates (x'+a, y', 0) will emerge from the lens in a direction with direction cosines

$$\frac{x_1' + a}{f_1} \quad , \quad \frac{y'}{f_1} \quad , \quad \frac{\sqrt{1 - (x_1' + a)^2 - y_1'^2}}{f_1}$$

Thus, if a circular aperture of radius r centred at (x', y', 0) is used, the light emerging from the lens diverges around a central direction of direction cosines,

$$\frac{x_1'}{f_1} \quad , \quad \frac{y_1'}{f_1} \quad , \quad \frac{1 - x_1'^2 - y_1'^2}{f_1}$$

and with divergence $\frac{2r}{f}$.

To produce the required beams, two apertures are used. The directions of the beams must be such that if one beam has direction cosines (l,m,n) the direction cosines of the other beam should be either (m,l,n) or (-m,-l,n). This condition will be satisfied if the centres of the apertures are (x', y', 0) and either (y', x', 0) or (-y', -x', 0).

If the power dissipated in the crystal is 1 watt at $2.5GH_2$ then the angles made by the two beams with respect to the optic axis of the crystal should be of the order of 2.10^{-3} radians. If a lens of focal length 0.2m. is used, and a screen situated in the focal plane of the lens, containing two pinholes, separated by 1mm, with the pinholes situated at a distance 0.5mm above or below a horizontal line perpendicular to the optic axis of the lens, then the beams emerging from the lens when the pinholes are illuminated make angles with the optic axis of the lens of about 3.10^{-3} rad. in air, The angles in the crystal will be reduced

by approximately $1/n_1$, where n_1 is the refractive index for waves travelling along the z-axis of the crystal. For ADP, $n_1 = 1.53$. The direction cosines of the two beams are then, to a good approximation

$$(2.10^{-3},\ 0,\ 1)\ ,\quad (0,\ 2.10^{-3},\ 1)$$

To obtain interference, the two beams must be superimposed. The fringe separation is determined by the angle at which the two beams cross. This can be shown as follows.

Consider the case of two plane waves (Fig.4.6). The amplitudes of the waves at AB and CD can be represented by

$$A_1 = A\ \mathrm{Sin}(\omega t) \qquad A_2 = A\ \mathrm{Sin}(\omega t + \delta)$$

where δ is constant.

Interference fringes are observed along EF. The amplitude at a point P is given by

$$A_p = A\ \mathrm{Sin}\left(\omega t + \frac{2\pi}{\lambda} QP\right) + A\ \mathrm{Sin}\left(\omega t + \frac{2\pi}{\lambda}.RP + \delta\right)$$

$$= 2A\ \mathrm{Sin}\left[\omega t + \frac{\pi}{\lambda}(PR + RQ) + \delta\right] \mathrm{Cos}\left[\frac{\pi}{\lambda}(QR - RP) - \delta\right]$$

The terms PR + RQ, and QP - RP can be evaluated with reference to Fig.(4.7).

$$PQ = QS + SP = AE + SP = AE + EP \tan\frac{\varphi}{2}$$

$$PR = TR - TP = EC - TP = AE - EP \tan\frac{\varphi}{2}$$

$$\therefore\ PQ + PR = 2AE$$

$$PQ - PR = 2\,EP \tan\frac{\varphi}{2} \simeq EP.\varphi \quad \text{if } \varphi \ll 1$$

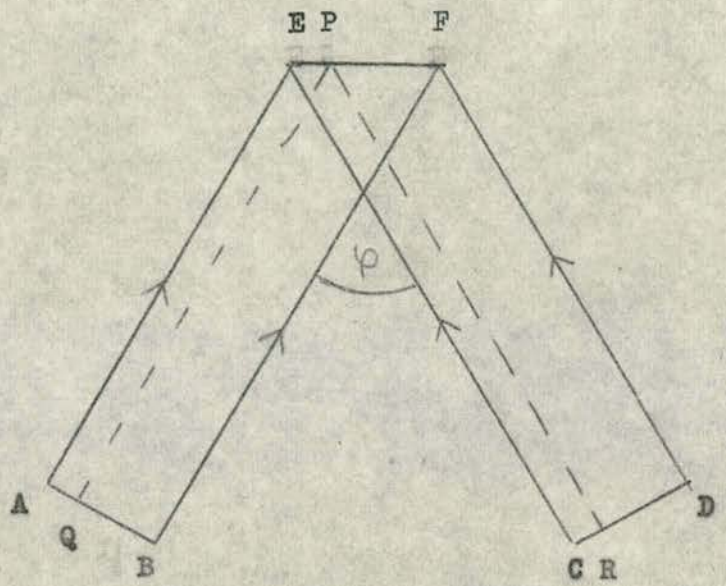

Fig.4.6

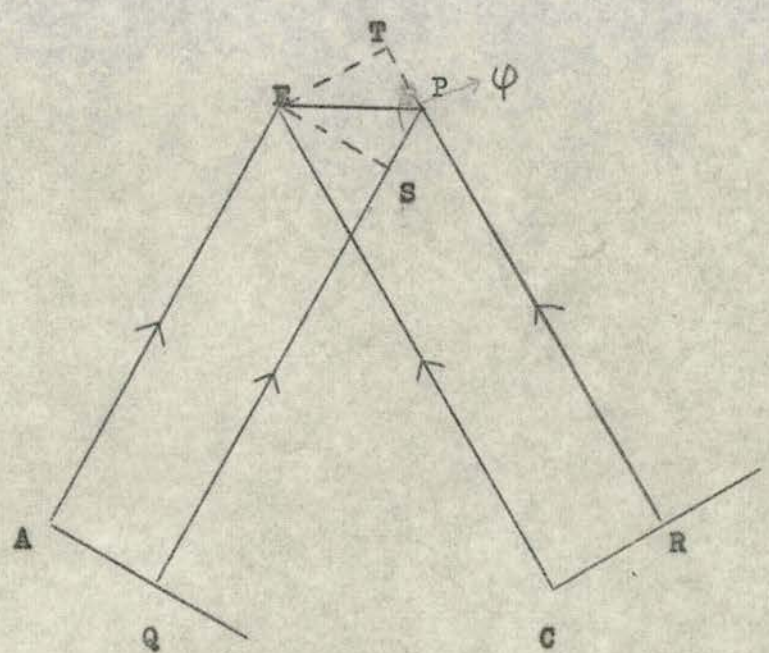

Fig.4.7

Thus

$$A_p = 2A \sin\left(\omega t + c.\frac{\pi}{\lambda}.AE + \delta\right).\ \cos\left(\frac{\pi\varphi}{\lambda}.EP\right)$$

The average intensity at P is

$$I_p = \frac{\omega}{2\pi}\int_0^{\frac{2\pi}{\omega}} A_p\, dt = 2A^2 \cos^2\left(\frac{\pi\varphi}{\lambda}.EP\right)$$

Thus, as the position of P is varied, the intensity varies. The separation of the maxima is given by

$$\Delta d = \frac{\lambda}{2\varphi}$$

Thus the separation of the fringes increases as the angle between the beams is decreased.

The two beams could be superimposed simply by rotating one beam with a mirror, so that the two beams overlap. This would, however, produce an interference pattern whose dimensions would be the dimensions of the beams. This would not be very convenient for detection purposes.

Instead, the two beams are passed through a concave lens, one of the beams having first been rotated, so that the beams overlap at a suitable angle. Interference is observed in the overlap region. The separation of the fringes is found as follows.

Consider first the case of parallel beams (Fig.4.8). Two divergent beams emerge from the lens and these beams apparently come from two point sources S_1 and S_2. The distance between these points is $f_2\alpha$, where α is the angle between the two beams, and is small, and f_2 is the focal length of the lens. The system is now effectively the same as that discussed in Chapter 2, Section 1. The separation of the fringes in such a system is well-known (see, for example, Jenkins and White[7]) to be $\frac{\lambda D}{d}$, where λ is the wavelength of the light, d is the separation of

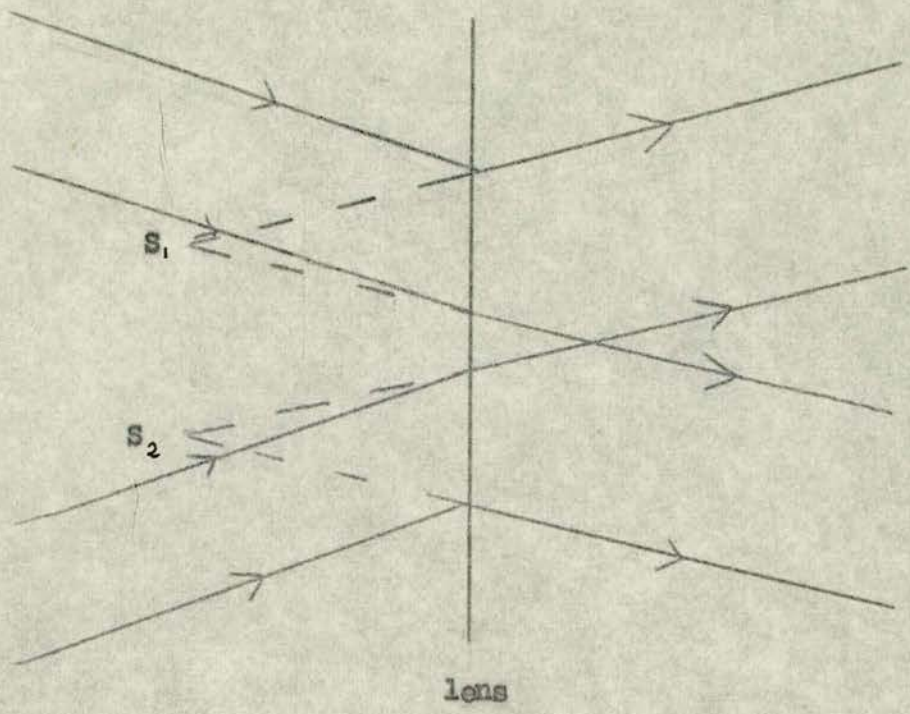

Fig.4.8

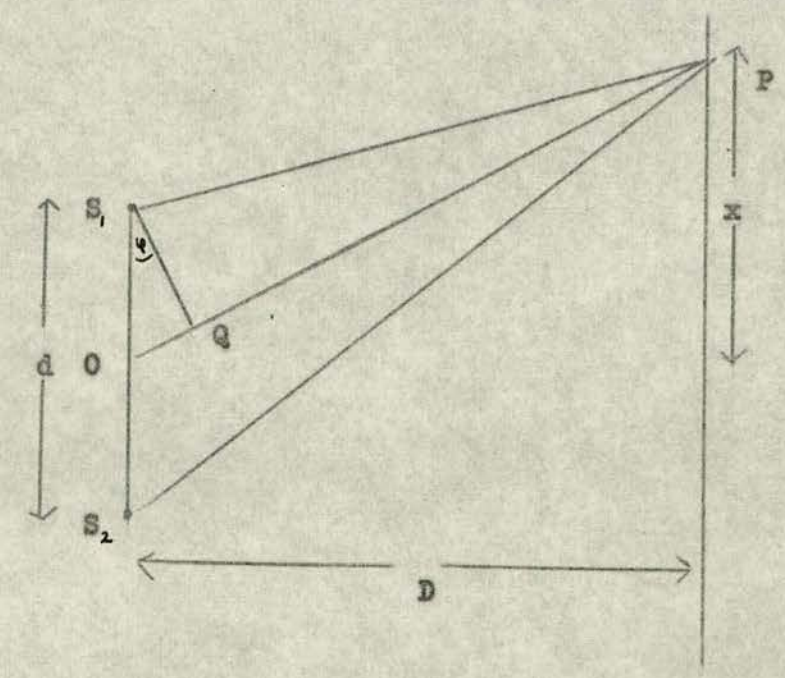

Fig.4.9

the point sources, and D is the distance between the sources and the plane of observation, as shown in Fig.(4.9).

The effect of the finite divergence of the beams can be shown with the help of Fig.(4.10). The beams can be considered as coming from sources of finite size, S_1 and S_2. The lens produces virtual, erect and reduced images of these sources. The interference obtained is the same as is obtained with two finite pinholes.

It can be shown that if the amplitudes at all points in S_1, are given by A sinωt and at all points in S_2 by A sin$(\omega t + \delta)$, the fringe pattern is the same as that which would be obtained using point sources. This is shown as follows.

In Fig.(4.11), the two sources are shown. The amplitude at any point P on the screen is the sum of the amplitudes contributed by each point in the two sources. Consider a point R in the source S_1. The amplitude due to R at P is

$$A_{PR} = A \sin\left(\omega t - \frac{2\pi}{\lambda} RP\right)$$

and $$RP = OP - OX = OP - OR.\frac{x}{D}$$

If the distance between any point in the sources from the point O is represented by y, then

$$A_{PR} = A \sin\left[\omega t - \frac{2\pi}{\lambda}\left(OP - \frac{y}{D}x\right)\right]$$

The total amplitude contributed by S_1, is

$$A_{P_1} = \int_{y_1}^{y_2} A \sin\left[\omega t - \frac{2\pi}{\lambda}\left(OP - \frac{y}{D}x\right)\right] dy$$

$$= A \sin\left[\omega t - \frac{2\pi}{\lambda}\left(OP - \frac{x}{D}(y_1+y_2)\right)\right].\cos\left[\frac{\pi x}{\lambda D}(y_1 - y_2)\right]$$

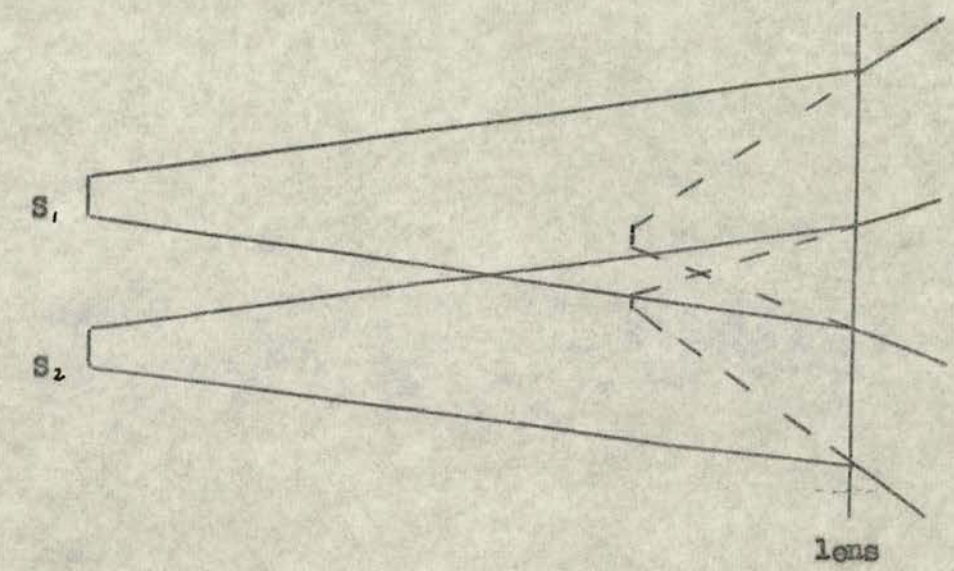

Fig. 4.10

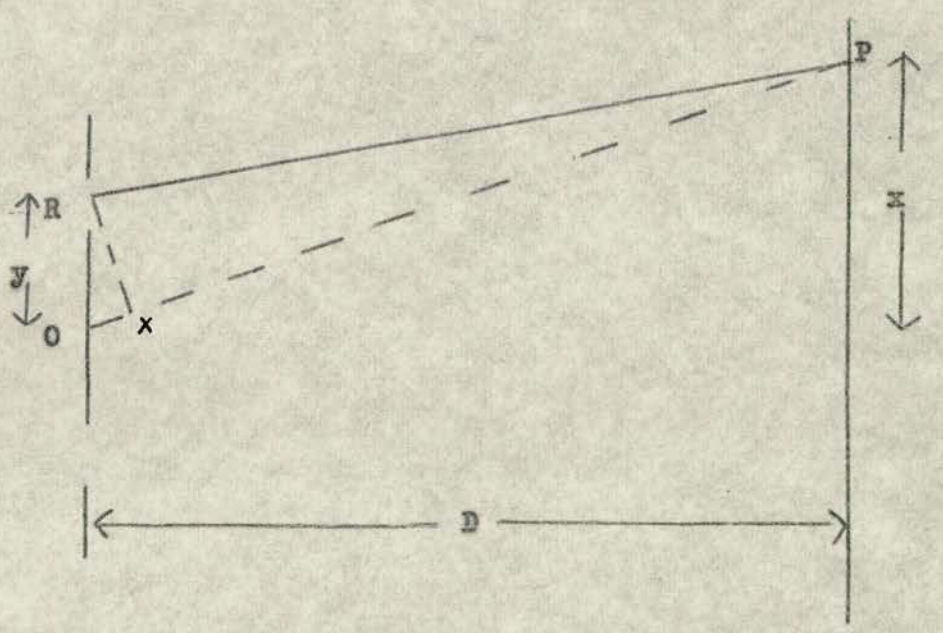

Fig.4.11

Similarly, the total amplitude contributed by S_2 is

$$A_{s_2} = A \sin\left[\omega t - \frac{2\pi}{\lambda}(OP - \frac{x}{2D}(y_1+y_2)) + \delta\right] \cdot \cos\left[\frac{\pi x}{\lambda D}(y_1-y_2) + \delta\right]$$

The average intensity at P is then

$$\langle I_p \rangle = \frac{1}{T}\int (A_{s_1} + A_{s_2})^2 dt$$

$$= \left\{\frac{A^2}{2} + \frac{A^2}{2} + A^2 \cos\left[\frac{\pi x}{\lambda D}(y_1+y_2) + \delta\right]\right\} \cos^2\left[\frac{\pi x}{\lambda D}(y_1-y_2)\right]$$

$$= kA^2\left[1 + \cos\left(\frac{\pi x}{\lambda D}(y_1+y_2)\right)\right]$$

where $K = \cos^2\left[\frac{\pi x}{\lambda D}(y_1-y_2)\right]$

Thus, the intensity on the screen fluctuates between 0 and $2kA^2$, and the separation of the maxima is

$$\Delta x = \lambda \frac{D}{d} = \frac{\lambda D}{f_2 \alpha}$$

Where α is the angle between the two light beams incident on the lens.

As the light source used is a laser, the amplitudes across the beam can be represented by A sinωt. Hence, the optical system described produces interference fringes whose visibility when the light is unmodulated, is 1.

The separation of the fringes in the experiment was .6mm, with $D \sim 100cm$, $f \sim 20cm$, $\lambda \sim 6.10^{-5}cm$.

III. MICROWAVE MODULATOR

The microwave cavity used is the same as that designed by Fox and Mansell[8]. It is shown in Fig.(4.12) to Fig.(4.16). This cavity employs two ADP crystals. This increases the modulation produced for a given voltage.

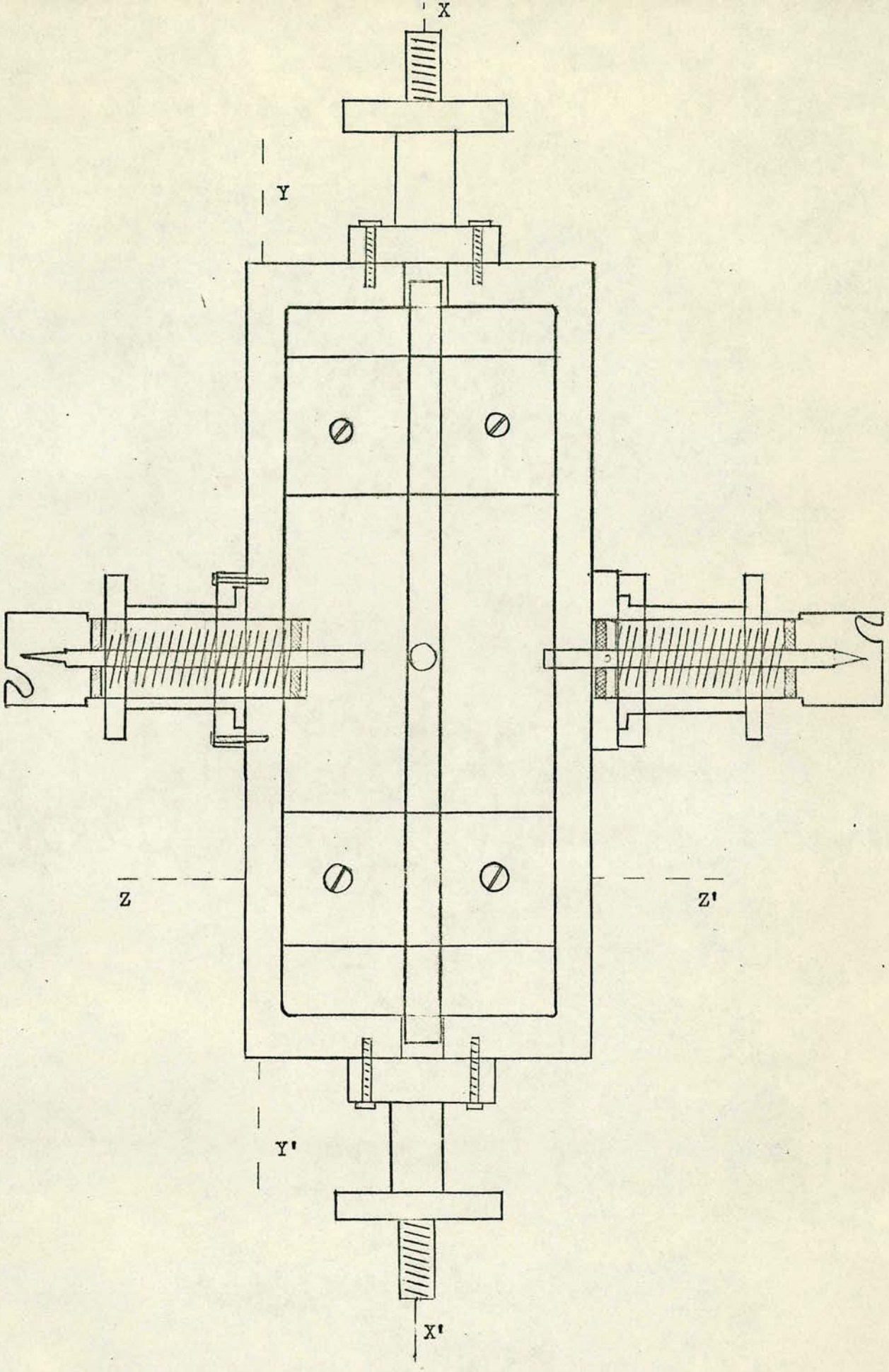

PLAN - SCALE 1:1

Fig.4.12

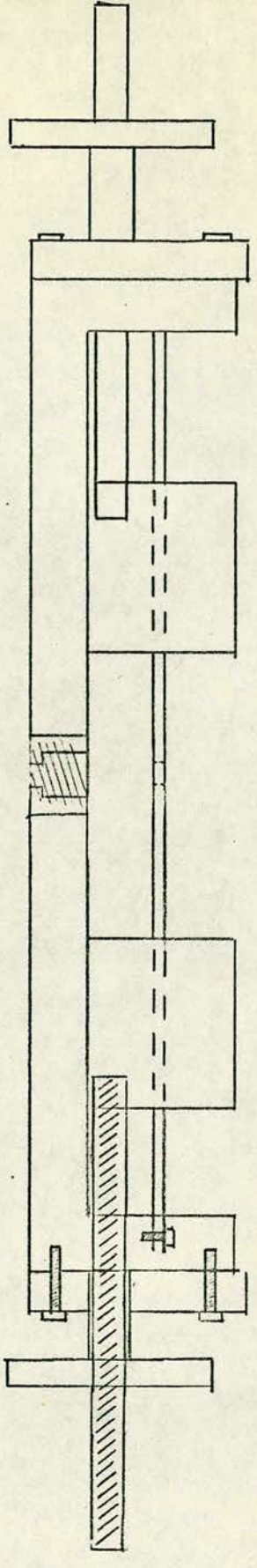

VERTICAL CROSS-SECTION XX'

SCALE 1:1

Fig.4.13

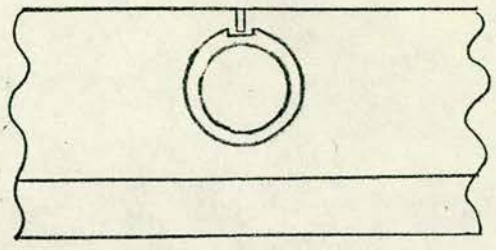

LOCATING PIN FOR PROBE

VERTICAL CROSS-SECTION YY'

FIG.4.14

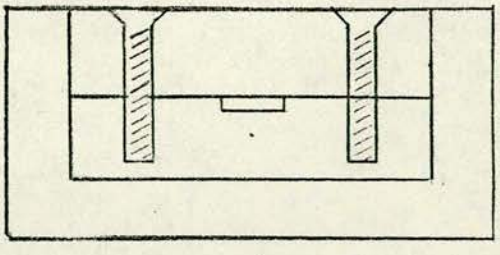

PLUNGER

VERTICAL CROSS-SECTION ZZ'

FIG.4.15

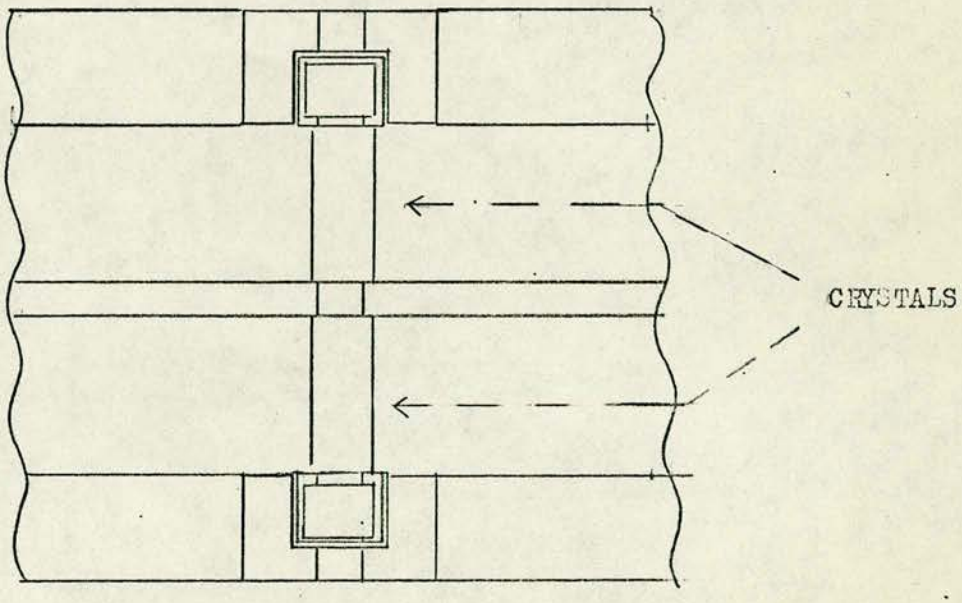

CRYSTAL MOUNTING

SCALE 2:1

FIG.4.16

The cavity is rectangular with a small rectangular-section central conductor. The ends of the cavity are formed by two moveable shorting plungers. The cavity can thus be tuned to the required frequency by adjusting the position of the plungers. The ADP crystals are placed on either side of the central conductor with their optic axes normal to the conductor.

The ADP crystals are 10mm along the z-axis, and the faces normal to the z-axis, which are 4x4 mm square, are optically polished. The x- and y-axes of the crystal are at 45^{o} to the edges of the square. The cavity is mounted in an optical bench saddle, so that the central conductor is at 45^{o} to the horizontal, and the x- and y-axes of the crystal are horizontal and vertical.

The microwave power is coupled to the cavity by an adjustable probe. A second probe is used to monitor the power.

The cavity resonates in a TEM mode, so that the electric field is applied to the crystals parallel to their optic axes. The fields on the two crystals are in opposite directions, so that one crystal must be rotated through 90^{o} with respect to the other in order that the modulation in the two crystals add.

The cavity is made of brass, with all internal surfaces silver-plated.

Small optical flats are attached to the optically polished surfaces of the crystals. This is necessary because ADP is hygroscopic, and the optical surface quickly deteriorates if exposed to air. The flats are attached, using Canada balsam. The crystals are stuck to the central conductor with nail varnish. This was found to be more satisfactory than available glues, because it is very easily removed with acetone,

thus facilitating the removal or re-alignment of the crystals. It is also easily cleaned off the surface of the crystal and off the cavity. The alignment of the crystals with respect to the cavity and with respect to one another will be discussed later in this section.

The limit to the modulation voltage which may be applied to the crystal is set by the amount of power which the crystal can dissipate. At the frequency used, this is a few watts at most. The relationship between the power dissipated W and the amplitude of the electric field amplitude, V_o, is

$$W = \frac{1}{2} V_o^2 \omega_M C \tan\delta$$

where tan δ is the loss tangent of the crystal, and ω_M is the angular frequency of the modulation, and C is the capacitance of the crystal. The di-electric constant of ADP at this frequency is 14, and its loss tangent $6.10^{-3(9)}$. When the power dissipated is 1 watt, the voltage across the crystal is 330V.

The microwave source is a magnetron, JP2-02, which oscillates at 2.45GHz.

It is necessary to know the voltage which is being applied to the crystal. This could be done by measuring the power which is being dissipated in the crystals. Apparatus was not available, however, to do this. It will be shown later in this section that the voltage across the crystal could be estimated by observation of the modulated light. It is still necessary to monitor the power being dissipated in the crystals even though an absolute measurement of this power is not required.

The magnetron unit has a power meter. A reflected power meter is included between the magnetron and the cavity. A rectifying crystal is

coupled to the second probe in the cavity, and the voltage across this crystal is measured by a galvonometer. It was not clear which, if any, of these meters gave a reading which was proportional to the power dissipated in the crystal. The readings did not seem to be correlated. A simple experiment was performed to see if the power could be monitored by means of any of these meters.

The crystals are heated when the microwave power is applied. The rise in temperature of the crystal increases as the power increases. The temperature of the crystal cannot be readily measured while the microwave power is being applied, but can be measured immediately after the power is turned off. This increases the uncertainty in the measurement of the temperature, but as the time taken for the crystal to cool down to room temperature is about 5 minutes, the error is not too serious.

The microwave power is turned on, and left on for about a few minutes, to allow the cavity to reach equilibrium. The readings on the three meters are noted, and the power turned off. The lid is then removed from the cavity, and a thermo-couple is held to one of the crystals. The voltage across the thermo-couple is measured with a galvonometer. Many readings are taken, with variations of the three parameters - see Table 4.1. The only clear correlation with the temperature increase of the crystal is the voltage across the rectifying crystal. This is shown graphically in Fig.(4.17).

Thus, the rectifying crystal produces a voltage which varies with the power dissipated in the crystals. This reading can then be used to monitor the power.

The operation of the modulator is critically dependent on the alignment of the light with respect to the crystal axes, as well as the align-

G	MM	RPM	T
7.9	11.0	6.5	1.8
8.0	9.2	6.0	1.5
8.0	11.7	6.6	0.8
8.0	10.7	6.5	0.9
8.0	12.5	7.0	0.9
8.0	12.3	6.8	1.4
8.0	8.3	5.5	1.0
8.0	9.0	5.5	1.3
8.0	8.2	5.5	0.7
8.0	7.2	5.8	1.3
8.0	9.0	5.8	1.0
8.1	7.7	5.7	1.1
8.1	7.5	5.8	1.4
8.1	8.3	5.5	2.1
8.1	11.0	6.5	1.9
8.1	11.3	6.5	1.3
8.1	9.5	6.0	1.5
8.1	8.7	6.0	0.9
8.2	11.2	6.4	1.8
8.3	8.5	5.8	1.3
8.3	7.5	5.2	1.3
8.5	11.2	6.2	1.2
10.0	10.7	6.5	1.8
10.0	10.7	6.2	1.4
10.8	10.3	6.5	1.3
10.0	9.80	5.5	1.2
10.0	11.2	6.5	1.4
10.0	6.8	2.5	2.4
10.0	8.5	5.5	1.4
10.0	5.0	2.5	2.0
10.0	9.0	5.5	1.8
10.1	9.2	6.0	1.9
10.1	10.2	6.0	1.5
10.1	11.7	6.5	2.0
10.2	8.3	5.5	1.9
10.2	11.2	6.2	2.1
10.2	10.7	6.2	1.3
10.3	8.20	5.0	1.4
10.3	6.8	5.2	1.8
10.3	7.2	4.8	1.5
10.4	8.3	5.5	1.4
10.4	8.0	5.2	1.5
10.4	8.0	5.3	1.9
11.8	7.2	3.0	2.0

G	MM	RPM	ΔT
12.0	10.7	6.0	2.7
12.0	10.9	6.0	1.6
12.0	6.2	1.0	2.3
12.0	7.5	3.0	2.6
12.0	6.0	1.0	1.8
12.0	8.2	5.0	2.0
12.0	8.7	3.0	1.8
12.0	5.0	1.0	1.8
12.1	8.7	5.7	1.7
12.1	8.4	5.5	1.7
12.1	11.7	6.5	2.2
12.1	10.5	6.2	1.7
12.2	11.6	6.5	1.8
12.2	7.0	1.0	2.9
12.4	10.5	5.8	2.2
12.4	10.5	6.3	1.7
12.4	10.8	6.0	1.6
12.4	7.8	4.5	2.1
12.5	7.3	4.8	1.9
12.5	10.3	6.1	2.2
12.5	11.5	6.2	2.1
13.5	6.8	1.0	2.2
13.7	10.0	5.3	1.5
13.7	8.5	5.0	1.9
13.8	8.0	5.0	2.7
13.8	6.5	2.0	2.8
13.8	7.2	4.0	2.0
14.0	10.8	5.8	3.0
14.0	11.8	5.8	2.5
14.1	6.8	1.0	2.6
14.2	7.5	4.0	2.8
14.2	8.6	5.0	3.5
14.2	10.5	6.0	2.3
14.2	11.2	5.7	2.7
14.2	9.8	5.5	2.8
14.3	10.8	5.8	3.2
14.3	7.2	3.0	3.6
14.4	8.3	5.2	2.5
14.5	10.0	6.0	1.8
14.5	10.3	5.8	2.5
14.5	10.5	6.3	1.8
14.5	6.3	0.2	2.9
14.5	8.0	2.5	2.9
15.0	6.8	1.0	3.0

G:Galvonometer. MM:Magnetron meter. RPM:Reflected power meter.
ΔT:Change in crystal temperature.

Table 4.1

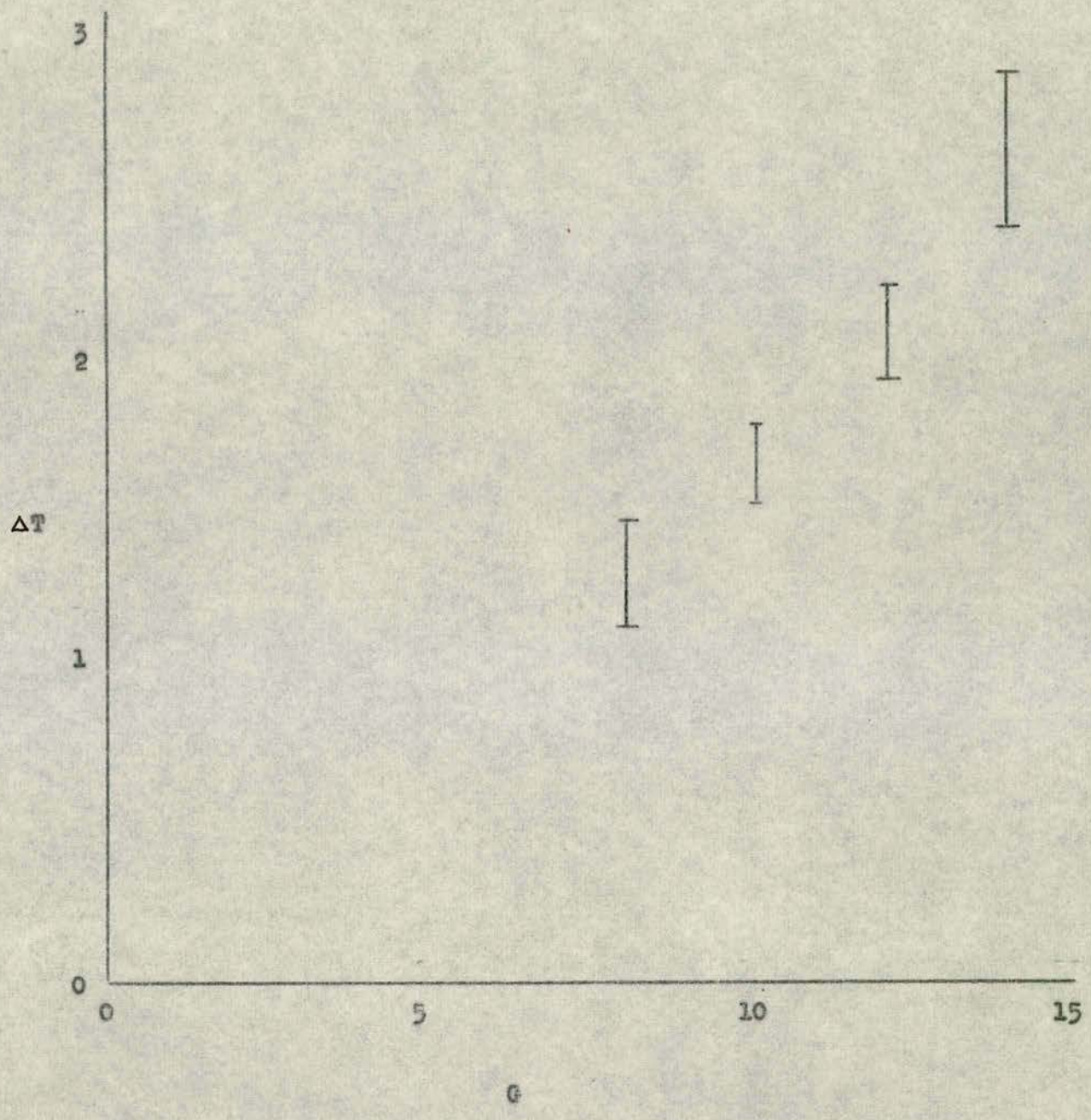

(All error bars denote two standard errors)

Fig.4.17

ment of the one crystal with respect to the other. The discussion of Section VIII, Chapter 3, shows that the modulation envelope of the light is significantly changed when the orientation of the beams is altered. With an applied field of 300V, a change of orientation of the beams with respect to the y-axis 3.10^{-3} rad to 1.10^{-3} rad when the angle between the beams and the x-axis is 2.10^{-3} rad. changes $M_{12}(\tau)$ from -.33 to -.71. It is clear that any misalignment of the crystals with respect to one another must be significantly less than this. A minimum requirement of alignment better than 10^{-4} rad was decided upon.

The interference produced when light is passed through a bi-refringent crystal placed between crossed polarisers can be used to align the crystals. This can be discussed with the help of the equations derived in Section III, Chapter 3.

It is only necessary to consider the case of a uni-axial crystal. The index ellipsoid may be written

$$A(x^2+y^2) + Bz^2 = 1$$

If the direction cosines of a wave travelling through the crystal are l.m.n with respect to the x-, y-, z-axes, then the rotation matrix (3.22) is

$$\begin{pmatrix} \frac{ln}{(l^2+m^2)^{1/2}} & \frac{mn}{(l^2+m^2)^{1/2}} & -(l^2+m^2)^{1/2} \\ \frac{-m}{(l^2+m^2)^{1/2}} & \frac{-l}{(l^2+m^2)^{1/2}} & 0 \\ l & m & n \end{pmatrix}$$

The refractive indices for waves polarised in the directions X and Y where

$$\underline{X} = \ell_x \underline{i} + m_x \underline{j} + n_x \underline{k} \qquad \underline{Y} = \ell_y \underline{i} + m_y \underline{j} + n_y \underline{k}$$

are given by

$$\frac{1}{n_x^2} = A(\ell_x^2 + m_x^2) + B n_x^2$$

$$= A\left[1 + \frac{B-A}{A}(\ell^2 + m^2)\right]$$

$$\frac{1}{n_y^2} = A(\ell_y^2 + m_y^2) + B n_y^2 = A$$

As $B - A < A$, and $l^2 + m^2 \ll 1$

$$n_x \simeq \frac{1}{\sqrt{A}}\left[1 - \frac{1}{2}\frac{B-A}{A}(\ell^2 + m^2)\right]$$

and $n_y = \frac{1}{\sqrt{A}}$

$$\therefore n_y - n_x = \frac{1}{2}\frac{B-A}{\sqrt{A^3}}(\ell^2 + m^2)$$

The phase difference between the two components after travelling through a crystal of length d, whose faces are perpendicular to its z-axis, is given by

$$\delta = \frac{2\pi d}{\lambda n}(n_y - n_x) = \frac{2\pi d}{\lambda n}\frac{(B-A)}{2\sqrt{A^3}}(\ell^2 + m^2) \qquad (4.1)$$

If the directions of the polariser and analyser are

$$\underline{P} = \frac{1}{\sqrt{2}}(\underline{i} + \underline{j}) \qquad \underline{Q} = \frac{1}{\sqrt{2}}(\underline{i} - \underline{j})$$

then the transmitted amplitude is given by

$$A_T = P_x Q_x \sin\delta$$

where $P_x = \{[1 - \ell(\ell+m)]\ell_x + [1 - m(\ell+m)]m_x - n(\ell+m)n_x\}/P_o$

$$Q_x = \{[1 + \ell(\ell-m)]\ell_x - [1 - m(\ell-m)]m_x - n(\ell-m)n_x\}/P_o$$

and P_o and Q_o are normalisation factors which can be shown to be approximately equal to $\sqrt{2}$ when l and m are much less than 1.

P_x and Q_x become

$$P_x \simeq \frac{l_x + m_x}{\sqrt{2}} \qquad Q_x = \frac{l_x - m_x}{\sqrt{2}}$$

since $n_x \ll l_x$, and $n_x \ll m_x$.

Thus

$$A_T = \frac{l_x^2 - m_x^2}{2} . \sin\delta = \frac{(l^2 - m^2)\, n^2}{2(l^2 + m^2)} . \sin\delta . \cos(\omega t + \delta) \qquad (4.2)$$

The transmitted intensity is proportional to the square of this quantity. This clearly varies as l and m are varied.

The transmitted intensity is zero when l = m, and when $\sin\delta = 0$, but otherwise some light is transmitted. Thus, an interference pattern is obtained when the crystal is illuminated with divergent light. The interference can be observed by focussing the light onto a screen, as all the waves travelling in a given direction will be focussed at a particular point on the screen, so that the intensity will vary over the screen.

The two polarisation components will travel in different directions when they emerge from the crystal, but the difference in direction small enough to be neglected. This can be seen as follows.

The refractive index at the boundary may be taken to be $\frac{1}{\sqrt{A}} = n_1$. It is seen from eq.(3.37) that this is correct to 1 in 10^7, when l and m are $\sim 10^{-3}$ rad.

The direction cosines l'm' of the emergent wave are then

$$l' = n_1 l \qquad m' = n_1 m \qquad n' = (1 - l'^2 - m'^2)^{1/2} \sim 1 .$$

If a lens of focal length f is used, and a co-ordinate system x', y', z' is constructed with x' and y' in the plane of a screen which is in

the focal plane of the lens, and with the z-axis along the optic axis of the lens, then the co-ordinates of the point at which a wave with direction cosines l', m', n', is focussed are

$$x' = \frac{\ell'}{f} = n_1 \frac{\ell}{f} \qquad y' = \frac{m'}{f} = n_1 \frac{m}{f}$$

Thus, the co-ordinates of the point at which a wave in a given direction is focussed, are proportional to the direction cosines of the direction in which the wave travels in the crystal.

The structure of the interference pattern can now be seen from eq.(4.2), and is shown in Fig.(4.18). When l = m, the intensity is zero, so that dark lines are obtained along the lines x' = y', and x' = -y'. The intensity is also zero when $\sin\delta = 0$, i.e. when

$$\frac{\omega d}{n} \cdot \frac{B-A}{\sqrt{A^3}} \cdot (\ell^2 + m^2) = 2p\pi \qquad \text{where p is an integer}$$

i.e., when

$$(\ell^2 + m^2) = \frac{P\sqrt{A^3}}{B-A} \cdot \frac{cn}{\omega d}$$

$$\simeq \frac{P\sqrt{A^3}}{B-A} \cdot \frac{c}{\omega d} \qquad \text{since } n \simeq 1$$

Thus, there will be a series of dark concentric circles of radii

$$r_p = \frac{\sqrt{\ell^2 + m^2}}{f} = \frac{1}{f}\left[\frac{\sqrt{A^3}}{B-A} \cdot \frac{c}{\omega d}\right]^{1/2} p^{1/2}$$

These fringes are often known as the "rings and brushes".

With an ADP crystal of length 1 cm and a lens of focal length 10 cm, the radius of the first dark ring is about 1 cm.

Equation(4.1) may be re-written remembering that $A = 1/n_1^2$ and $B = 1/n_1^2$, as follows

$$\delta = \frac{2\pi d}{\lambda} \frac{\left[\frac{1}{n_3^2} - \frac{1}{n_1^2}\right]}{2 \cdot \frac{1}{n^2}} (\ell^2 + m^2) \simeq \frac{2\pi d}{\lambda}(n_1 - n_3)$$

Surfaces of constant phase difference are found at values of l, m satisfying

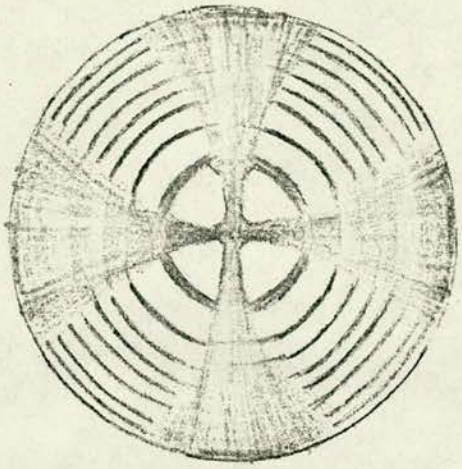

FIG.4.18

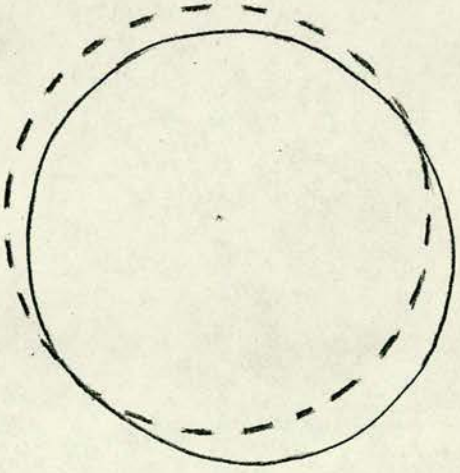

FIG.4.19

$$\ell^2 + m^2 = \frac{\lambda}{d(n_1 - n_3)} \qquad (4.3)$$

The first dark ring in the interference pattern is found at directions satisfying the equation

$$(\ell^2 + m^2)(n_1 - n_3).\frac{d}{\lambda} = 1$$

It is necessary to consider what happens to the fringe pattern when two crystals are placed in series. If the crystals are in exact alignment, the effect will be the same as if one crystal of twice the length were used. The first dark ring is found at directions

$$\ell^2 + m^2 = \frac{\lambda}{2d(n_1 - n_3)} = r_0^2$$

When the crystals are not exactly aligned, the result is rather more complicated. Light travelling in a given direction suffers a phase change δ_1 in the first crystal, and δ_2 in the second crystal, where

$$\delta_1 = \frac{2\pi d}{\lambda}(n_1 - n_3)(\ell_1^2 + m_1^2) \qquad \delta_2 = \frac{2\pi d}{\lambda}(n_1 - n_3)(\ell_2^2 + m_2^2)$$

l_1, m_1, n_1, and l_2, m_2, n_2 are the direction cosines of the wave with respect to the principal axes of the first and second crystals respectively. Let the direction cosines of the z-axis of the second crystals with respect to the z-axis of the first be (sin Ø, 0, cos Ø). (This can be done without any loss of generality since the directions of the x- and y-axes are not defined in a uni-axial crystal).

The angle between the z-axis of the second crystal and the wave is given by

$$\cos\theta = \ell_1 \sin\phi + n_1 \cos\phi = n_2$$

Hence

$$\sin\theta = \ell_2^2 + m_2^2 = 1 - n_2^2$$

$$= 1 - (\ell_1 \sin\phi + n_1 \cos\phi)^2$$

Thus the total phase change of the wave is

$$\delta = \delta_1 + \delta_2 = \frac{2\pi d}{\lambda}(n_1 - n_3)[\ell_1^2 + m_1^2 + 1 - (\ell_1 \sin\phi + n_1 \cos\phi)^2]$$

If the misalignment of the crystals if small, i.e. $\phi \ll 1$, then

$$\delta \simeq \frac{2\pi d}{\lambda}(n_1 - n_3)[2(\ell_1^2 + m_1^2) + 2\ell_1 \sin\phi + \sin^2\phi]$$

The first dark ring is now found at directions given by

$$(\ell_1^2 + m_1^2) + \ell_1 \sin\phi + \frac{\sin^2\phi}{2} = \frac{\lambda}{2d(n_1 - n_3)}$$

The shape of this depends on the value of sin ϕ, but if sin $\phi < 0.1 r_0$ it is of the form shown in Fig.(4.19), where the dotted line shows the first dark ring for crystals which are fully aligned. It is seen that the ring is distorted by misalignment, the maximum distortion being in the x direction. It is also seen that the centre of the pattern is shifted. This can be understood as follows.

The wave in the first dark ring when the crystals are fully aligned and when $m_1 = 0$, satisfies the condition

$$\ell_0 = \pm r_0$$

When the crystals are misaligned, the wave with $m_1 = 0$ in the first dark ring satisfies the condition

$$\ell = \pm r_0 (1 - \tfrac{1}{2}\sin^2\phi) - \tfrac{1}{2}\sin\phi \simeq \pm r_0 - \tfrac{1}{2}\sin\phi$$

Hence, the distortion of the ring along the x-axis is proportional to where $l = l - l_0$. This is given by

$$\frac{\delta\ell}{\ell_0} = \frac{\ell - \ell_0}{\ell_0} = -\frac{\sin\phi}{2r_0}$$

Similarly, the distortion of the first dark about the y-axis is found by putting $l_1 = 0$, so that the wave in the first dark ring satisfies

$$m_1 = \pm r_0\left(1 - \frac{\sin^2\phi}{4r_0^2}\right)$$

Hence, the distortion of the ring in the y-direction is proportional to $\frac{\Delta m}{m_0}$, given by

$$\frac{\Delta m}{m_0} = \frac{m - m_0}{m_0} = \left(\frac{\sin\phi}{2r_0}\right)^2$$

Clearly the distortion is greater in the x-direction than in the y-direction.

It is also seen that the centre of the pattern is shifted in the x-direction by an amount proportional to

$$\frac{1}{2}\sin 2\phi$$

The interference pattern produced by a single crystal can be observed in a travelling microscope with two-dimensional motion, and the co-ordinates of the centre of the pattern located. If a second crystal is aligned in series with the first, then the position of the centre of the interference pattern will be unchanged. A second crystal is then placed in series with the first, and the centre of the interference pattern located. The amount and direction of the misalignment can be found from the difference between this position and the position of the centre with only one crystal. It is possible to align the second crystal with the first.

The experimental set-up is shown in Fig.(4.20) The aperture in the microwave cavity is illuminated by a mercury lamp. A green filter is used, as it is necessary to have a quasi-monochromatic source in order

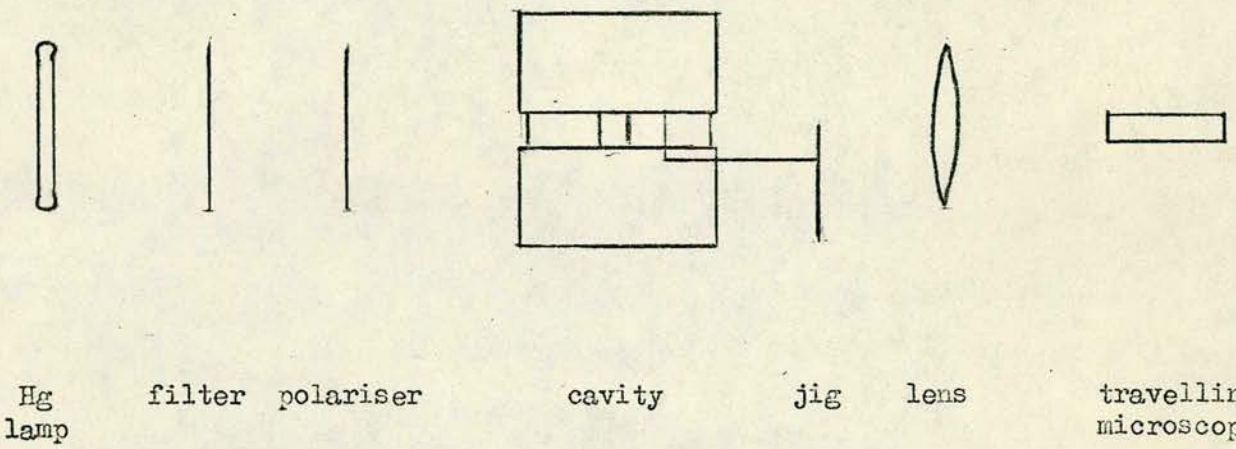

Fig.4.20

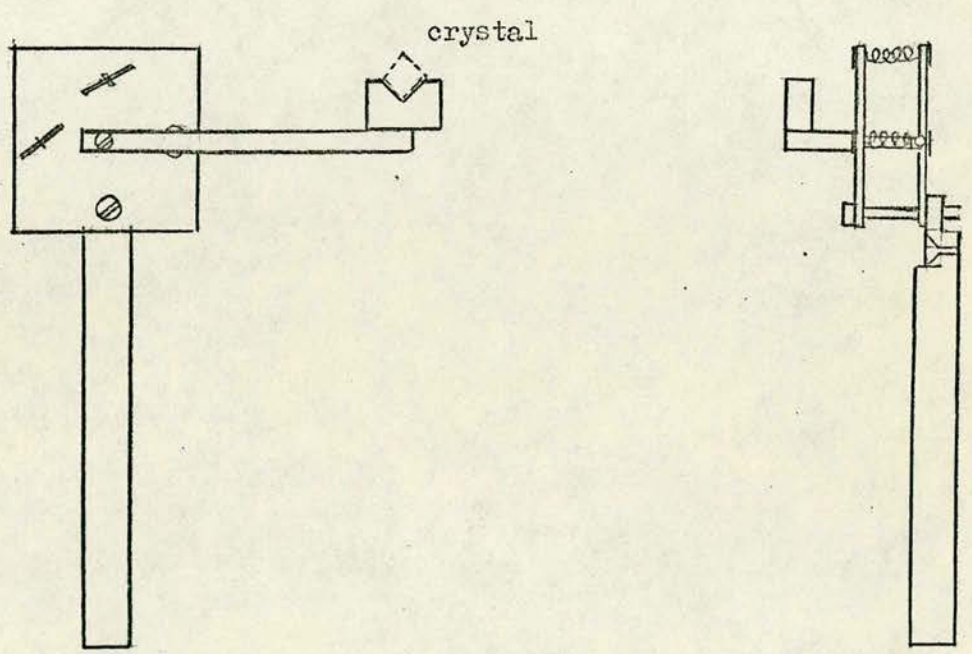

Fig.4.21

that the fringes will be clearly defined, and a laser may not be used since it is necessary to look directly at the pattern.

The crystal is mounted by means of a jig, which is shown in Fig.(4.20) This allows the crystal to be rotated about two orthogonal axes, each at 45^{o} to the horizontal axis. The jig is mounted in an optical bench saddle which can be moved up and down.

The interference pattern is focussed by a convex lens. It is observed with the travelling microscope which can be traversed in two horizontally and vertically in a plane which is perpendicular to the optic axis of the crystal.

The inner crystal is first mounted. It must be situated so that a line through its centre passes roughly through the centre of the apertures in the cavity. This is done by observing the position of the fringe pattern with respect to the apertures with the eye and adjusting the alignment of the crystal until the centres coincide. The crystal is then attached to the central conductor in the cavity.

The interference pattern is then observed in the microscope. The cross-hair is set on the darkest part of the first dark ring on the left hand side and then on the right hand side, and the microscope reading noted in this case. This gives the horizontal co-ordinate of the centre of the pattern. The vertical co-ordinate is found by a similar process, setting the cross-hair on the top and bottom of the first dark ring. A series of such readings are shown in Table 4.2, where it can be seen that the co-ordinates of the centre can be measured with a standard deviation of 0.002 mm. The diameter of the ring is 9 mm. The angular diameter of

	L.H.S.		R.H.S.
	13.883		12.970
	13.884		12.972
	13.880		12.970
	13.880		12.970
	13.884		12.969
	13.877		12.970
	13.878		12.972
	13.880		12.966
	13.884		12.970
	13.881		12.970
Mean value	13.881	Mean value	12.970
Standard deviation	0.0024	Standard deviation	0.002

Table 4.2

this ring can be found from eq.(4.3), so that 0.02 mm corresponds to 6.10^{-5} rad. The crystals are to be aligned to better than 10^{-4} rad. The direction of the optic axis of the crystal, which is the direction of the wave at the centre of the pattern, is determined to 6.10^{-5} rad, so that the alignment is possible.

The second crystal is then mounted in the jig and put in place. It is adjusted initially using the eye. It was found that it was possible to align the crystals to within 1.10^{-3} rad with the eye. The pattern is then viewed through the microscope. The centre is located as before. The orientation of the crystal is then adjusted by means of the jig, and the position of the centre found again. This process is continued until the centre of the two-crystal pattern is the same as that of the one-crystal pattern to within 0.01 mm. Sufficient readings are taken so that two standard errors of readings of the co-ordinates are 0.01 mm. In this case, the optic axes of the crystals are aligned to 1.10^{-4} rad. This can be done with about four adjustments if done carefully.

The crystal is then stuck to the central conductor. Unfortunately, it was found that when the adhesive dried out, the orientation of the crystal was changed. This was probably due to the downward gravitational force on the system. A very much more rigid jig would be required to overcome this problem.

Instead of designing such a jig, it was decided to operate the cavity using only one crystal. The operation of the cavity can be tested by looking at the pattern with the microwaves on and off. The central dark spot should brighten when the microwave power is applied to the crystal. This was observed to occur.

A more objective test can be made by measuring the intensity of the centre of the fringe pattern by means of a photomultiplier connected to a high sensitivity galvonometer, and observing the change in intensity when the microwave power is applied. The variation of the intensity with time is shown in Table 4.2. There is clearly a period of about five minutes during which the light intensity is changing. After that it has reached thermal equilibrium, and the light intensity is constant, except for intensity fluctuations of the light source.

A laser beam was passed along the optic axis of the crystal in the cavity, and the output light, when the microwave power was applied was examined in a scanning Fabry-Perot interferometer. Side-bands of the central light frequency were observed, confirming that amplitude modulation of the light was taking place. It was not possible to make any measurements in this system, due to the non-availability of the Fabry-Perot interferometer.

It is necessary to align the two light beams, produced by the two pinhole-lens system described in the previous section, in the required direction with respect to the optic axis of the crystal. This can be done by using the interference pattern produced by divergent light passing through the crystal. The x- and y- axes of the crystal are horizontal and vertical. The arms of the 'cross' of the interference pattern are horizontal and vertical, when the polariser and analyser are suitably oriented. The light beams must be symmetrically oriented with respect to the y-axis. If the pinholes are illuminated with an ordinary light bulb, the stray light is sufficient to produce the interference pattern. If the crystal is viewed with the eye focussed at infinity, the images of

the pinholes should be symmetrically situated about the vertical arm of the 'cross'.

This alignment can be made to about 10^{-4} rad. This was shown by setting the pinholes so that they were definitely asymmetric about the vertical arm on either side. The readings on the scale on the screen were noted. The difference between these readings was .08mm, which means that the difference in angle between the two settings was 4.10^{-4} rad.

The horizontal setting of the beams can be adjusted by traversing the screen containing the pinholes vertically. This allows the variation of the visibility of the fringes with alignment with respect to the x-axis to be measured. Hence, a suitable alignment of the beams can be located for the 'alternating slit' experiment to be performed.

IV. DETECTION SYSTEM

A slit is placed on the region where the two light beams overlap. The slit is parallel to the fringes, and is mounted in an optical bench saddle which can be traversed across the interference pattern. Behind the slit is the photo-multiplier (EMI 9524S), whose output current is measured by an electrometer.

The dark current of the photo-multiplier and the instability of laser intensity were the main sources of noise, as the laboratory was in complete darkness except for the laser itself, the pilot lights on the instrument panels, which were covered with black cloths, and a torch which was needed to read and record the electrometer current (this was

done under a black cloth so that there was no noticeable leakage of its light on the photo-multiplier). The slit was isolated from the rest of the interferometer by a black curtain which had a small hole to allow the two beams through.

The quantity to be measured is $M_{12}(\tau)$, as defined in eq.(2.7). It is shown below that an absolute measurement of the visibility of the fringes is not required. Hence, neither the slit-to-fringe-width ratio nor the accuracy of alignment of the slit with the fringes need be known.

The relation of the visibility of the fringes to $M_{12}(\tau)$ is given by eq.(2.10), and is

$$V_M = \frac{I^M_{MAX} - I^M_{MIN}}{I^M_{MAX} + I^M_{MIN}} = |M_{12}(\tau)|\,|\gamma_{12}(\tau)|\,\frac{2\beta_M}{1+\beta_M^2}$$

where $M_{12}(\tau)$ is real, β_M^2 is the ratio of the intensities of the beams, and I^M_{max} and I^M_{min} are the maximum and minimum intensities in the interferogram.

The visibility of the fringes produced by the same two beams when the modulator is removed is given by eq.(2.6) and is

$$V = |\gamma_{12}(\tau)|\,\frac{2\beta}{1+\beta^2}$$

where I_{max} and I_{min} are the maximum and minimum intensities in the interferogram, and β^2 is the ratio of the intensities of the two beams. In fact, at any given point in the interferogram $\beta = \beta_M^2$, but since the visibility is measured for several fringes and the intensities of the beams vary across the pattern, the ratio of the intensities may vary from fringe to fringe, and must be measured at each fringe.

$M_{12}(\tau)$ is given by

$$|M_{12}(\tau)| = \frac{V_M}{V}$$

Because of the finite slit width, the quantities I_{max} and I_{min} cannot be measured accurately. It is shown below that the measured visibility is proportional to the true visibility, the constant of proportionality being dependent on the slit width.

The energy passing a given point per second in the interference pattern where the path difference between the beams is $c\tau$ may be represented by

$$dE = (I_0 + I_1 \cos\omega\tau)\, d\tau$$

where ω is the frequency of the light in the case of a monochromatic source, or the central frequency in the case of a quasi-monochromatic source.

If a slit is placed in the overlap region of the two beams, with the path difference between the two beams at the centre of the slit being $c\tau$, and at the edges of the slit being $c(\tau_0 \pm \frac{\Delta\tau}{2})$, the energy passing through the slit per second is given by

$$E = \int_{\tau_0 - \frac{\Delta\tau}{2}}^{\tau_0 + \frac{\Delta\tau}{2}} dE = I_0 \Delta\tau + I_1 \cos\omega\tau_0 \cdot \sin\left(\frac{\omega\Delta\tau}{2}\right) \cdot \frac{1}{\omega}$$

The maximum and minimum energies passing through the slit per second are

$$E_{MAX} = I_0 \Delta\tau + 2 I_1 \sin\left(\frac{\omega\Delta\tau}{2}\right) \cdot \frac{1}{\omega}$$

$$E_{MIN} = I_0 \Delta\tau - 2 I_1 \sin\frac{\omega\Delta\tau}{2} \cdot \frac{1}{\omega}$$

The measured visibility is

$$V_{OBS} = \frac{2I_1}{I_0} \sin\left(\frac{\omega\Delta\tau}{2}\right) \cdot \frac{1}{\frac{\omega\Delta\tau}{2}}$$

and the true visibility is

$$V_{TRUE} = \frac{2I_1}{I_0} \cdot \sin\left(\frac{\omega\Delta\tau}{2}\right) \cdot \frac{1}{\frac{\omega\Delta\tau}{2}}$$

Hence

$$V_{OBS} = \sin\left(\frac{\omega\Delta\tau}{2}\right) \cdot \frac{1}{\frac{\omega\Delta\tau}{2}} \cdot V_{TRUE}$$

The visibility which is measured is a fraction of the true visibility the fraction being constant for a given fringe-to-slit-width ratio. It is seen that

$$V_{OBS} \rightarrow V_{TRUE} \quad \text{when} \quad \omega\Delta\tau \rightarrow 0$$

and

$$V_{OBS} \rightarrow 0 \quad \text{when} \quad \omega\Delta\tau \rightarrow \pi$$

The measurement of visibility becomes more accurate as the slit width is decreased, but the signal strength is also reduced. Some value of between 0 and $\frac{1}{2}w$ must be chosen for the slit width, where w is the width of one fringe, which gives a signal which can be measured. A slit width of approximately half a fringe width was used, giving

$$V_{OBS} = 0.64\, V_{TRUE}$$

The signal strength was about the same as the dark current of the photomultiplier with this slit.

The measured visibilities V_{OBS} and V_{MOBS} are related to the true visibilities by

$$V_{OBS} = V \sin\left(\frac{\omega\Delta\tau}{2}\right) \cdot \frac{1}{\frac{\omega\Delta\tau}{2}} \qquad V_{MOBS} = V_M \sin\frac{\omega\Delta\tau}{2} \cdot \frac{1}{\frac{\omega\Delta\tau}{2}}$$

Hence

$$|M_{12}(\tau)| = V_{MOBS} / V_{OBS}$$

The quantities measured are then (1) i_{max} and i_{min}, the maximum and minimum photo-multiplier currents obtained when the slit is scanned across the interference pattern produced by the unmodulated beams, (2) i_1 and i_2, the photo-multiplier currents obtained when one and then the other beam is blocked off, (3) i^m_{max} and i^m_{min}, the maximum and minimum currents obtained when the slit is scanned across the interference pattern produced by the modulated beams, (4) i^m_1 and i^m_2, the currents obtained when one and then the other modulated light beams is blocked off, (5) i_B, the current obtained when both beams are blocked off. V_{OBS} and V_{MOBS} are given by

$$V_{OBS} = \frac{(i_{MAX} - i_B) - (i_{MIN} - i_B)}{(i_{MAX} - i_B) + (i_{MIN} - i_B)} \cdot \frac{2\sqrt{(i_1 - i_B)(i_2 - i_B)}}{(i_1 - i_B) + (i_2 - i_B)}$$

and

$$V_{MOBS} = \frac{(i^M_{MAX} - i_B) - (i^M_{MIN} - i_B)}{i^M_{MAX} - i_B + i^M_{MIN} - i_B} \cdot \frac{2\sqrt{(i^M_1 - i_B)(i^M_2 - i_B)}}{(i^M_1 - i_B) + (i^M_2 - i_B)}$$

A program was written which evaluated $M_{12}(\tau)$ from the experimental results and calculated the standard error of each result.

The measurement process described above gives the numerical value of $M_{12}(\tau)$ but not its sign. This can be found as follows.

When modulation system of cavity, polariser and analyser are removed the intensity at a given point in the interferogram is given by (from eq. (2.5))

$$I(Q) = I^{(1)} + I^{(2)} + 2\sqrt{I^{(1)}}\sqrt{I^{(2)}}\,|\gamma_{12}(\tau)|\cos(\alpha_{12}(\tau) - 2\pi\bar{\nu}\tau)$$

When the modulator is included, the intensity at the same point is

given by (from eq.(2.9))

$$I(Q) = \langle G_1^2(t)\rangle [\, I^{(1)} + I^{(2)} + 2\,|M_{12}(\tau)|\,|\gamma_{12}(\tau)|\cos(\alpha_{12}(\tau) - 2\pi\bar{\nu}\tau)]$$

Hence, if $M_{12}(\tau)$ is positive the maxima of the modulated light pattern occur at the same values of path difference as those of the unmodulated light pattern, and if $M_{12}(\tau)$ is negative, the maxima of the modulated light pattern occur at values of path difference where there are minima in the unmodulated light pattern.

Hence, by comparing the positions of the mexima in the interference pattern obtained with the unmodulated light with the positions of the maxima in the modulated light interferogram, it is possible to determine the sign of $M_{12}(\tau)$.

An interference pattern can be observed on the screen containing the slit, which is almost the same as the interference pattern which would be obtained with the cavity and polariser removed. This is the case because (a) the addition of a polariser to the system simply reduces the intensity of the pattern without changing the relative intensities of the maxima, and (b) the effect of the crystal is to produce a small component perpendicular to the initial polarisation direction, but to leave the component in the initial polarisation direction almost unchanged (see eq. (3.42)). (It should be noted that the interference pattern which is to be observed if the analyser was placed beforethe slit is to be shifted by half a fringe with respect to the pattern obtained with the modulator removed. This can be seen by substituting $\beta_0 = 0$ into eq.(3.41).)

To find the sign of $M_{12}(\tau)$, the position of the slit is adjusted so that it coincides with a minimum in the interference pattern. The photo-multiplier current is noted when the microwave power is applied, and by

traversing the slit, it can be seen whether the intensity at the first setting is a maximum or a minimum, and hence the sign of $M_{12}(\tau)$ is found.

The photo-multiplier current can be calibrated in terms of photons incident on the photo-cathode per second. This is done as follows.

The photo-cathode is illuminated by the laser used in the interferometer, its intensity being reduced by polarisers. The photo-multiplier current is noted, and the dark current measured by screening the photo-cathode.

The pulses from the photo-multiplier are then counted with a scaler, readings again being made for laser and dark current. This done for various values of the pulse dicrimination height of the scaler. The number of pulses recorded per second increases as the discrimination level is decreased, but the number of pulses from the laser which is found by subtracting the background count from the background plus signal count-rate, levels off. This is the number of photo-electrons emitted by the photo-cathode.

To find the number of photons incident on the photo-cathode, it is necessary to know its quantum efficiency. The cathode used was an S-type, whose quantum efficiency at 632.8nm is 0.2%.

In this way, the number of photons producing a giving photo-multiplier current is found.

CHAPTER 5

I. MEASUREMENTS MADE

The amplitude of the modulating electric field was found. A suitable alignment of the beams could thus be found for the performance of the experiment. The variation of the visibility of the fringes with path difference was found for this alignment of the beams. In addition the variation of the visibility with path difference of the fringes produced by two beams which suffered phase reversal was measured. Lastly, the photo-multiplier current was calibrated.

II. MEASUREMENT OF THE ELECTRIC FIELD AMPLITUDE

The pinholes were situated so that when they were illuminated and viewed through the aperture in the cavity, which was placed between crossed polarisers, they appeared to be symmetrically located about the vertical arm of the 'cross' of the interference pattern discussed in Chapter 4, Section III. The pinholes were traversed vertically, and the visibility of the fringes produced by the unmodulated and modulated beams measured for various settings of the pinholes. The sign of $M_{12}(\tau)$ was also found.

The results are listed in Table 5.1 and are shown graphically in Fig.(5.1). In Fig.(5.1) are also shown calculated curves of $M_{12}(\tau)$ for beams with the separation of the beams in the experiment, and for electric field amplitudes 100V; 130V; and 160V.

Comparison of the experimental and theoretical curves show that the electric field amplitude lies in this range.

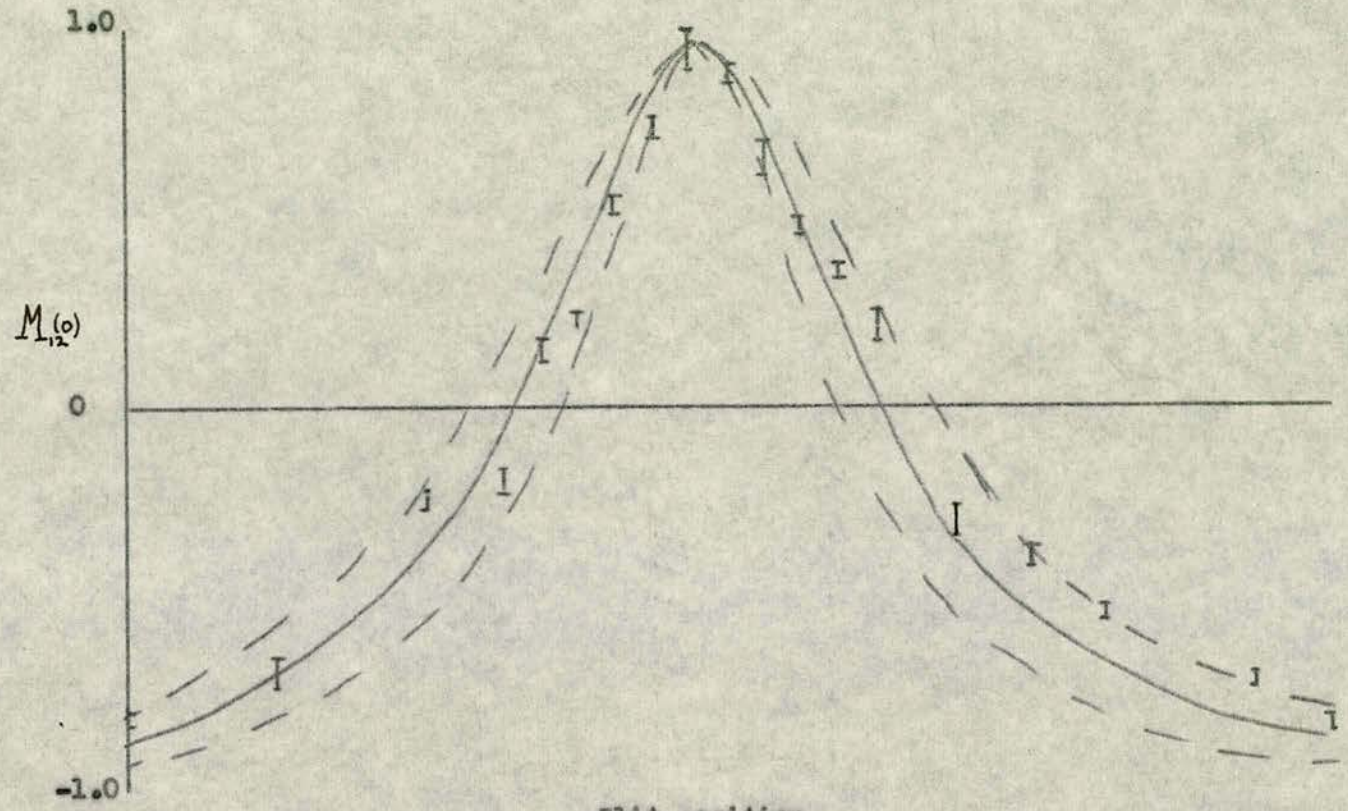

Fig.5.1

Slit position (mm.10)	$M_{(o)}$	Standard deviation
0	-0.82	.02
2	-0.70	.04
4	-0.25	.02
5	-0.20	.02
5.5	0.15	.03
6	0.23	.02
6.5	0.54	.02
7	0.74	.06
7.5	0.94	.02
8	0.80	.04
8.5	0.65	.02
9	0.48	.02
9.5	0.36	.05
10	0.22	.04
11	-0.30	.03
12	-0.40	.03
13	-0.55	.02
15	-0.72	.02
16	-0.84	.03

Table 5.1

III. THE EXPERIMENT PROPER

A visibility contour diagram for E_z = 130V is shown in Fig.(5.2). The pinhole-lens system used produced beams of angular divergence (1.5) $.10^{-3}$ rad. whose angular separation in the crystal was $(4.2).10^{-3}$ rad. One of these beams is indicated by the circle centred about P in Fig. (5.2)

It is seen that when the beam is located as indicated here, and the other beam is symmetrically located on the opposite side of the axis, the beams suffer very little phase reversal, since this occurs only when $M_{12}(0) < \frac{1}{3}$ (i.e. $2\text{lm} < \beta_o^2$).

The visibility of the fringes produced by the two beams thus aligned was measured with path differences between the two beams of from 0 to 30 cms. The results are shown in Fig.(5.3) and listed in Table 5.2. The theoretical variation of $M_{12}(\tau)$ is also shown in Fig.(5.3).

The slit width was approximately half a fringe width. The value of $I_1 + I_2$ never exceeded 1nA. Hence, the number of photons per fringe can be found when the photo-multiplier has been calibrated.

IV. CALIBRATION OF THE PHOTO-MULTIPLIER CURRENT

The calibration of the photo-multiplier current gave the results listed in Table 5.3 and shown in Fig.(5.4). It is seen that the value of the photon count per second due to the light signal levels off at a value of $3.6.10^3$. The photo-multiplier current produced by this signal was 28nA. The quantum efficiency of the photo-cathode for light of wavelength 0.63uA is 0.2%.

Hence, when the photo-multiplier current is 1nA, the rate at which photons are incident on the photo-cathode is $1.25.10^6$/sec.

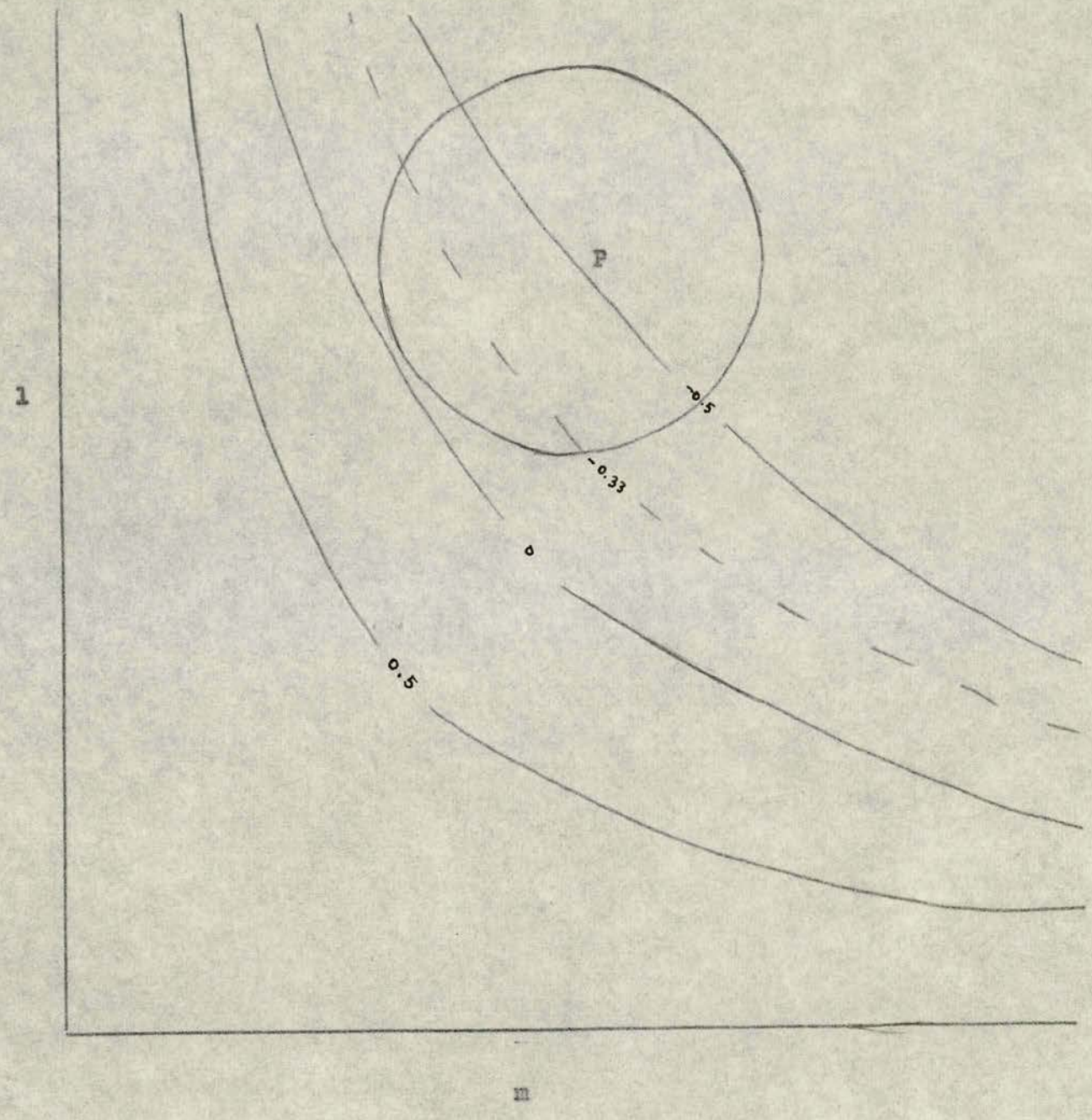

Fig.5.2

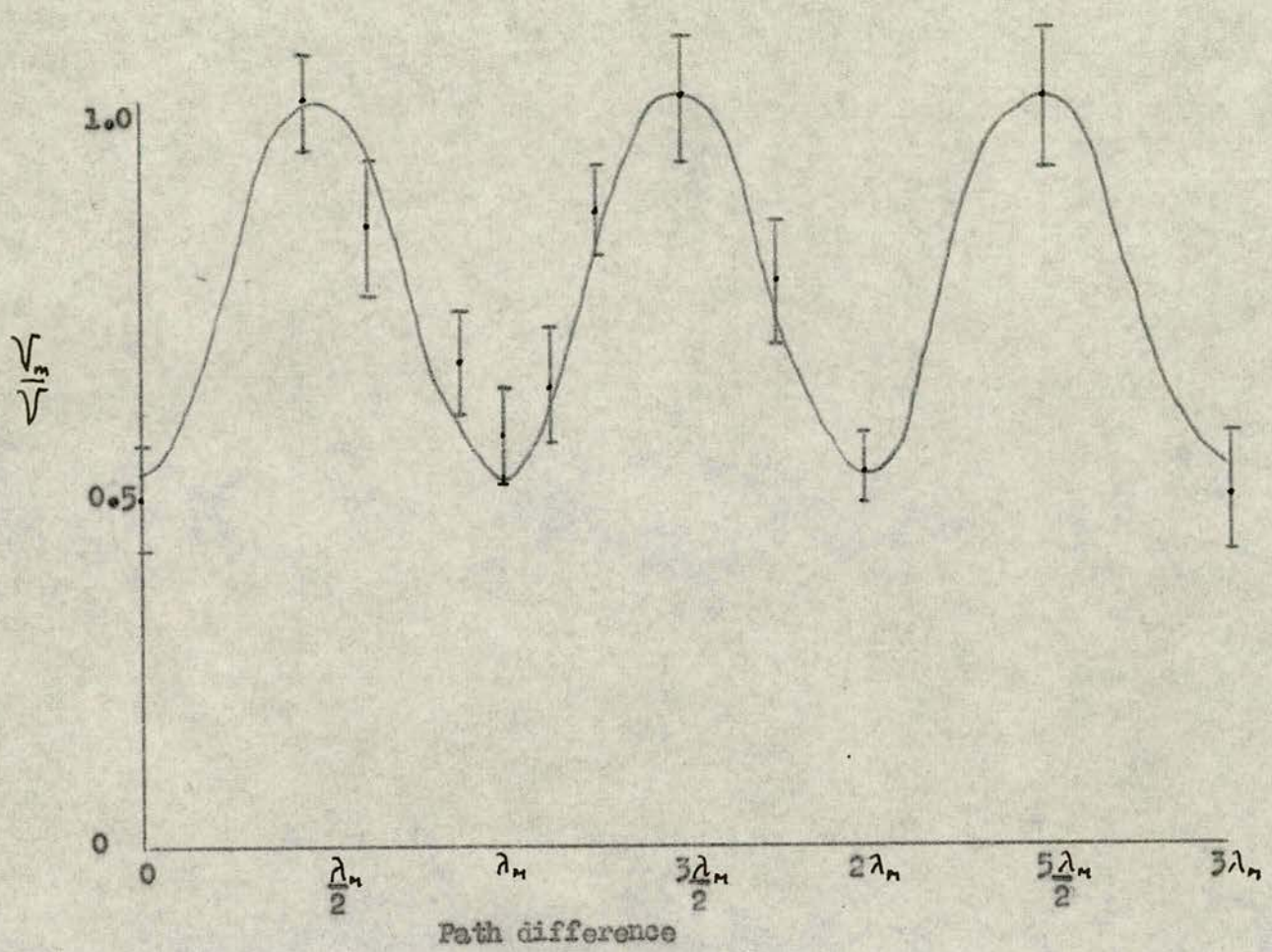

FIG.5.3

Path difference	V_m/V	Standard deviation
0	0.47	.07
5.5	1.00	.06
7.7	0.83	.09
10.8	0.65	.07
12.2	0.55	.06
13.8	0.62	.03
15.3	0.86	.07
18.3	1.00	.08
21.7	0.76	.08
24.4	0.50	.05
30.5	1.00	.10
36.6	0.47	.08

TABLE 5.2

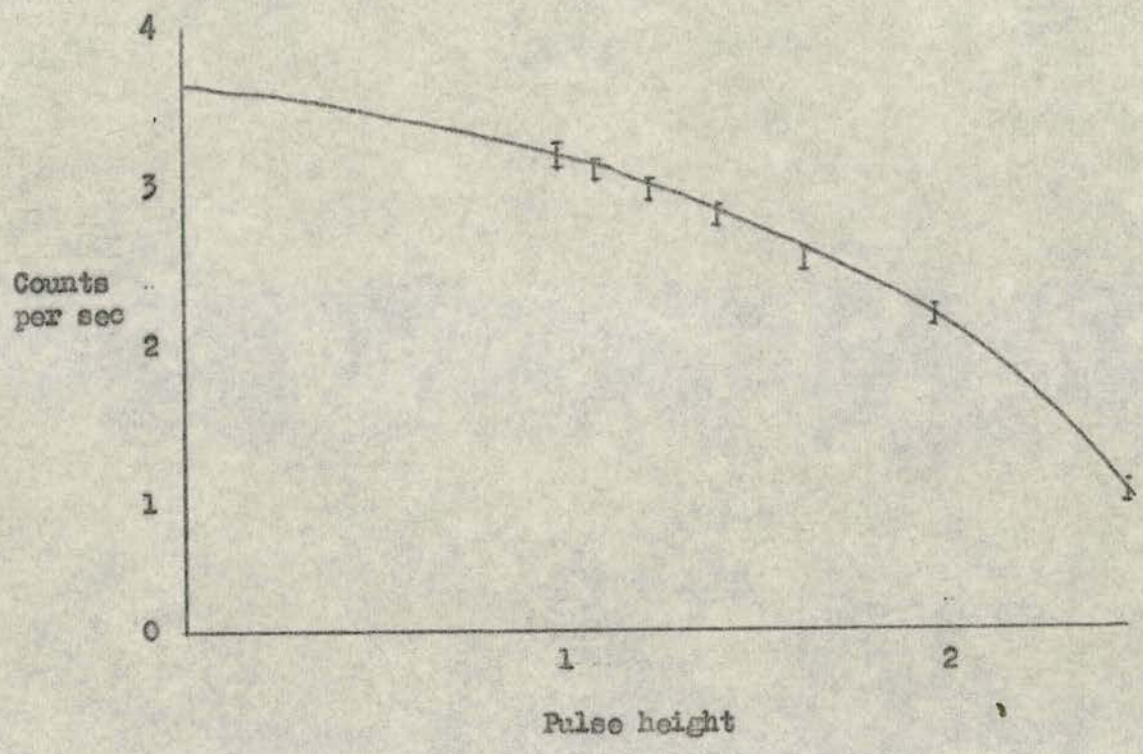

Fig.5.4

Pulse height (arb.units)	Counts/sec $\times 10^{-4}$	Standard deviation
1	3.12	.07
1.11	3.04	.05
1.25	2.89	.07
1.42	2.73	.06
1.66	2.42	.04
2.00	2.08	.01
2.50	0.81	.02

Table 5.3

V. DISCUSSION OF RESULTS

It was required to show that when a particle is scattered by a scatterer which can be at either of two positions at any time, but never at both, interference is obtained in the probability distribution of the scattered particle.

A beam of photons was scattered by a double scatterer consisting of two pinholes, lens, and electro-optic crystal placed between crossed polarisers, with an alternating electric field applied. Though the two scatters were not fully orthogonal, since the amount of light coming from each was at all times non-zero, they approximated fairly closely to the required condition. The variation of the transmitted intensities of each scatterer during the period of the modulation is shown in Fig.(5.5). By measuring the area under each curve for the first half of the modulation period, it is found that the total transmitted intensity of the first is eight times that of the second scatterer. This situation is reversed during the second half period. Hence, a photon incident on the screen is eight times as likely to be scattered by the first scatterer as by the second during the first half of the modulation period, whereas during the second half of the modulation period these probabilities are interchanged. The system behaves effectively as a scatterer which can occupy two positions, but is largely at one position half the time and largely at the other the rest of the time. It was found that when the path difference was zero the interference effect was significantly reduced, but that at a suitable path difference, the visibility was the same as if both scatterers were operating all the time.

The experiment performed demonstrated the single-photon nature of

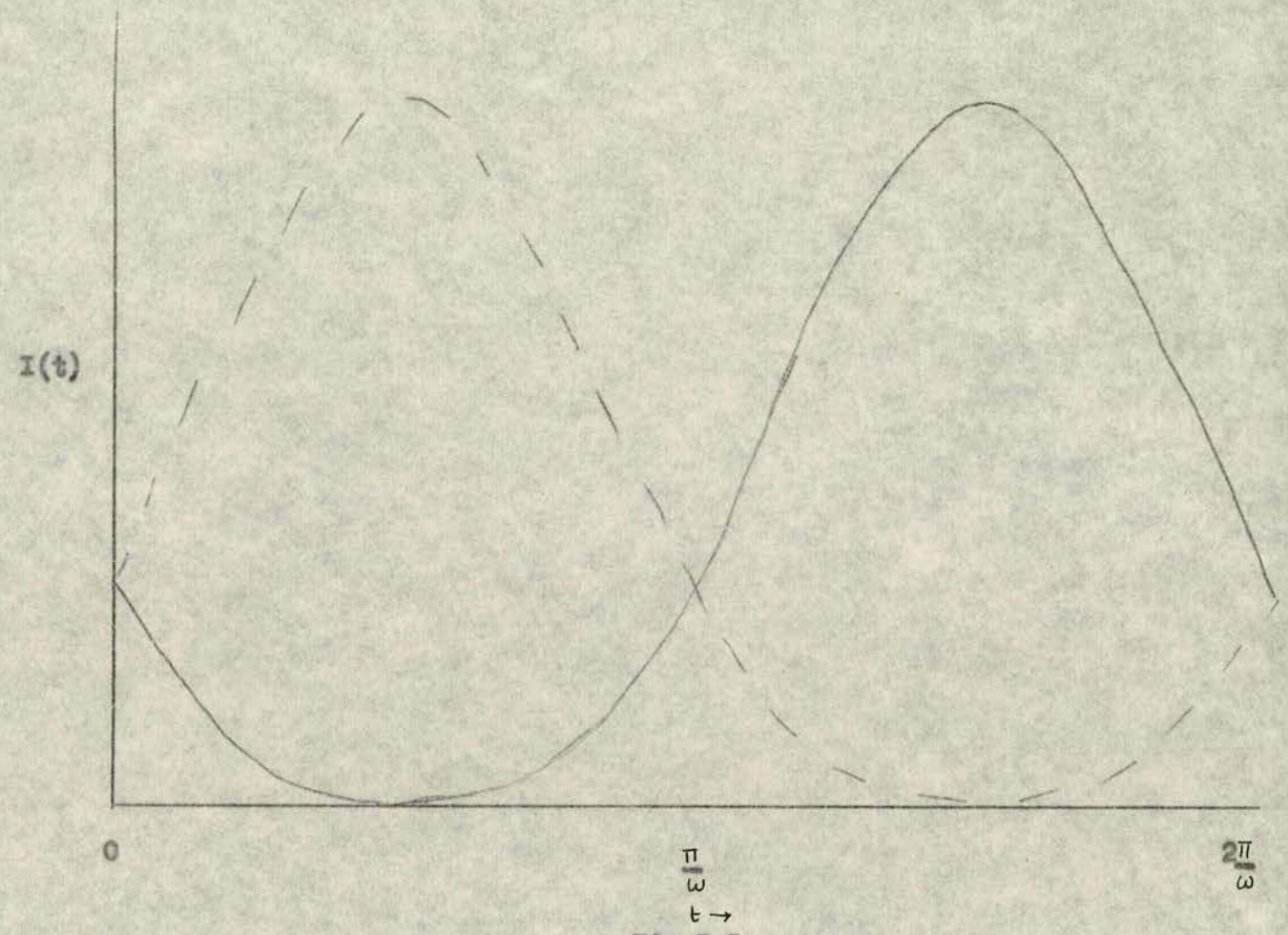

Fig.5.5

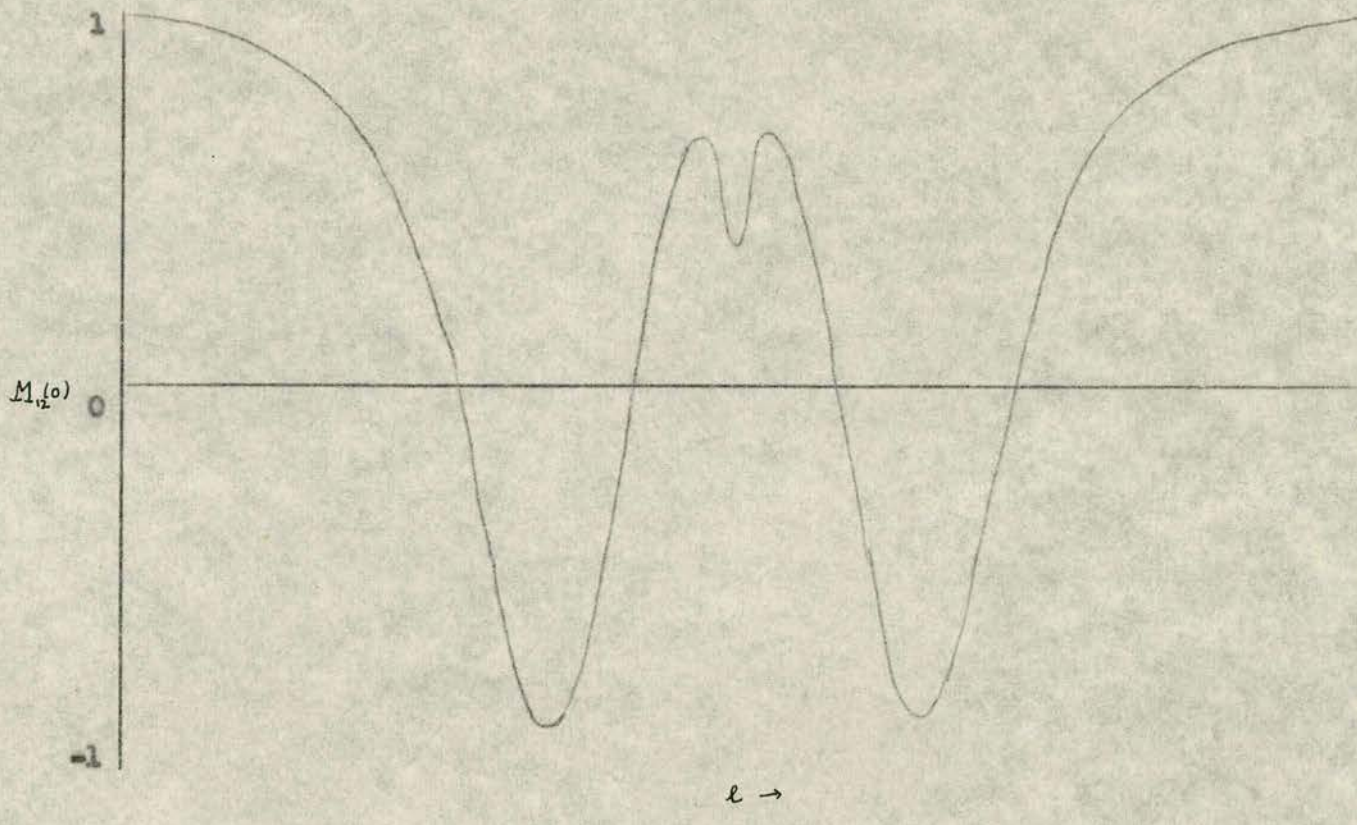

Fig.5.6

the effect, since it can be shown that one photon in an interference fringe is absorbed by the detector long before the next is emitted by the source. This is seen as follows.

The number of photons present in the apparatus i.e. between the screen and the interference region, is given by

$$n = \frac{N}{\epsilon} \tau_T$$

where N is the number of photo-electrons measured per fringe, τ_T is the time taken for a photon to travel through the apparatus, and ϵ is the quantum efficiency of the photo-cathode.

Since the length of the apparatus is 3m, τ_T must be 10^{-8}_{s}. Then, N, from the results given in Sections III and VI of this chapter is $1.25.10^{6}$. Hence, there is only one photon per fringe every 80 transit times.

Though the coherence length of the photons is much longer than the length of the apparatus ($c\tau_{coh} \sim 10\,Km$), the argument is nonetheless valid, since the photons spend most of their lifetimes in the laser cavity, and the time spent by them actually in the interferometer is just the transit time τ_T.

Hence, it has been shown that a single photon incident on a scatterer which occupies only one of two positions can nonetheless show interference in its probability distirbution.

VI. POSSIBLE APPLICATIONS

This kind of interferometer could be used to measure electro-optic constants at high frequencies (i.e. at constant strain).

In Section II of this chapter, it was shown that the amplitude of the applied electric field could be found by measuring the variation of the

visibility of the fringes as the orientation of the light beams is varied. The curve obtained depends on the electric field amplitude, and also on the value of the electro-optic constant of the crystal. If the electric field is known, the electro-optic constant can be found from the curve.

As an example, the constant r_{41} for ADP is not known. It has been shown by a further modification of the program that if an alternating electric field is applied in the x-direction, and the two beams are symmetrically oriented about the y-axis, and are rotated about the x-axis, then the visibility variation is as shown in Fig.(5.6) for three values of $r_{41}E_x$. It should be noted that the maximum angle made by the optic axis with the z-axis for a given electric field amplitude is a lot less than for a field applied in the z-direction, if $r_{41} \sim r_{63}$. The effect is significant only for waves making angles of the same order, or less than the angle made by the optic axis with respect to the z-axis. Hence, the angle between the beams would have to be reduced. This could be done by using a lens of longer focal length, and also using a lower modulation frequency (10MHz) so that a higher electric field amplitude could be used.

Another application of the interference of modulated light beams is to the measurement of the velocity of light. The interferogram has maxima and minima, and the separation L of the maxima (say) in terms of the increase in path difference from one to the next, is simply the distribution travelled by the light in one perion T of the modulation. The velocity of light is then given by $c \frac{L}{T}$. The length measurement can be made in terms of fringes which can be directly compared with a length standard. The time measurement is made by means of a frequency standard. It should thus be possible to measure the velocity of light to the accuracy of the length standard, this being the less accurate of the two.

REFERENCES

(1) Janossy & Nagy, Ann. Physik. 17, 115 (1956)

(2) Mandel, J. Opt. Soc. Am. 49, 931, (1959)

(3) Mehta & Sudarshan, Phys. Rev. 138, B274 (1965)

(4) Born & Wolf, 1959, Principles of Optics (Pergamon Press) Chap X, Sec. 1-4.

(5) Rice, Bell System Tech. J. 23, 282 (1944)

(6) Born & Wolf, as above, Chap. XIV, Sec. 1-2

(7) Jenkins & White, 1957, (McGraw Hill), Chap. 13, Sec. 3

(8) Fox & Mansell, paper delivered at the I.P.P.S. conference on non-linear, electro- and magneto-optics, York, 1966

(9) Kaminow & Turner, Proc. IEEE 54, 1374, (1966)

```
E.R.C.C.  IMP(AA) COMPILER  RELEASE 5 VERSION 7 DATED 15/10/70

%BEGIN
    %REALSLONG
    %REAL A,B,C,W,Z,L,M,D,PX,PY,QX,QY
    %REAL N,Q11,Q12,LX,MX,NX,LY,MY,NY,R,S,FAC,AA,BB,CC,LAM,NORM,PO,QO
    %REAL AMP,MEANINT,MEANCORR
    %REAL FIELD
    %INTEGER I,J,K,H,X
    %REALARRAY DEL(1:19),PHASE(1:2),LL(1:2),MM(1:2),INT(1:34),CORR(1:34
    %REALARRAY AD(1:2)
    %REALARRAY DELTA(1:3)
    PRINTSTRING('VISIBILITY CALCULATION')
    NEWLINE
    READ(A);READ(B);READ(C);READ(W);READ(Z)
    A=1/A**2;B=1/B**2
    W=6.2832*C/W
      %CYCLE J=1,1,3
       READ(DELTA(J))
      %REPEAT
    1:READ(X);%IF X=99%THEN%STOP
    PRINT(X,2,0)
    READ(LL(1));READ(MM(1))
    LL(1)=LL(1)*.0001;MM(1)=MM(1)*.0001
    LL(2)=MM(1);MM(2)=LL(1)
    PRINT(LL(1),0,5);PRINT(MM(1),0,5);SPACES(4)
      %CYCLE  I=1,1,3
    NEWLINE;SPACES(3)
        PRINT(DELTA(I),1,9)
      %CYCLE J=1,1,19
        DEL(J)=SIN(3.1416*(20-2*J)/36)*DELTA(I)
       D=DEL(J)
       %CYCLE K=1,1,2
       L=LL(K);M=MM(K)
          N=SQRT(1-L**2-M**2)
          AA=A+A*D*(M**2-L**2)/(M**2+L**2)
          BB=((N**2)*A)+(A*D*(L**2-M**2)*(N**2)/(L**2+M**2))%C
          +(B*(L**2+M**2))
          CC=2*A*L*M*N*D/(L**2+M**2)
          LAM=(AA+BB+SQRT((AA-BB)**2+4*CC**2))/2
          NORM=SQRT(CC**2+(AA-LAM)**2)
          %IF NORM<1@-14 %THEN%START
            Q11=0;Q12=1
          %FINISH%ELSE%START
            Q11=CC/NORM;Q12=(AA-LAM)/NORM
          %FINISH
          FAC=SQRT(L**2+M**2)
          LX=(-M*Q11+L*N*Q12)/FAC
          MX=(L*Q11+M*N*Q12)/FAC
          NX=-Q12*FAC
          LY=-(M*Q12+L*N*Q11)/FAC
          MY=(L*Q12-M*N*Q11)/FAC
          NY=Q11*FAC
          R=SQRT(A*(1+D)*LX**2+A*(1-D)*MX**2+B*NX**2)
          S=SQRT(A*(1+D)*LY**2+A*(1-D)*MY**2+B*NY**2)
```

```
      PO=SQRT((1-L*(L+M))**2+(1-M*(L+M))**2+(N*(L+M))**2)
      QO=SQRT((1-L*(L-M))**2+(1+M*(L-M))**2+(N*(L-M))**2)
      PX=((1-L*(L+M))*LX+(1-M*(L+M))*MX-N*(L+M)*NX)/PO
      QX=((1-L*(L-M))*LX-(1+M*(L-M))*MX-N*(L-M)*NX)/QO
      PHASE(K)=W*Z*.1*((1/R)-(1/S))/(C*N)
      AMP=PX*QX
      AD(K)=AMP*SIN(PHASE(K))
      %REPEAT
      CORR(J)=AD(1)*AD(2)
      INT(J)=AD(1)**2
    %REPEAT
MEANINT=(INT(1)+INT(19))/2
      %CYCLE J=2,1,18
      MEANINT=MEANINT+INT(J)
     %REPEAT
MEANCORR=(CORR(1)+CORR(19))/2
      %CYCLE J=2,1,18
     MEANCORR=MEANCORR+CORR(J)
      %REPEAT
PRINT(MEANCORR/MEANINT,1,4)
  %REPEAT
NEWLINE;SPACES(3)
->1
%ENDOFPROGRAM
```

APPENDIX II

To find the directions of the bisectors of the angles between two lines whose directions are given.

The equations of the two lines are $y = m_1x+c_1$, $y = m_2x+c_2$. Any point such as P(x,y) (Fig.II.I) is equidistant from the two lines. These distances PR and PS are given by

$$PR = \frac{m_1x - y + c_1}{\sqrt{1+m_1^2}} \qquad PS = \frac{m_2x - y + c_2}{\sqrt{1+m_2^2}}$$

The loci of all points such as P are given by the equations

$$\frac{m_1x - y + c_1}{\sqrt{1+m_1^2}} = \pm \frac{m_2x - y + c_2}{\sqrt{1+m_2^2}}$$

where the two signs occur because the square roots can be negative or positive. These equations are the equations of two straight lines, which are the bisectors of the angles between L_1 and L_2. The equations may be written

$$x(m_1\sqrt{1+m_2^2} \mp m_2\sqrt{1+m_1^2}) - y(\sqrt{1+m_2^2} \mp \sqrt{1+m_1^2}) + c = 0$$

The slopes of the two lines are

$$M_- = \frac{m_1\sqrt{1+m_2^2} - m_2\sqrt{1+m_1^2}}{\sqrt{1+m_2^2} - \sqrt{1+m_1^2}} = \frac{m_1m_2 - 1 - \sqrt{(1+m_1^2)(1+m_2^2)}}{m_1+m_2} \qquad \text{(II.I)}$$

$$M_+ = \frac{m_1\sqrt{1+m_2^2} + m_2\sqrt{1+m_1^2}}{\sqrt{1+m_2^2} + \sqrt{1+m_1^2}} \qquad \frac{m_1m_2 - 1 + \sqrt{(1+m_1^2)(1+m_2^2)}}{m_1+m_2}$$

It is necessary to determine which of the slopes corresponds to bisector B_1, and which to B_2. This is done as follows.

The slopes of all the lines are unaffected by transformation of the

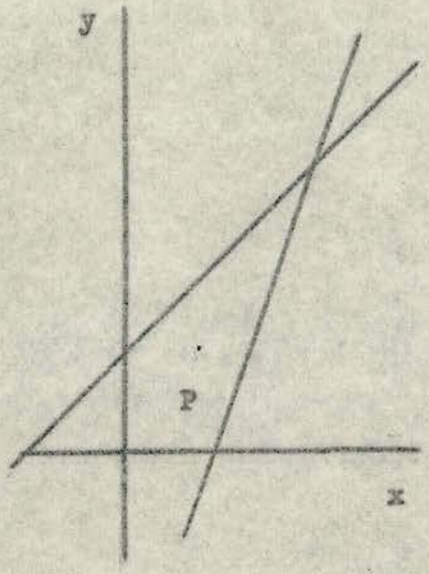

Fig.II.1

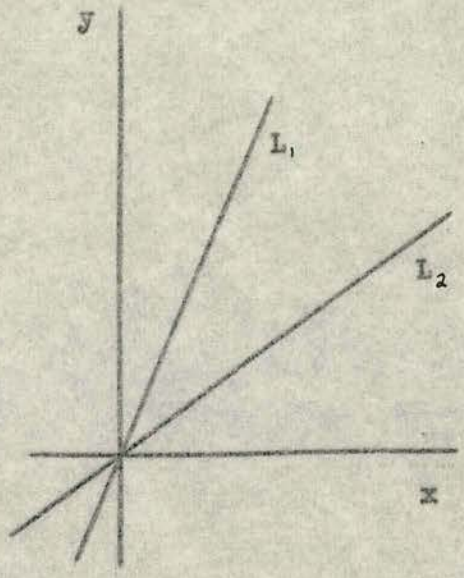

Fig.II.2

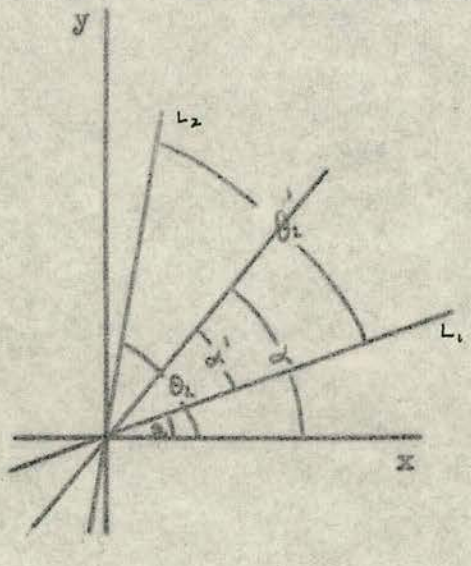

Fig.II.3

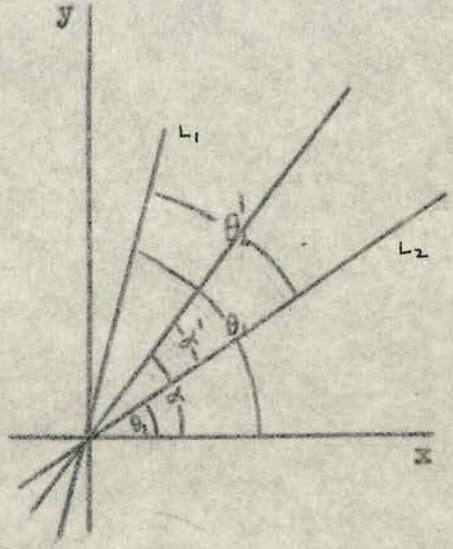

Fig.II.4

origin of the co-ordinate system, as long as the axes are not rotated. The origin can be shifted so that it coincides with the point of intersection of L_1 and L_2.

The case is first considered where L_1 is in the direction of the x-axis, i.e. $m_1 = 0$. The slopes of the bisectors then become

$$M_+ = \frac{-1 + \sqrt{1+m_2^2}}{m_2} = -\frac{1}{m_2} + \sqrt{1+\frac{1}{m_2^2}}$$

$$M_- = \frac{-1 - \sqrt{1+m_2^2}}{m_2} = -\frac{1}{m_2} - \sqrt{1+\frac{1}{m_2^2}}$$

It is seen that, whether m_2 is positive or negative, M_+ is always positive and M_- is always negative. Hence the bisector of slope M_+ always lies in the first and third quadrant, and the bisector of slope M_- always lies in the second and fourth quadrant.

This determines which slope corresponds to which bisector in this particular case, and can be used to do the same thing for the general case, as follows.

Neither of the lines now coincides with the x-axis (Fig.(II.2)). The origin of the co-ordinate system is again shifted so that it coincides with the point of intersection of the two lines.

The slopes of the bisectors are given by eq.(II.I). The co-ordinate system is rotated so that the slope of L_1 is zero and the slope of $L_2 = m_2^1$

The slopes of the bisectors in the rotated system are given by

$$M_+^1 = \frac{-1 + \sqrt{1+m_2^{1\,2}}}{m_2^1} \qquad M_-^1 = \frac{-1 - \sqrt{1+m_2^{1\,2}}}{m_2^1} \qquad \text{II.3}$$

In the case where $m_1 < m_2$, it can be shown that the bisector of slope M_+^1 is the bisector of slope M_+, and when $m_1 > m_2$ it is the bisector of slope M_-. This is seen as follows.

The case is first taken where $m_1 < m_2$. The bisector of slope M_+^1 in the rotated system has slope M* in the unrotated system where they are related by

$$M^* = \frac{M_+ + m_1}{1 - M_+ m_1}$$

since

$$M_+^* = \tan\alpha \qquad M_+^1 = \tan\alpha'$$

$$m_1 = \tan\theta_1 \qquad \alpha = \alpha' + \theta_1$$

where the angles are those shown in Fig.II.3.

It is seen that $\theta_2 = \theta_2 - \theta_1$, hence

$$m_2 = \frac{m_2 - m_1}{1 + m_1 m_2}$$

When this is substituted into eq.(II.3), it becomes

$$M^* = \frac{-1 + m_1 m_2 + \sqrt{(1+m_1^2)(1+m_2^2)}}{m_1 + m_2}$$

The bisector of slope M_+^1 lies in the first quadrant of the rotated system. Since $m_1 < m_2$, this bisector must be the bisector of the angle through the x-axis does not pass.

When $m_1 > m_2$, the bisector of slope M_+^1 in the rotated system has slope M** in the unrotated system, and these are related by

$$M^{**} = \frac{M_+ + m_1}{1 - M_+ m_1} \qquad \text{(II.4)}$$

since

$$M^{**} = \tan\alpha \qquad M_+^1 = \tan\alpha'$$

$$m_1 = \tan\theta' \qquad \alpha = \alpha' + \theta_1$$

where the angles are shown in Fig.II.4.

In this case $\theta_2' = \theta_1 - \theta_2$, so that

$$m_2' = \frac{m_1 - m_2}{1 + m_1 m_2}$$

When this relationship, and that of eq.(II.2) are substituted into eq.(II.4), that equation becomes

$$M^{**} = \frac{-1 + m_1 m_2 + \sqrt{(1+m_1^2)(1+m_2^2)}}{m_1 + m_2} = M_-$$

The bisector of slope M_+^1 lies in the first quadrant of the rotated system. Since $m_1 > m_2$, this bisector of slope M_+^* must be the bisector of the angle through which the x-axis does pass.

Hence, the bisector of slope M_- is the bisector of the angle containing the x-axis, and the bisector of slope M_+ is the bisector of the angle which does not contain the x-axis.

```
BEAM1 =0;BEAM2 =0
%CYCLE J=1,1,25
%CYCLE K=1,1,2
L=LL(J,K);M=MM(J,K)
N=SQRT(1-L**2-M**2)
AA=A+A*D*(M**2-L**2)/(M**2+L**2)
BB=((N**2)*A)+(A*D*(L**2-M**2)*(N**2)/(L**2+M**2))+(B*(L**2+M**2)
CC=2*A*L*M*N*D/(L**2+M**2)
LAM=0.5*(AA+BB+SQRT((AA-BB)**2+4*CC**2))
NORM=SQRT(CC**2+(AA-LAM)**2)
%IF NORM<1@-14 %THEN%START
Q11=0;Q12=1
%FINISH%ELSE%START
Q11=CC/NORM;Q12=(AA-LAM)/NORM
%FINISH
FAC=SQRT(L**2+M**2)
LX=(-M*Q11+L*N*Q12)/FAC
MX=(L*Q11+M*N*Q12)/FAC
NX=-Q12*FAC
LY=-(M*Q12+L*N*Q11)/FAC
MY=(L*Q12-M*N*Q11)/FAC
NY=Q11*FAC
S=SQRT(A*(1+D)*LY**2+A*(1-D)*MY**2+B*NY**2)
R=SQRT(A*(1+D)*LX**2+A*(1-D)*MX**2+B*NX**2)
PHASE(K)=W*Z*((1/R)-(1/S))/(C*N)
P0=SQRT((1-L*(L+M))**2+(1-M*(L+M))**2+(N*(L+M))**2)
Q0=SQRT((1-L*(L-M))**2+(1+M*(L-M))**2+(N*(L-M))**2)
PX=%C
((1-L*(L+M))*LX+(1-M*(L+M))*MX-N*(L+M)*NX)/P0
QX=((1-L*(L-M))*LX-(1+M*(L-M))*MX-N*(L-M)*NX)/P0
AD(K)=PX*QX
%REPEAT
BEAM1=BEAM1+AD(1)*SIN(PHASE(1)/2)
BEAM2=BEAM2+AD(2)*SIN(PHASE(2)/2)
%REPEAT
INT(I)=BEAM1**2
CORR(I)=BEAM1*BEAM2
%REPEAT
MEANINT=(INT(1)+INT(19))/2
    %CYCLE I=2,1,18
     MEANINT=MEANINT+INT(I)
    %REPEAT
MEANCORR=(CORR(1)+CORR(19))/2
    %CYCLE I=2,1,18
    MEANCORR=MEANCORR+CORR(I)
     %REPEAT
PRINT(MEANCORR/MEANINT,1,4)
  %REPEAT
NEWLINE;SPACES(3)
->1
%ENDOFPROGRAM
```

APPENDIX III

E.R.C.C. IMP(AA) COMPILER RELEASE 5 VERSION 7 DATED 15/10/70

```
%BEGIN
  %REALSLONG
  %REAL A,B,C,W,Z,L,M,N,P,Q,Q11,Q12,LX,MX,NX,LY,MY,R,S
  %REAL D,NY,PX,PY,QX,QY,FAC,BEAM1,BEAM2
  %REAL AA,BB,CC,LAM,NORM,PO,QO,F,G
  %REAL MEANINT,MEANCORR,VISIBILITY
  %REAL FIELD
  %REALARRAY DEL(1:19),AD(1:2),BD(1:2),DX(1:2),DY(1:2)
  %REALARRAY CORR(1:19) ,INT(1:19)
  %REALARRAY LL(1:25,1:2),MM(1:25,1:2),PHASE(1:2)
  %REALARRAY DELTA(1:3)
  %INTEGER H,I,J,K,X
  PRINTSTRING('VISIBILITY CALC. EFFECT OF DIVERGENCE')
  NEWLINE
  READ(A);READ(B);READ(C);READ(W);READ(Z)
  A=1/A**2;B=1/B**2
  W=6.2832*C/W
    %CYCLE J=1,1,3
     READ(DELTA(J))
    %REPEAT
  1:READ (X);%IF X =99 %THEN%STOP
  NEWLINE;PRINT(X,2,0)
  READ(LL(1,1));READ(MM(1,1))
  LL(1,1)=LL(1,1)*.0001;MM(1,1)=MM(1,1)*.0001
  PRINT(LL(1,1),0,5);PRINT(MM(1,1),0,5)
  LL(1,2)=MM(1,1)
  MM(1,2)=LL(1,1)
  G=0.5*SQRT(LL(1,1)**2+MM(1,1)**2)
     %CYCLE J=1,1,8
     F=3.1416*((J/4)-1)
      LL(1+J,1)=LL(1,1)+G*SIN(F)
      MM(1+J,1)=MM(1,1)+G*COS(F)
      MM(1+J,2)=LL(1+J,1)
      LL(1+J,2)=MM(1+J,1)
     %REPEAT
     %CYCLE J=1,1,16
     F=3.1416*((J/8)-1)
      MM(9+J,1)=MM(1,1)+2*G*COS(F)
      LL(9+J,1)=LL(1,1)+2*G*SIN(F)
      LL(9+J,2)=MM(9+J,1)
      MM(9+J,2)=LL(9+J,1)
     %REPEAT
    %CYCLE H=1,1,3
  NEWLINE;SPACES(3)
      PRINT(DELTA(H),1,9)
  %CYCLE I=1,1,19
      DEL(I)=SIN(3.1416*(20-2*I)/36)*DELTA(H)
      D=DEL(I)
```

E.R.C.C. IMP(AA) COMPILER RELEASE 5 VERSION 7 DATED 15/10/70

```
%BEGIN
    %REALSLONG
    %REAL A,B,C,W,Z,L,M,D,PX,PY,QX,QY
    %REAL N,Q11,Q12,LX,MX,NX,LY,MY,NY,R,S,FAC,AA,BB,CC,LAM,NORM,PO,QO
    %REAL AMP,MEANINT,MEANCORR
    %INTEGER E,H,I,J,K,X
    %REALARRAY DEL(1:51),PHASE(1:2),LL(1:2),MM(1:2),INT(1:34),CORR(1:34
    %REALARRAY SIG(1:110,1:2),AVSIG(1:34,1:2)
    %REALARRAY DELTA(1:3)
    PRINTSTRING('VISIBILITY CALC.INC.TRANSIT-TIME CORR.SIMP')
    NEWLINE
    READ(A);READ(B);READ(C);READ(W);READ(Z)
    A=1/A**2;B=1/B**2
    W=6.2832*C/W
      %CYCLE J=1,1,3
       READ(DELTA(J))
      %REPEAT
    1:READ(X);%IF X=99%THEN%STOP
    READ(LL(1));READ(MM(1))
    LL(1)=LL(1)*.0001;MM(1)=MM(1)*.0001
    LL(2)=MM(1);MM(2)=LL(1)
    PRINT(X,2,0)
    PRINT(LL(1),0,5);PRINT(MM(1),0,5);SPACES(4)
      %CYCLE  I=1,1,3
    NEWLINE;SPACES(3)
        PRINT(DELTA(I),1,9)
      %CYCLE J=1,1,51
        DEL(J)=SIN(3.1416*(52-2*J)/100)*DELTA(I)
       D=DEL(J)
       %CYCLE K=1,1,2
       L=LL(K);M=MM(K)
          N=SQRT(1-L**2-M**2)
          AA=A+A*D*(M**2-L**2)/(M**2+L**2)
          BB=((N**2)*A)+(A*D*(L**2-M**2)*(N**2)/(L**2+M**2))%C
          +(B*(L**2+M**2))
          CC=2*A*L*M*N*D/(L**2+M**2)
          LAM=(AA+BB+SQRT((AA-BB)**2+4*CC**2))/2
          NORM=SQRT(CC**2+(AA-LAM)**2)
          %IF NORM<1@-14 %THEN%START
            Q11=0;Q12=1
          %FINISH%ELSE%START
            Q11=CC/NORM;Q12=(AA-LAM)/NORM
          %FINISH
          FAC=SQRT(L**2+M**2)
          LX=(-M*Q11+L*N*Q12)/FAC
          MX=(L*Q11+M*N*Q12)/FAC
          NX=-Q12*FAC
          LY=-(M*Q12+L*N*Q11)/FAC
          MY=(L*Q12-M*N*Q11)/FAC
          NY=Q11*FAC
```

```
        R=SQRT(A*(1+D)*LX**2+A*(1-D)*MX**2+B*NX**2)
        S=SQRT(A*(1+D)*LY**2+A*(1-D)*MY**2+B*NY**2)
        PO=SQRT((1-L*(L+M))**2+(1-M*(L+M))**2+(N*(L+M))**2)
        QO=SQRT((1-L*(L-M))**2+(1+M*(L-M))**2+(N*(L-M))**2)
        PX=((1-L*(L+M))*LX+(1-M*(L+M))*MX-N*(L+M)*NX)/PO
        QX=((1-L*(L-M))*LX-(1+M*(L-M))*MX-N*(L-M)*NX)/QO
        PHASE(K)=W*Z*.1*((1/R)-(1/S))/(C*N)
AMP=PX*QX
SIG(J,K)=AMP*SIN(PHASE(K))
    %REPEAT
  %REPEAT
    %CYCLE K=1,1,2
      %CYCLE J=52,1,101
       SIG(J,K)=SIG(102-J,K)
      %REPEAT
      %CYCLE J=1,1,9
       SIG(101+J,K)=SIG(J+1,K)
      %REPEAT
    %REPEAT
     %CYCLE J=1,1,34
    %CYCLE K=1,1,2
      AVSIG(J,K)=0;H=3*J-2
      %CYCLE E=1,1,10
      AVSIG(J,K)=AVSIG(J,K)+SIG(H+E-1,K)
      %REPEAT
    %REPEAT
    CORR(J)=AVSIG(J,1)*AVSIG(J,2)
    INT(J)=AVSIG(J,1)**2
    %REPEAT
MEANINT=(INT(1)+INT(34))/2
     %CYCLE J=2,1,33
     MEANINT=MEANINT+INT(J)
     %REPEAT
MEANCORR=(CORR(1)+CORR(34))/2
     %CYCLE J=2,1,33
    MEANCORR=MEANCORR+CORR(J)
     %REPEAT
PRINT(MEANCORR/MEANINT,1,4)
   %REPEAT
NEWLINE;SPACES(3)
->1
%ENDOFPROGRAM
```